

POLITECNICO DI TORINO

Corso di Laurea Magistrale
in Ingegneria Civile

Tesi di Laurea Magistrale

A reliability comparison between different
robustness strategies in seismic zone



Relatore: Prof. Paolo Castaldo

Relatore: Prof. Taichiro Okazaki

Correlatore: Ing. Elena Miceli

Candidato:

Massimiliano Bruno Caredio

Marzo 2023

Summary

The theory of structural robustness has only recently emerged in the field of structural civil engineering, as a consequence of both minor and major collapses, one of which being the World Trade Center terrorist attack (New York, 11th September 2001).

Normally, buildings are designed to withstand normal actions, whose types and intensities are defined according to the building's importance. In reality, structures are not always able to withstand exceptional events, such as impacts, explosions, and fires; these scenarios have a low probability of occurring, but can have catastrophic results in terms of loss of life, environmental, economic, and patrimonial damage, as well as disruptions to public utility services.

By definition, structural robustness is an intrinsic characteristic of a structure and indicates its ability to avoid disproportionate or progressive collapses as a result of local damage. A structure is thus considered to be robust when, after the loss of one or more sections, it is able to establish other load paths and properly redistribute the forces to the remaining portions of the structural whole.

In this work of thesis, a probabilistic method is used to evaluate the robustness of a reinforced concrete building. This is done because a reliability evaluation of the issue may be useful talking about robustness analysis. This is done in order to take into consideration the uncertainties that can impact structural performance.

Two different frames are analysed, designed in an area of high seismicity according to the directives of the Italian and European regulations. The former has been designed according to code rules while the latter has been improved following other prescriptions, coming from previous experimental studies, to enhance structural robustness. Some changes were made relating to the geometry of the beams, the arrangement and continuity of the reinforcing bars, and the stiffness lateral of the structure.

One hundred different samples of the materials and load characteristics for each frame were taken into account applying a probabilistic approach, the Latin Hypercube Sampling (LHS).

A FEM software, called ATENA 2D, has been used. The main analyses that have been performed, for all the one-hundred scenarios for each frame, are of two types: a pushdown analysis and a reliability analysis. The former was necessary to compute the dynamic amplification coefficients, to be applied to the loads in the second type of analysis, after the column is removed. The latter is needed for the reliability evaluation of the structural robustness.

These dynamic amplification coefficients, which varied for each of the one hundred situations, were analysed using a technique given by Izzuddin et al. [1], which involves performing a pushdown analysis. The latter results in the static imposition of a monotonically increasing vertical displacement at the point of column removal, obtaining, as a result, at each step the strength that the rest of the structure is able to provide at the point itself. The resulting curves are the so-called load-displacement capacity curves, through which it was possible to become aware of the best behaviours in the different cases treated, with the aim of providing design indications and strategies useful for structural robustness. In reference to amplification coefficient once again, this refers to the point where the curves representing the internal energy and the external work meet. The structure will reach collapse if the equilibrium cannot be established (that is, if the curves do not intersect), which has happened for almost the 80% of the “weak frame” cases.

After that, the reliability analysis was carried out for each of the one hundred different scenarios for each frame, which made it possible to validate the procedure that Izzuddin had proposed; all of the scenarios in which the equilibrium could not be reached did not effectively meet convergence criteria in the probabilistic analysis, which confirmed the results of the initial phase.

In the end, the strains at different points of frames' sections were monitored to determine the local probability of failure. This was done for both the concrete and the reinforcing components of the structures. As a

direct consequence of this, a global reliability evaluation and a critical comparison between two different designing criteria were carried out.

Ringraziamenti

Vorrei ringraziare tutti coloro che mi hanno supportato durante la mia carriera universitaria e preparazione della tesi.

Innanzitutto vorrei ringraziare i supervisori di questo lavoro, il professor Paolo Castaldo, per avermi dato l'opportunità di svolgere questo progetto di tesi all'estero, per aver messo a disposizione la sua competenza e per la sua disponibilità durante tutto il percorso, tenendo conto delle numerose difficoltà sorte data la mia lontananza. Il professor Okazaki, per avermi accolto con calore nel suo team di ricerca, per avermi dato la possibilità di cimentarmi nei vari studi sperimentali in laboratorio, un'esperienza indimenticabile. Ringrazio Elena per la sua pazienza, disponibilità e consigli utili in ogni occasione, è riuscita a supportarmi nel mio percorso nonostante le molte interferenze e ostacoli.

Ringrazio tutti i ragazzi che ho conosciuto nel corso di questi 5 anni, Luca, Antonio, Enrico e tutti gli altri con cui ho lavorato, scherzato e condiviso momenti, abbiamo creato un bel team!

Grazie a tutti i ragazzi conosciuti nel periodo di scambio in Giappone, mi hanno accolto con calore nella loro quotidianità e fatto sentire a casa nonostante fossi dall'altra parte del mondo.

Un immenso ringraziamento va ai miei genitori che, nonostante i numerosi diverbi, con il loro esempio mi hanno insegnato a vivere con sani principi, che hanno sostenuto ogni mia decisione e che con tanti sacrifici hanno permesso la realizzazione di uno dei miei più grandi obiettivi.

Grazie a tutta la mia famiglia, nonna Franca, nonna Mirella, nonno Valter, zia Tiziana, Zio Alessandro, ai miei cugini Francesco e Beatrice che mi sono stati vicini lungo tutto il mio percorso.

Infine voglio dedicare un pensiero ai miei nonni Bruno e Giuseppe che mi guardano da lassù, se sono qui è anche grazie a voi e a tutto quello che avete fatto per me. Spero di avervi reso orgogliosi.

*Questa tesi è dedicata a
mio Nonno Bruno che mi
protegge da lassù*

Contents

Preface.....	1
1 Structural Robustness.....	3
1.1 Concept of robustness.....	3
1.1.1 Definition.....	3
1.1.2 Robustness in current regulations.....	4
1.2 Accidental actions.....	5
1.2.1 Classification.....	6
1.2.2 Accidental actions modelling.....	8
1.3 Disproportionate collapse risk.....	11
1.3.1 The concept of risk.....	11
1.3.2 Risk analysis – probabilistic method.....	12
1.3.3 Different scenarios.....	13
1.4 Reduction of the risk.....	13
1.4.1 Analysis of the consequences.....	16
1.4.2 Possible strategies to reduce risk.....	17
1.5 Robustness design.....	17
1.5.1 Design approaches.....	18
1.5.2 Structural modelling.....	19
1.5.3 Analysis types.....	20
1.5.4 Reinforced concrete structures placed into use.....	21
2 Structural Reliability.....	28
2.1 Limit states design, basic principles and uncertainties.....	29
2.1.1 Uncertainties and their classification.....	30
1.1.2 General formulation of the structural reliability problem.....	33

2.1.2	Probability of failure.....	34
2.1.3	Reliability index assessment.....	35
2.2	Methods of reliability and theoretical model.....	36
2.2.1	Methods of Level III.....	37
2.3	Safety formats for reinforced concrete structures.....	39
2.3.1	Levels of approximation.....	40
2.3.2	Probabilistic safety format.....	41
2.3.3	Partial factor format.....	41
2.3.4	Global resistance format.....	42
3	Design of a multi-storey reinforced concrete frame in a seismic zone	44
3.1	General description	44
3.2	Geometrical properties.....	46
3.3	Material properties.....	47
3.3.1	Concrete.....	47
3.3.2	Steel	47
3.4	Durability	48
3.5	Actions	51
3.5.1	Permanent actions.....	53
3.5.2	Variable actions	56
3.5.3	Seismic action.....	58
3.6	Modal analysis	60
3.7	Dimensioning and verification.....	61
3.7.1	Beam design: bending at ULS.....	61
3.7.2	Beams – shear at ULS	64
3.7.3	Beams – SLS	67
3.7.4	Column: bending and compression at ULS.....	69
3.7.5	Column: shear at ULS	70

3.7.6	Joints.....	72
3.7.7	Capacity design - Design solutions' summary	74
3.7.8	Design characteristics of the improved frame	75
3.7.9	Previous robustness evaluation's summary	75
3.7.10	Robustness analysis - Design solutions' summary	76
4	ATENA 2D	78
4.1	The Software.....	78
4.2	Pre-processing.....	80
4.2.1	Graphical interface	80
4.2.2	Materials definition	81
4.2.3	CCT material description	85
4.2.4	Geometrical definition.....	86
4.2.5	Loads and supports	90
4.2.6	Analysis settings.....	95
4.2.7	Parameters	97
4.3	Post-processing	97
4.3.1	Outputs	98
5	Fundamental variables sampling.....	100
5.1	Action fundamental variables	103
5.1.1	Reinforced-concrete specific-weight ρ	103
5.1.2	Permanent structural load of the slab $G1$	104
5.1.3	Floor variable loads Qp	106
5.1.4	Roofing variable loads Qc	107
5.2	Resistance basic variables.....	108
5.2.1	Concrete compressive strength f_c	108
5.2.2	Reinforcement yield strength f_y	109
5.2.3	Reinforcement ultimate strength f_u	111

5.2.4	Reinforcement ultimate strain ϵ_{su}	112
5.2.5	Reinforcement Elastic Modulus E_s	113
5.3	Correlation coefficients.....	114
6	Reliability analysis by using FEM models.....	117
6.1	Introduction.....	117
6.2	Constitutive laws.....	118
6.2.1	Concrete (Model by Saatcioglu and Razvi, 1992).....	119
6.2.2	Steel	122
6.2.3	Geometry	123
6.3	Analysis 1 - Pushdown analysis.....	125
6.3.1	Introduction	125
6.3.2	Load cases in Atena.....	127
6.3.3	Steps of the analysis and results	127
6.3.4	Dynamic amplification coefficient - DAF.....	128
6.4	Analysis 2 - Reliability Analysis	132
6.4.1	Load cases in Atena.....	132
6.4.2	Steps of the analysis	133
6.4.3	Outputs	135
6.4.4	Computation of P_{fmax} : local probability of failure	136
7	Conclusions	142
8	References	144

List of Figures

Figure 1.1: Damaged building's formation of catenary activity (http://www-personal.umich.edu/eltawil/catenary-action.html).....	14
Figure 1.2: Tie forces (DoD 2016 [16]).....	15
Figure 1.3: Column is removed, and the resulting catenary effect(CNR, 2018)	16
Figure 1.4: Technique used to decrease risk.....	17
Figure 1.5: Building with transfer plan (CNR, 2018).....	18
Figure 1.6: : Example of alternative load path (CNR, 2018).....	19
Figure 1.7: Membrane stresses in structural elements (CNR, 2018).....	22
Figure 1.8: Two-dimensional reinforced concrete frame (Lew et al. [19])	23
Figure 1.9: Diagram of imposed displacement-reaction (CNR-DT 214 2018) ..	23
Figure 1.10: Diagram of imposed displacement-horizontal displacement (CNR-DT 214 2018).....	24
Figure 2.1:Limit state domain with X_1 and X_2 as two random variables.	34
Figure 2.2: Relationship between the probability of failure P_f and reliability index β	36
Figure 2.3: The approximation levels approach as outlined by Muttoni	40
Figure 3.1: Building front view	46
Figure 3.2: Building plan view	46
Figure 3.3: Slab design	53
Figure 3.4: Design for the interior walls.....	54
Figure 3.5: Response spectrum at ULS	59
Figure 3.6: Response spectrum at SLS	59
Figure 4.1: Main features of Athena 2D (www.cervenka.cz).....	78
Figure 4.2: Atena 2D	80
Figure 4.3: Graphical interface	81

Figure 4.4: Definition of the fundamental concrete characteristics.....	82
Figure 4.5: Concrete's traction model definition.....	83
Figure 4.6: Concrete's compression law definition.....	83
Figure 4.7: Concrete's shear behaviour definition	84
Figure 4.8: Concrete's specific gravity and thermal expansion coefficient definition.....	84
Figure 4.9: Steel's fundamental parameters definition.....	85
Figure 4.10: Steel's specific gravity and thermal coefficient definition.....	85
Figure 4.11: Material's CCT command description	86
Figure 4.12: Material's CCT command description	86
Figure 4.13: Joints definition.....	87
Figure 4.14: CCT command for joint definition.....	87
Figure 4.15: Lines' definition.....	88
Figure 4.16: CCT command for line definition	88
Figure 4.17: Definition of macro-elements.....	89
Figure 4.18: CCT command for Macro-elements definition and mesh characteristics.....	89
Figure 4.19: Definition of the reinforcement area and the interaction with concrete	90
Figure 4.20 Defining the position of the reinforcing bars	90
Figure 4.21: Fixed support load case definition	91
Figure 4.22: Supports load case application	91
Figure 4.23: CCT command for Supports load case definition	92
Figure 4.24: 2D frame illustration	92
Figure 4.25: <i>Body force load case</i> introduction.....	93
Figure 4.26: CCT commands for <i>Body force load case</i> introduction.....	93
Figure 4.27: <i>Forces load case</i> introduction	93
Figure 4.28: <i>Forces load case</i> allocation.....	94

Figure 4.29: CCT commands <i>Forces load case</i> allocation.....	94
Figure 4.30: distributed line loads applied to 2D frame	94
Figure 4.31: <i>Prescribed deformation load case</i> allocation to the junction above the main column.....	95
Figure 4.32: CCT command for allocation of <i>Prescribed deformation load case</i>	95
Figure 4.33: Examples of analysis steps	96
Figure 4.34: CCT commands for Analysis steps implementation	96
Figure 4.35: Solution parameters (General solution).....	97
Figure 4.36: Solution parameters (Conditional Break-Criteria section).....	97
Figure 4.37: Post processing visualization	98
Figure 4.38: Text printout button.....	99
Figure 5.1: Reinforced concrete specific-weight - Normal distribution: a) Probability density function; b) Histogram and Distribution fit; c) Scatter plot	104
Figure 5.2: Scatterplots for specific weight: a) reinforced concrete (independent sampled variable); b) concrete cover (dependent variable)	104
Figure 5.3: Permanent structural load - Normal distribution: a) Probability density function; b) Histogram and Distribution fit; c) Scatter plot.....	105
Figure 5.4: Permanent non-structural load - Normal distribution: a) Probability density function; b) Histogram and Distribution fit; c) Scatter plot	106
Figure 5.5: Floor variable load - Gumbel distribution: a) Probability density function; b) Histogram and Distribution fit; c) Scatter plot.....	107
Figure 5.6: Roofing variable load - Gumbel distribution: a) Probability density function; b) Histogram and Distribution fit; c) Scatter plot.....	108
Figure 5.7: Concrete compressive strength - Lognormal distribution: a) Probability density function; b) Histogram and Distribution fit; c) Scatter plot	109
Figure 5.8: Steel yield strength - Lognormal distribution: a) Probability density function; b) Histogram and Distribution fit; c) Scatter plot.....	110

Figure 5.9: Steel ultimate strength - Lognormal distribution: a) Probability density function; b) Histogram and Distribution fit c) Scatter plot.....	112
Figure 5.10: Steel ultimate strain - Lognormal distribution: a) Probability density function; b) Histogram and Distribution fit; c) Scatter plot.....	113
Figure 5.11: Steel Elastic Modulus - Lognormal distribution: a) Probability density function; b) Histogram and Distribution fit; c) Scatter plot.....	114
Figure 5.12: Reinforcement basic variables correlation: a) correlation between f_y and f_u ; b) correlation between f_y and ϵ_u ; c) correlation between f_u and ϵ_u ; d) correlation between f_y and E_s	115
Figure 6.1: Scheme for Material 1 (Beam D), Material 2 (Beam ND), Material 3 (Column) and Material 4 (Joints) and Material 5 (NC Concrete).....	119
Figure 6.2: Model of Saatcioglu and Razvi (1992)	120
Figure 6.3: Concrete strength curves according to confinement	121
Figure 6.4: Joints representation: left model with column, right model without column	123
Figure 6.5: Lines representation: left model with column, right model without column	124
Figure 6.6: Representation with joints, lines and macro-elements: left model with column, right, model without the column.....	124
Figure 6.7: Representation of longitudinal and transversal reinforcement: left model with column, right model without the column.....	125
Figure 6.8: Pushdown analysis's scheme	126
Figure 6.9: Pushdown analysis' scheme	127
Figure 6.10: Results of pushdown analysis on the N simulations: a) curve displacement-load – Standard frame; b) curve displacement-load – Improved frame;	128
Figure 6.11: Energy balance approach (Izzuddin [1])	130
Figure 6.12: Energy curves: a) case where the equilibrium is reached b) case where the equilibrium is not reached.....	131

Figure 6.13: DAF sampled values for Standard frame (on the left) and Improved frame (on the right)	131
Figure 6.14: Load amplification's CCT format: simulations where equilibrium is reached (on the left); simulations where equilibrium is not reached (on the right)	134
Figure 6.15: Strains evaluation's visualization: section location (on the left); nodes' location (on the right).....	135
Figure 6.16: Scheme of the sections: indirectly affected members (on the left); directly affected members (on the right).....	136
Figure 6.17: Convolution integral for the maximum Pf of directly affected sub-sections: beam confined concrete strain (on the left); beam reinforcement strain (on the right)	138
Figure 6.18: Scheme of the failure probabilities at each sub-section, standard frame	139
Figure 6.19: Scheme of the failure probabilities at each sub-section, improved frame	139
Figure 6.20: Failure probabilities and reliability indices of the standard frame's nodes: a) 3D plot of Pf ; b) 3D plot of β ; c) Contour plot of Pf ; d) Contour plot of β	140

List of tables

Table 3.1: Forms of construction (Table 2.4.I of DM2018).....	45
Table 3.2: Values of the use coefficient C_U	45
Table 3.3: Concrete characteristics.....	47
Table 3.4: Steel characteristics	47
Table 3.5: Exposure level for corrosion caused by carbonation.....	48
Table 3.6: Limiting parameters for the composition and characteristics of concrete are prescribed.....	49
Table 3.7: According to exposure class XC, the recommended structural categorization.....	49
Table 3.8: In terms of bonds, the minimal cover needed.....	50
Table 3.9: In terms of durability, the minimum cover needed	50
Table 3.10: Coefficients of combination	53
Table 3.11: Permanent structural load of the slab	54
Table 3.12: Slab's permanent non-structural load	54
Table 3.13: Weight of internal walls	55
Table 3.14: Exposure coefficient c_e , as function of the height	57
Table 3.15: Relationship between wind pressure and height.....	57
Table 3.16: 12 initial vibration modes of modal analysis.....	60
Table 3.17: Peculiarities of beams' geometry	61
Table 5.1: Correlation coefficients [-]	102
Table 5.2: Mechanical properties of tested rebars (monotonic tensile tests)....	112
Table 5.3: Correlation coefficients [-]	115
Table 5.4: Sampled basic variables summary.....	116
Table 6.1: SBeta Material inputs	121

Table 6.2: Tensile, Compressive, Shear and Miscellaneous inputs for SBeta Material.....	122
Table 6.3: Steel characterization.....	122
Table 6.4: Pushdown analysis's load cases	127
Table 6.5: Reliability analysis's load cases	132

Preface

Mechanical strength, functionality, stability, ductility, and durability are the traditional fundamental characteristics of a structure. To meet specified needs, these qualities may typically be managed using standardized design techniques.

As a result, structural designers have traditionally concentrated on cost efficiency while satisfying regulatory standards. However, during their service life, structures may be subjected to some unusual and unanticipated occurrences, such as crashes, explosions, or fires. These incidents often produce minor structural damage, which might progress into the collapse of a substantial portion or possibly the entire building.

Recent occurrences have shown how dangerous it is to presume that structures designed for regular conditions can resist unexpected or unintentional load levels.

The ability of a structure to avoid, or at least substantially limit, this type of collapse, is called structural Robustness, and today represents a further requirement to be considered in the fundamental characteristics of a structure, which becomes particularly important and urgent in the case of critical or strategic structures with regard to Civil Protection.

Recently, structural civil engineering has shown a growing interest in structural strength. As a result, many experimental and numerical studies as well as the majority of technical standards have been conducted. Although these studies do not indicate actual quantitative analytical evaluations, they have revealed design-type criteria and procedures that should be followed in order to strengthen the structures.

Reliability analysis may be a highly effective approach for evaluating a structure's robustness. To do this, a probabilistic analysis may be performed in order to assess the local probability of failure, which can then be transposed to the global scale in subsequent analyses.

A reinforced concrete building built following seismic standards has been the subject of a probabilistic study for the purposes of this thesis. Different options for the structural design have been presented, particularly with regard to the longitudinal reinforcement, as previous tests on the same structure have shown that capacity design is unable to provide enough robustness.

The Chapter 1 concerns the fundamental concepts surrounding structural robustness, in particular, the term's meaning in accordance with several code standards is provided. The notions of accidental events and risk scenarios are then illustrated, and solutions for risk reduction are deepened.

The Chapter 2 deals with key aspects about structural reliability. The dissertation then analyses reliability analysis techniques with a focus on the reliability target before coming to a conclusion with safety format aspects.

The Chapter 3 is about the design process for the analysed structure, particularly, recommendations for capacity design are followed. The definition and quantification of actions come after a consideration of the material properties and durability features. The structural dimensioning and verification using SLS and ULS are then shown.

The Chapter 4 is a description of the program ATENA 2D that is separated up into two sections: pre-processing and post-processing. Basic information on material, shape, load, and support modelling is provided in the former. The output and graph tools are described in the latter.

The Chapter 5 is about the fundamental variables sampling, all involved distributions are illustrated. It presents the description of the basic actions and materials sampling according to the Latin Hypercube Sampling (LHS).

The Chapter 6 is about the core of this work of thesis: reliability analysis to evaluate the robustness of the structure under analysis. The fundamentals of the finite element model are initially specified in terms of the mesh, material, and geometry. Then, Pushdown Analysis and Reliability Analysis will be provided as the two key analyses. In order to estimate the local and global probability of failure, the reliability analysis' results are elaborated in terms of the principal total strains. This made it possible to calculate the structure's structural reliability.

1 Structural Robustness

Before explaining the analysis performed for this thesis work, it is necessary to clarify the idea of robustness thoroughly. This is the goal of the subsequent chapter, which begins with a description of robustness, analyses accidental acts and risk scenarios, then discusses risk reduction tactics, not proportional collapse and progressive collapse notions, and finally robustness design. The entirety of the material in this chapter is based on the DT 214 of 2018[4], "Istruzioni per la valutazione della robustezza delle costruzioni," a report created by the CNR (National Council of the Researches).

1.1 Concept of robustness

Different definitions of robustness may be found in the literature of the various domains of study and technology, such as computer engineering, statistics, ecosystems, etc. For instance, in statistics, a technique is regarded as robust when it is insensitive to tiny fluctuations in parameters (Adam et al, 2018).

Given the broad scope of structural strength in the subject of structural civil engineering, it is difficult to provide a clear description. Various definitions of progressive collapse, disproportionate collapse, and robustness have been suggested in research papers, publications, building regulations, and guidelines after many years of study and applications on the evaluation and application of risk mitigation with respect to extraordinary loads on buildings. Even while professional engineers and other stakeholders, such as construction contractors, owners, credit institutions, insurers, governmental organizations, and emergency planners, require a widespread consensus on language and particularly methods, this is still not the case.

1.1.1 Definition

In accordance with what is required by the coding standards, specific sorts of actions and combinations are employed while designing a structure. These activities include seismic loads, fluctuating loads, and permanent loads. The goal is always to achieve a given level of safety, which is based on the significance of

the building and the potential effects of a certain damage. Additionally, code regulations dictate that structures ought to be sufficiently strong. In this contest, the capacity to prevent disproportionate damage—damage that shouldn't be excessive in relation to the extraordinary action that has produced it—is described as a structure's robustness with regard to an exceptional action. The adjective extraordinary denotes that the activity was not planned for, or that it was planned but with a reduced intensity.

1.1.2 Robustness in current regulations

The *Eurocode – Basis of structural design*, in § 2.1 indicates that a structure must be designed and executed in such a way that it is not damaged by events such as explosion, impacts and consequences of human errors, to an extent disproportionate to the cause of origin. Potential damage shall, as a rule, be limited or avoided by the appropriate choice of one or more of the following:

- avoiding, eliminating or reducing the risks to which the structure is exposed;
- choosing a structural form that is poorly sensitive to the risks considered;
- choosing a structural form and design scheme that can adequately withstand the exceptional elimination of an element;
- avoiding as much as possible structural systems that can collapse without warning;
- providing the structure of adequate chaining.

Eurocode 1 – Actions on structures - Part 1-7: General actions - Accidental actions, at § 3.2 means various approaches to ensuring that the property possesses such property, including:

- design of some "key components " to increase the probability of survival of the structure after an exceptional event;
- design of adequate construction details and with ductile materials and structural elements;
- realization of a sufficient hyperstaticity in the structure to facilitate the transfer of actions by exploiting alternative load paths.

In Italy, the *New Technical Standards for Construction* of 2018, in § 3.6 classify exceptional actions as those that occur during events such as fires,

explosions and impacts and states that it is appropriate that the buildings possess an adequate degree of robustness, depending on the intended use of the construction, identifying or risk scenarios and actions exceptional relevant to its design. Therefore, in § 2.2.5 they suggest several design strategies to refer to ensure an adequate level of robustness:

- design of the structure able to withstand exceptional actions of a conventional nature, combining nominal values of exceptional shares with other explicit project actions;
- prevention of the effects of exceptional measures to which the structure may be subject or reduction of their intensity;
- adoption of a structural form and typology that is not very sensitive to the exceptional actions considered;
- adoption of a structural shape and type such as to tolerate localized damage caused by an exceptional action;
- realization of structures as redundant, resistant and / or ductile as possible;
- adoption of control systems, passive or active, suitable for the actions and phenomena to which the work may be subjected.

Last but not least, the fib Model Code 2010 [2], at 3.3.1.3, notes that robustness plays a significant part in a structure's capacity to preserve its functioning when unexpected actions are present or as a result of human mistake. It highlights how crucial it is to maintain robustness for the preservation of human life, protection of human assets and the environment, and maintenance of operations.

1.2 Accidental actions

Before approaching any type of analysis, it is first necessary to correctly define the possible exceptional actions that may affect the construction.

In general, actions can be defined as forces, acting in a static or dynamic way, the magnitude of which depends on the probability of occurrence considered, or through the definition of a specific scenario, as in the case of constructions of great importance, or of particular exceptional events, such as terrorist attacks, which by their nature cannot be treated on a probabilistic basis with classical methods.

By definition, an exceptional action is an action, usually of short duration but of significant magnitude, with a very small probability of occurrence on a given structure during the useful life of the project of the structure itself.

They are usually related to *low-probability and high-consequence LPHC (high-probability)* those events that, on the one hand, have a much lower probability of occurring than that of normal events and, on the other, can cause huge losses, such as victims, repair costs and downtime.

The main and problematic in the management of such scenarios of actions on structures is represented by the difficulty of formulating and identifying risk scenarios and the difficulty in ensuring that designing against such actions is effectively effective in reducing the possibility of structural collapse.

1.2.1 Classification

The exceptional actions are very different from the classic ones considered in the design of structures and below is illustrated a classification, defined in chapter 2 of the *Instructions for the evaluation of the robustness of buildings* (National Research Council – CNR, 2018).

First of all, exceptional events can have a natural or anthropogenic origin and three categories of dangers can be identified:

- 1) dangers deriving from natural phenomena or involuntary human activity: the former may be earthquakes, logical meteor phenomena and landslides while the latter concern explosions and non-arson;
- 2) intentionally man-made actions, such as vandalism and terrorist attacks;
- 3) hazards resulting from errors in the design, design or execution of the construction.

From the point of view of the interaction between the event and the construction, these dangers can act on the structure such as:

- distributed loads of exceptional magnitude;
- impact loads;
- accelerations impressed during a seismic action;

- induced deformations and displacements.

Actions can also be classified on the basis of their duration, although exceptional actions are in most cases very short in relation to the useful life of the structure; in structural modelling, they can be applied to the structure in a static, dynamic way, or with an impulsive trend.

The way in which the model is built varies according to the type of danger:

With regard to Category 1 hazards (of natural origin or arising from involuntary human activity), four models should be prepared to assess the effects on construction: a model describing, from a statistical point of view, the frequency of occurrence of a given phenomenon, one that describes the effects at a distance, another that describes the intensity of the action and how the natural phenomenon interacts with the construction, and finally a model that describes the effects of any interventions mitigation of the action and consequent reduction of danger; through this procedure is possible to achieve a risk scenario sufficiently suitable to formulate an assessment of the structural response to the scenario under consideration.

For the dangers of Category 2 (vandalism and terrorism), it is not possible to take into account the statistics of past events, so they can give indications regarding the possible occurrence of an act of vandalism the strategic role of the construction, the potential relevance of the attack and the type of service of the building; usually in these cases it is not possible to build a model of the intensity of the phenomenon as the modes of attack can be varied and diversified.

The hazards of Category 3 (errors in design, design and construction) cannot be treated statistically except, at least in part and in relation to the construction aspect, in the case of prefabricated modular constructions; the effects of these errors can be mitigated through the control and adoption of a quality and verification process in the various phases of design and construction of the work.

Below is an illustration of some of the possible exceptional actions that may affect a structure in the case of natural and anthropogenic hazards.

1.2.2 Accidental actions modelling

Following the classification of the activities, it is required to decide how to model these loads in order to explain their intensity, their impacts on the structure, assess the risk, and determine the appropriate mitigation measures. The category being evaluated affects these models.

To create a plausible scenario for the Category 1 (hazards with a natural cause or unintentional human cause) and better assess the effects on a structure, the following is required:

1. Create a model that describes the event's recurrence frequency. It is not always simple to define a model of the occurrences for those events brought on by human behaviour.
2. locate a model that forecasts the consequences
3. provide a model that explains the action's level of intensity and its application (load pressure, impulsive load, ...)
4. provide a model that illustrates the results of potential risk reduction and mitigation measures

The inability to establish an occurrence model for threats falling under Category 2 (vandalism or terrorist activities) stems from the fact that prior occurrences are not significant from a probabilistic perspective. Furthermore, because human behaviour influences how intense an action is, it might be difficult to determine because human behaviour is always changing. The lone exception is when someone commits vandalism using explosive explosives, in which case it is conceivable to simulate the wave pressure in proportion to the amount of TNT utilised.

In conclusion, Category 3 risks (conceptual, design, and execution faults) cannot be handled statistically but may be avoided with quality control procedures used both throughout the design and construction stages.

1.2.2.1 Natural phenomena or resulting from involuntary human activity

Among the natural phenomena or deriving from involuntary human activity are the earthquake, the tidal wave, landslides, floods, tornadoes, fires and explosions.

The earthquake is evaluated by the standards through non-epicentral seismic actions, which are obtained considered laws of attenuation of the accelerometric components. In the case of epicentral actions, the reduced distance between the epicenter and the structure hit by the seismic action does not allow adequate damping, and this leads to an increase in substantial with regard to regulatory actions, which may therefore be insignificant.

The tsunami is a natural phenomenon due to underwater movements that determine the onset and propagation in the sea of waves that can have a considerable height when approaching the coast, leading to widespread flooding. Based on the topography of the coastal zone, it is possible to evaluate the extent of areas flooded by a tidal wave due to seismic action, as well as the height of the sum and the speed of the flow. The effects on construction, although variable, can essentially be attributable to impact pressures caused by the moving flow, by concentrated forces due to the debris carried by it, and to hydrostatic thrusts.

Landslides are phenomena due to the loss of stability and/or cohesion of a mass of soil / fractured rock, only of natural origin but sometimes also caused by anthropogenic action; the impact force of a landslide is a function of the speed and type of the mass of soil concerned from the phenomenon.

Flooding is a natural phenomenon due to precipitation or breakage of hydraulic works along the hydrographic network which leads to the rise of surface water and the subsequent flooding of normally dry areas. The effects of this phenomenon on buildings are many: static and dynamic pressures exerted by water at rest or in motion, impacts of objects transported by the current, saturation of underground soils, localized erosion.

The whirlwinds are violent air vortices that form at the base of the clouds and reach the ground; these meteorological phenomena are generated by a center of low pressure around which the air masses rotate producing strong winds and

copious precipitation. The winds that are generated during this type of weather phenomena can seriously damage buildings, knock down plants and power lines, move cars from the road, etc. Therefore, during meteorological phenomena of such magnitude and power, it is good to consider two distinct actions on constructions: the wind pressure on the surfaces and the point forces of impact of the objects moved.

Fires can cause the combustion of structural and non-structural elements; the method of calculating the action, the response of structures to fire and prevention are extensively detailed in many regulatory documents that can be referred to.

In explosions, the pressure wave forms a shock surface that moves at a very high speed and carries a considerable amount of energy; the arrival of the shock wave on a surface, placed at a certain distance from the explosion point, involves a quasi-instantaneous increase in pressure. The amount of pressure on the surfaces of a building is different in cases of confined and unconfined environment.

Impacts on structures can be assessed by means of an equivalent static analysis or through a dynamic analysis. The forces that the impacting body transmits to the impacted structure depend both on the type of impact and on the stiffness and deformability of each of the two bodies.

1.2.2.2 Vandalism and terrorism

The evaluation of actions due to vandalism and terrorism is much more complex than what was indicated above for other types of action, as it is first necessary to analyze the intentions and motivations that push individuals, or the group, to cause damage to society.

The objectives of the vandalism action are usually chosen on the basis of the degree of difficulty in being able to generate damage, on the basis of the degree of protection and surveillance of the facilities/infrastructure, based on the number of persons needed to carry out the terrorist act.

The theory emphasizes the fact that, when primary targets are too protected or difficult to attack, the focus shifts to secondary, simpler goals. In general, terrorists use similar modes of attack, based on previous attempts that have proven effective, until a good mode of attack emerges that turns out to be particularly effective.

1.2.2.3 Design or execution errors

Although they are not to be considered in all respects real actions, the mistakes that can be made in all phases of design and construction of a structure are possible scenarios in respect of which to evaluate the robustness.

These errors lead to the creation of a structure unsuitable to support the project actions, varying the structural behavior with respect to what is indicated by the designer. This type of hazard is closely linked to the quality of the process and the control procedures used.

Structural design errors are those that affect the overall behavior of the structure subject to the project actions.

Design errors concern the final performance of the project, including the construction details to be carried out on site or in the factory.

Finally, the execution errors are those concerning the realization of the structure, including the links between the elements, by the workers.

1.3 Disproportionate collapse risk

The meaning of "disproportionate collapse" refers to a collapse whose features are severe in terms of extent relative to the event that has produced the harm. This concept is sometimes confused with "progressive collapse," which occurs when local damage gradually affects the majority or the whole structure (like a domino effect). While the first collapse focuses mostly on the magnitude of the damage, the second collapse describes the manner in which something collapses.

When dealing with robustness analysis, it is of the crucial relevance to determine the degree of risk acceptance associated with a certain occurrence, given that risk elimination is impossible.

1.3.1 The concept of risk

All exceptional actions can generate stresses on structures capable of causing their collapse, consequently, all types of structures are potentially exposed to the risk of disproportionate collapse, although each type has a different level of

vulnerability to the same.

The events that can trigger disproportionate collapse on the one hand are characterized by very low probabilities of occurrence; in general terms, the risk is determined by the combination of three factors, hazard (P), vulnerability (V), and exposure (E):

$$R = P(*)V(*)E \quad (1.1)$$

Risk can be differently conceived and perceived by the multiplicity of actors involved in decision-making processes. For example, most people tend to be risk-averse, which implies a low perception of the same, on the other hand, large companies often resort to taking out private insurance, in order to neutralize the negative consequences of a strongly adverse event. From a social point of view, however, communities generally have a different perception of catastrophic events, even if they involve a limited number of individuals, compared to more common and that, for this reason, can globally involve a large number of people: a typical example is represented by the perception of risk towards an air accident (which generally causes a higher number of fatalities than the individual road accident and of which the media deals with more attention) rather than road accidents, in fact more frequent and, from a statistical point of view, more risky.

The probability of disproportionate collapse can be calculated by characterizing the conditional probabilities of two levels of damage: local damage, given the occurrence of an exceptional event; global damage, or disproportionate collapse, given the drawing of local damage.

1.3.2 Risk analysis – probabilistic method

Let H (*Hazard*) be a harmful event, with a low probability of occurrence but serious consequences expected in the event of its occurrence, in particular due to the occurrence of a disproportionate collapse, and both SL a state of damage local to the structure, induced by H. Identify with C the disproportionate collapse caused by SL. The basic mathematical model for assessing the probability of collapse is the following equation:

$$P[C] = P[C|SL] \cdot P[SL|H] \cdot P[H] \quad (1.2)$$

where:

- $P[C]$ represents the annual probability of structural collapse C due to event H , related to the "collapse resistance" of the system;
- $P[H]$ is the probability of occurrence of event H , assumed to be equal to the average annual rate of occurrence λH ;
- $P[SL|H]$ represents the conditional probability of local damage, given H ;
- $P[C|SL]$ represents the conditional probability of disproportionate collapse given the local damage state SL .

$P[C|SL]$ defines the robustness of the structure and is the only term on which a structural civil engineer can really act, in order to reduce it; its evaluation in probabilistic terms, can be complex, requiring, strictly speaking, the use of advanced analysis methodologies, such as nonlinear dynamic analysis, performed on models detailed and realistic numbers.

1.3.3 Different scenarios

A considerable amount of data is required to obtain a credible metric for calculating the yearly occurrence probability of an event ($P[H]$). When unusual occurrences occur, such as terrorist attacks, calculating the occurrence frequency is difficult, thus a new technique, a deterministic one, characterized as risk

analysis based on a scenario S , is required. The equation is as follows:

$$P[C|S] = P[C|SL] \cdot P[SL|H] \quad (1.3)$$

1.4 Reduction of the risk

The design for the reduction of the risk of disproportionate collapse turns out to be different from the traditional one, in fact it is necessary to consider the occurrence of extreme events, whose probability is extremely low, during the nominal life of the structure.

Risk reduction can be implemented through a few steps:

- definition of requirements or performance in the presence of risk scenarios;
- calculation of the probability of non-compliance with the requirements;
- assessment of the consequences of any failure to meet the requirements.

Among the requirements that the structure must possess, there are some of a general nature, valid for any structural type, and others that are instead related to the intended use of the construction.

Different design approaches can be identified to mitigate the risk of disproportionate collapse; among the various classifications we find that between direct and indirect method:

- indirect design method: the goal is to reach an alternative equilibrium configuration through catenary action, which means the development of large deformation so that loads are mainly taken by vertical components of axial forces that develop in the beams, these components are indeed the catenary forces. Of course, to be this phenomenon efficient, the structural element should have enough ductility. This aspect is clearly explained in the

Figure 1.1:

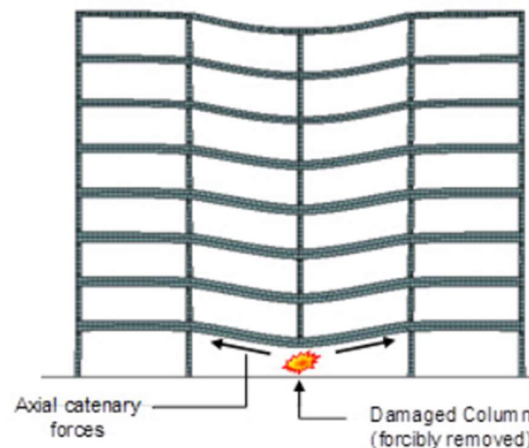


Figure 1.1: Damaged building's formation of catenary activity
(<http://www-personal.umich.edu/eltawil/catenary-action.html>)

To do this, the engineer should create three-dimensional tie systems such as corner, peripheral, and interior ties in both orthogonal slab directions, horizontal

connections between columns or walls, and vertical ties. Figure 1.2 depicts these mechanisms:

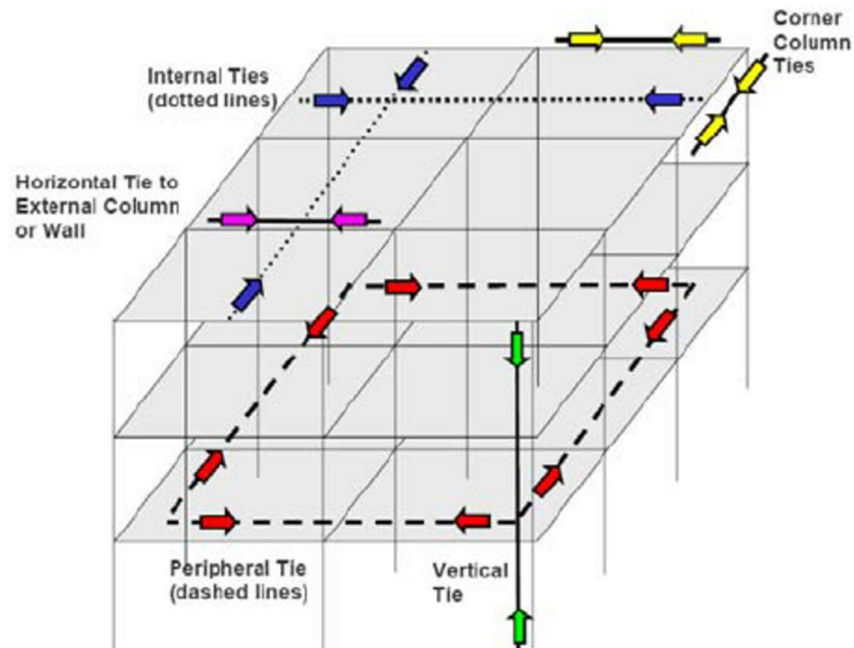


Figure 1.2: Tie forces (DoD 2016 [16])

- in the direct design method, the designer explicitly evaluates the capacity of the structure with regard to the evolution of disproportionate collapses, and can identify a structural solution capable of not collapsing completely even in the event of failure of a single membratura. An example would be the design of the structure so that it is able to continue to transfer loads following an alternative path following the removal of a structural element (Figure 1.3):

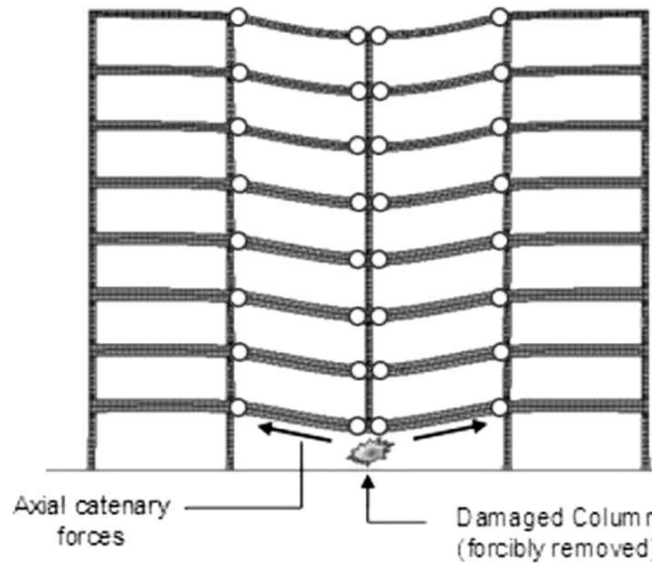


Figure 1.3: Column is removed, and the resulting catenary effect(CNR, 2018)

1.4.1 Analysis of the consequences

The systematic procedure for describing and/or calculating the consequences is called consequence analysis. The consequences are generally multidimensional, however, in specific cases can be described in a simplified way with a limited number of elements such as, for example, human deaths, damage to property, the environment and costs due to the unavailability of a structure.

The analysis of the consequences should begin with a technical and functional description of the system under consideration: the type of structure, its intended use, the planned activities, the number of people affected by a possible collapse, the strategic role of the building, government activities, medical services, etc.

Some consequences are independent of structural behavior. For example, many people may die or be injured by a fire in a building due to the effects of smoke and radiation. In such a case, where there is a time frame from the beginning of the danger to the perception of its effects, human lives can be saved by providing adequate alarm systems and adequate escape routes. There are ample models for calculating the probability of survival of people exposed during such events.

If the structural response is important, it is necessary to distinguish between

the direct response of the exposed elements and the subsequent behavior of the rest of the structure. If the direct response of a structural element is inadequate, then that element is considered vulnerable. If the failure of vulnerable elements is followed by inadequate behavior of the remaining part of the structure, this structure is defined as not very robust. Both the evaluation of direct and indirect results may require rather advanced structural analyses that consider, for example, nonlinear effects, dynamic effects and temperature effects.

1.4.2 Possible strategies to reduce risk

To mitigate the risk associated with an unintentional occurrence, non-structural methods for controlling the accidental action or structural measures to analyse the local damage and its progression may be implemented. Figure 1.4 depicts the technique to be used to decrease risk using the approaches provided in this sub-chapter:

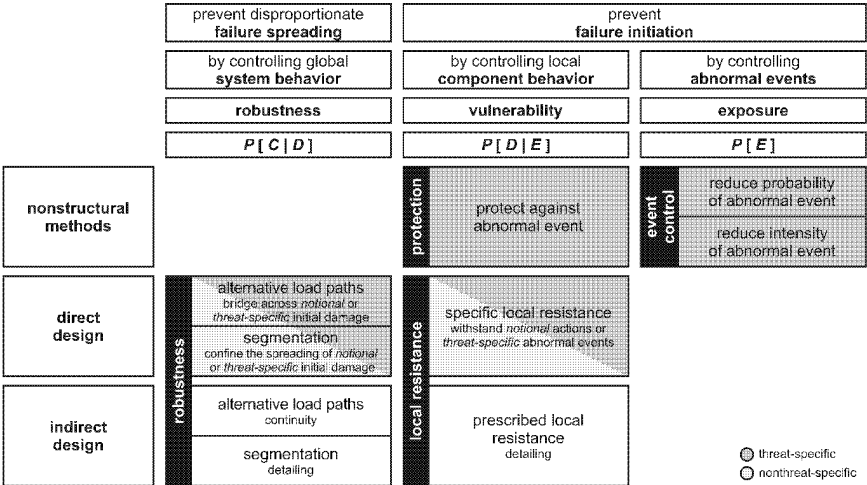


Figure 1.4: Technique used to decrease risk

1.5 Robustness design

A proper understanding of the structure may help to reduce the danger of disproportionate collapse. The following factors contribute to minimizing year propagation and increasing total structural strength: redundancy, chaining, ductility, uniform distribution of structural parts, appropriate resistance to tangential tensions, and the capacity to resist reversal of actions and stresses.

Below are briefly illustrated the indications given in chapters 5 and 6 of the *Instructions for the assessment of the robustness of buildings* (CNR, 2018).

1.5.1 Design approaches

In terms of structural strength, there are basically three methods to use in the design:

- The **local resistance method** aims to prevent the triggering of a possible disproportionate collapse, and thus to avoid local damage to those elements whose collapse would lead to an uncontrolled propagation of the damage (key elements). It is often utilized in the presence of structural typologies in which an alternative channel of the loads is difficult to be developed and therefore, as a result, they are more vulnerable to local damage than others; they are often structures with a low degree of redundancy, such as in the presence of a transfer plane (Figure 1.5), where the loss of a column is unlikely to result in a disproportionate collapse given the huge light.

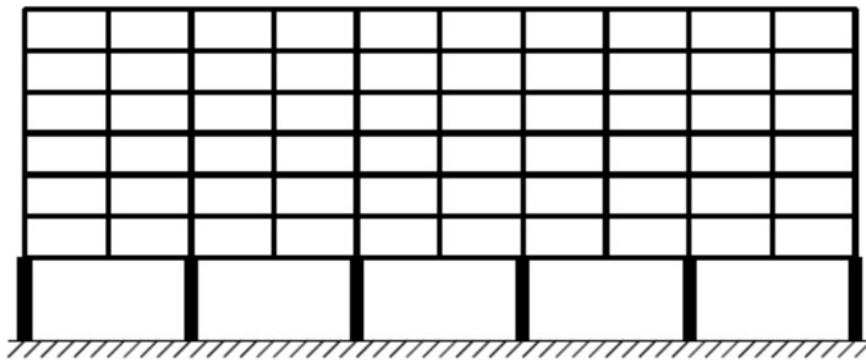


Figure 1.5: Building with transfer plan (CNR, 2018)

The key element is designed to resist previously identified threats through one of the following alternative modes: individually, i.e., without recalling the contribution of other structural elements, or by recalling the contribution of other structural elements participating in the same resistant mechanism.

To limit the possibility of disproportionate collapse, various steps should be implemented, such making the transfer beams continuous on several supports and encouraging an alternate path between the transfer beams through the warps perpendicular to them.

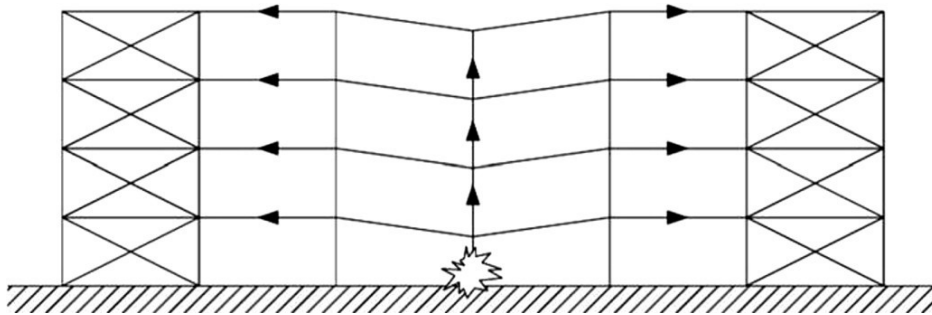


Figure 1.6: : Example of alternative load path (CNR, 2018)

- **The alternative load path approach** is designed to avoid the structure from collapsing disproportionately after a local collapse has occurred, and to shift the loads carried by the collapsed part to the remaining components (Figure 1.6). Usually, the designer removes a structural piece (typically a column) and does non-linear static or non-linear dynamic assessments to ensure that the remainder of the structure is still capable of transferring the unintended loading actions.

Alternative load routes may be created into structural systems with ductility, structural regularity, redundancy, and dissipative capacity more simply. This reduces the likelihood of a catastrophic collapse. As can be seen, then, there is a high degree of connection between this technique and the seismic design standards.

-By separating the collapsed piece of the building from the remaining structure, **compartmentalization** aims to reduce the amount of excessive collapse. The compartment's margins are produced by "strong" components that prevent the collapse of the compartment's "weak" elements, or vice versa, by weak elements that collapse by separating the injured portion from the remainder of the structure, which thus stays intact (structural fuses).

1.5.2 Structural modelling

The capacity to absorb and disperse energy after the creation of localised damage is directly related to the constitutive laws selected for the materials that make up the structural components and their connections, thus the sensitivity and expertise of the designers play a crucial part in the choice and calibration of the most appropriate constitutive laws to use. Structural modelling takes a basic relevance in the design for robustness.

In terms of constitutive laws and modelling, the following factors should be considered while performing structural analyses:

- Elastic-linear constitutive models. By a wide margin, the linear elastic constituent models are the simplest to use and comprehend; they are particularly helpful in the first investigation stages, when the non-linearities of the material are often neglected. While their simplicity is a benefit, it makes them inappropriate for the investigation of complicated processes such as disproportionate collapse.

- Nonlinear component models that are dependent/independent of load application speed. The broad study of disproportionate collapse entails the beginning of structural deformations that result in the development of inelastic deformations. The plasticization of the material contributes significantly to the process of energy dissipation and the redistribution of actions; thus, it cannot be disregarded in the studies. In the non-linear behaviour of traditionally utilised materials (concrete, steel, composite materials, masonry, etc.), the constitutive law is influenced by the rate of load application, particularly when the action is performed rapidly (for example in the case of explosion or impact of high-speed vehicles). This factor contributes to an increase in the strength and/or stiffness of the materials, which may be included into the evaluation of strength.

- Local models / global models:. Typically, it is acceptable to develop both global and local models. The former are used to collect general information, such as the trend of stress and displacement characteristics across the structure, while the latter are required to examine the behaviour in specific sections (zones of discontinuity, points of application of the load, zones of concentration of efforts, nodes, connections, etc ...).

1.5.3 Analysis types

Local damage or loss of an element might result in a quick transition from the original configuration to the damaged one, causing dynamic effects that can be accounted for in a variety of ways depending on the kind of analysis used.

- Linear static analyses can be used to amplify the effects using an appropriate dynamic amplification coefficient; however, linear analysis does not allow for the recording of important effects such as the

redistribution of stresses, geometric and mechanical non-linearities, and therefore the catenary effect;

- Nonlinear static analyses allow for the incorporation of nonlinearities and the accurate capture of the catenary effect;
- Linear dynamic studies allow for the consideration of the dynamic impacts associated with local damage/collapse, but do not provide the evaluation of the consequences associated with the non-linearity of the issue.
- To model the problem, dynamic-nonlinear studies are the most comprehensive and appropriate sort of study. Typically, the computation is conducted using three-dimensional, nonlinear models, under circumstances of substantial deformations, and taking the behaviour during the transitional period into consideration. However, not all calculating programmes can do this sort of analysis. Due to the complexity and large number of factors involved, only experienced designers can do this sort of study. The computational effort that these models impose must also be considered, particularly in the case of massive structures.

1.5.4 Reinforced concrete structures placed into use

Reinforced concrete constructions cast on-site have a number of helpful characteristics in terms of their response to exceptional and/or extreme events:

- structural continuity (and the resulting redundancy);
- ductile behaviour of sections and members subject to bending;
- columns that are not susceptible to instability;
- the high mass of the structure increases its response to explosions.

On the other hand, the mass of the structure can make it difficult to distribute loads because the force that must be transmitted along an alternative path is high; fragile resisting mechanisms (such as cutting, twisting, anchoring, and overlapping of the reinforcements) can prevent the development of ductile mechanisms, so it is necessary to use a design approach based on the hierarchy of resistances in a way that is similar to the design metonymy.

Membrane effects is a significantly contribute to the structural strength definition of reinforced concrete components such as beams and slabs. In order to

prevent overly pessimistic reinforcing methods (for existing structures) or design (for new structures), it is necessary to account for the strength reserves caused by membrane stresses when calculating structural strength.

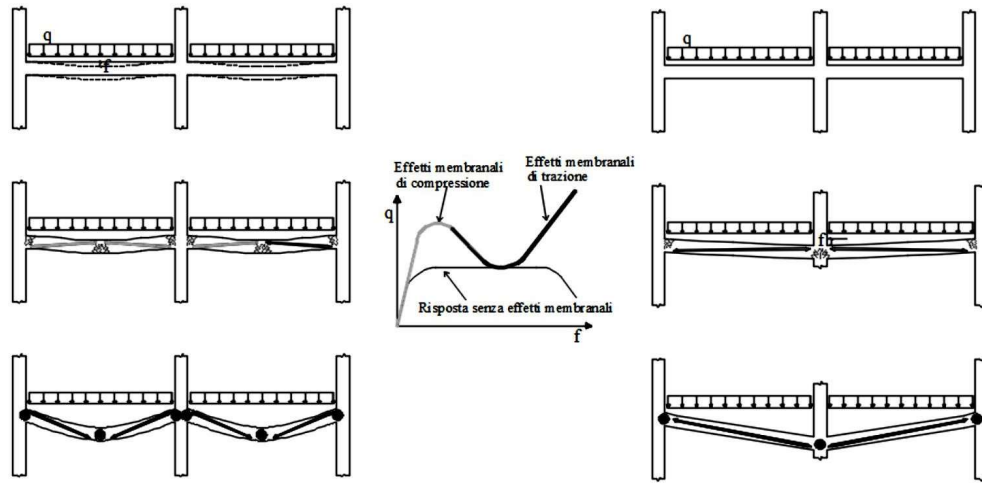


Figure 1.7: Membrane stresses in structural elements (CNR, 2018)

Figure 1.7 demonstrates that the advantageous impact of membrane stresses may be employed not only during an unplanned occurrence such as the removal of a column, but also during the application of loads exceeding those anticipated during the structure's design phase.

In the case of low loads, membranous compressive stresses are activated at low deformation values, however in the case of high loads, diaphragm compressive stresses are insignificant and tensile stresses considerably contribute to the resistance of deflected parts.

The membranous tensile stresses are not considerably dependent on the deformations of the concrete, but they are strongly dependent on the final deformations possible of reinforcing bars and the geometric reinforcement ratios.

The value of the membranous stresses depends significantly on the constraint conditions: the interlocking condition defines the upper limit of the value of the membranous stresses, which are decreased by reducing the stiffness of the external constraint without ever being completely depleted because the membrane efforts are also present in elements without constraints to lateral displacements due to structural continuity.

1.5.4.1 Column removal - Structural behaviour

A two-dimensional frame experiment may be used to illustrate the structural behaviour of a reinforced concrete structure subjected to column removal

A vertical displacement is imposed at the point P1 where the column was removed, and it may be monitored as a function of the response at point P1 (Figure 1.9) and the horizontal displacement at point P2 (Figure 1.10).

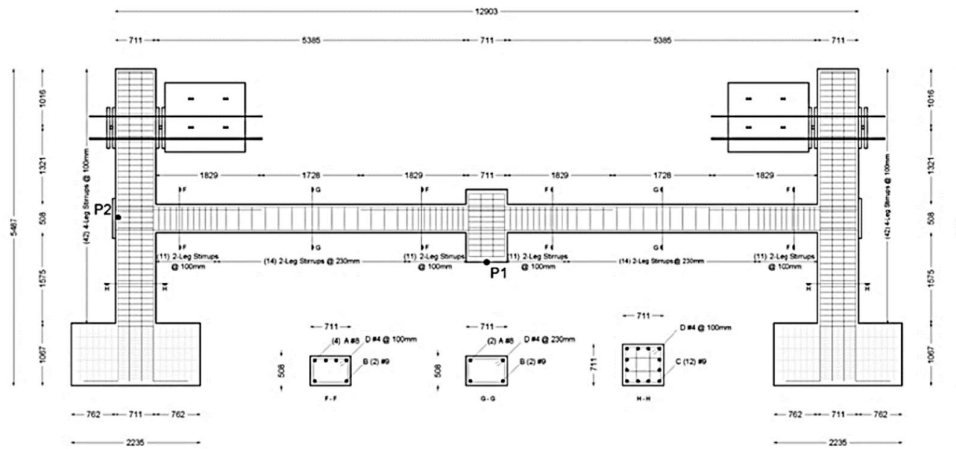


Figure 1.8: Two-dimensional reinforced concrete frame (Lew et al. [19])

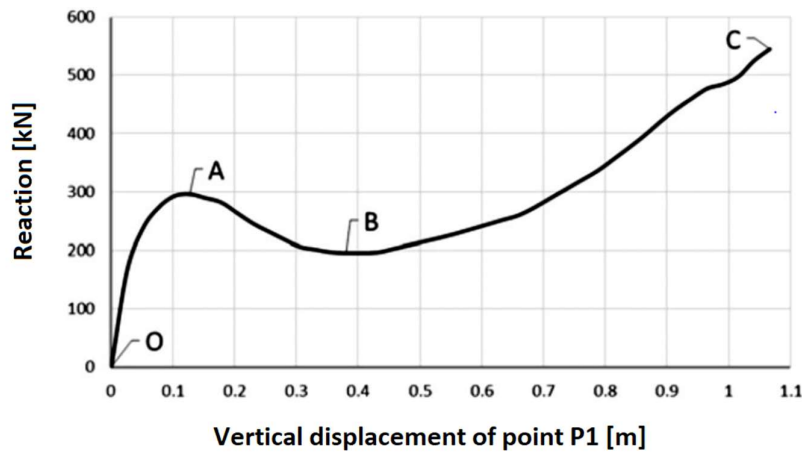


Figure 1.9: Diagram of imposed displacement-reaction (CNR-DT 214 2018)

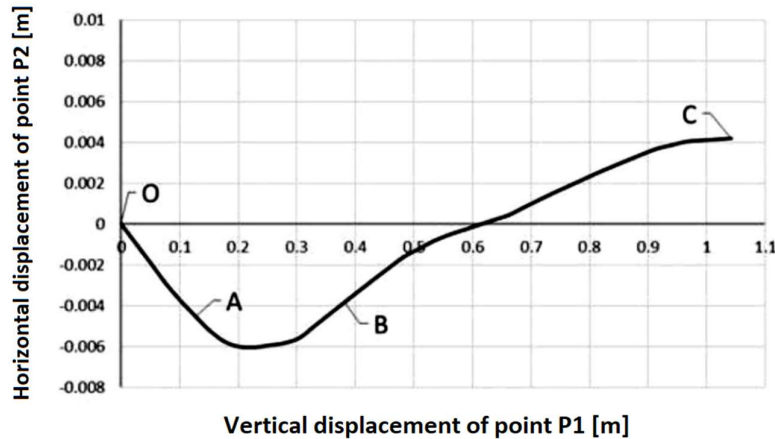


Figure 1.10: Diagram of imposed displacement-horizontal displacement (CNR-DT 214 2018)

The structural behaviour is explicable by examining three distinct phases:

- Line OA (flexural behaviour): it relies on the bending behaviour of the beam and persists with the development of plastic hinges at the beam-column connection sites (negative plastic moment in correspondence of the lateral columns and positive plastic moment at the central column). As a result of the beam's fissuration and subsequent elongation, the point P2 is shifted towards the beam's exterior (negative value). In addition, the beam is squeezed due to the column's rigidity, which resists the beam's elongation.

- Line AB (softening): marked by a softening phase and, therefore, a decrease in the response at point P1. The negative horizontal displacement starts to decrease. Additionally, compressing action is reduced.

- Line BC (catenary effect): the response rises again as the vertical displacement at point P1 increases. The horizontal displacement becomes positive (so the outer columns slide inward) and the beam is now under stress. This is the result of a combination of membrane tensional effects and reinforcing bar catenary effects.

Notably, if the reinforcement does not extend over the exterior columns, softening is not possible and only the flexural behaviour of the beam carries the load. This suggests that the process is stopped at point A, when the building collapses.

1.5.4.2 Column removal - Design

With appropriate simplifying hypotheses, it is possible to estimate the bearing capacity of a framed system in the event of an accidental removal of a supporting pillar.

The maximum load for purely flexural behaviour (point A of Figure 12) can be calculated with the theory of plasticity and with the principle of virtual works with the following formula:

$$P_{MAX,FL} = \frac{2(M_{PL}^+ + M_{PL}^-)}{L} \quad (1.4)$$

where M_{PL}^+ and M_{PL}^- are the plastic moment of the beam in correspondence of the connections with the column for positive moment and negative moment respectively.

Neglecting the armor in the compressed zone, in favor of safety, the plastic moments can be calculated in a simplified way as follows:

$$M_{PL}^+ = 0.9A_s^+ f_y d \quad (1.5)$$

$$M_{PL}^- = 0.9A_s^- f_y d \quad (1.6)$$

Where A_s^- and A_s^+ are the tense armatures of the beam at the connection with the column, respectively for positive moment and negative moment, d is the useful height of the beam, f_y is the yield strength of calculation of the reinforcement obtained by applying the relevant safety coefficients for accidental verification.

With regard to the catenary behavior (point B of Figure 12), the maximum or bearable load can be evaluated as:

$$P_{MAX,CAT} = 2 \frac{\delta}{L} A_{s,cont} f_t = 2\theta_u^- A_{s,cont} f_t \quad (1.7)$$

where δ is the displacement capacity of the point where the column was removed, $A_{s,cont}$ is the continuous reinforcement on the beam length 2L and f_t is the breaking tension of the reinforcement obtained by applying the safety coefficients relevant to the accidental verification.

For the evaluation of the rotation capacity and the following δ value, reference

should be made to experimental values.

It is critical to emphasise that the catenary effect is only advantageous if the load that generates can be absorbed by the component of the structure that is not directly affected by the damage. Therefore, emphasis must be paid to the crucial columns, such as the corner and perimeter ones. The catenary effect is only advantageous if it results in an effective increase in the load's resistance, so if $P_{MAX,CAT} \geq P_{MAX,FL}$.

Probabilistic and semi-probabilistic quantification of the robustness

Code regulations and standards do not account for a sufficient number of activities or circumstances that represent a risk to the safety and performance of a structural system, assuming the state of the art. This has required the consideration of hazards that were not previously analysed or addressed using a deemed-to-satisfy technique, i.e. a checklist of the event rather than real structural computation design.

Many events can be more or less hazardous depending on the target risk considered; for instance, an explosion can have a low hazard and thus a low impact on the risk evaluation if the target probability of collapse $P(C)$ is $10(-5)$ per year, but it can have a greater impact if the target is $10(-7)$ per year.

In addition, the risk assessment based on a 1-year time scale might have distinct effects on exposures whether the time period is 50 or 100 years. This has required the evaluation, within the design methods, of just those occurrences with a likelihood of collapse above a minimal threshold.

In addition, the risk assessment based on a 1-year time scale might have distinct effects on exposures whether the time period is 50 or 100 years. This has required the evaluation, within the design methods, of just those occurrences with a likelihood of collapse above a minimal threshold.

The assessment of the conditional probabilities stated in previous equation may be performed using a Probabilistic Risk Analysis (PRA), which, in the context of structural systems, can be seen as a Structural Reliability Analysis. According to this theory, failure occurs when the demand S (intended as the

actions' consequences) surpasses the resistance R . The failure probability can be thus be expressed by:

$$P_f = \int F_R(x) \cdot f_S(x) dx \quad (1.8)$$

, where $F_R(x)$ represents the cumulative distribution function of the resistance and $f_S(x)$ represents the probability density function of the demand.

When working with the particular occurrence of a collapse whose repercussions might decide life lost, it is feasible to specify the following target:

$$P(C) \leq p_{th} \quad (1.9)$$

where p_{th} is the *de minimis* risk, which is often between 10^{-5} and 10^{-7} , following Pate-Cornell [14].

For the particular instance of the alternative load route design approach, the probability of collapse as given by Equation (1.2) is reduced to the quantification of $P(C|SL)$ and may be assessed using the convolution integral of Equation (1.8).

Consequently, according to the equation (1.9), the likelihood of collapse may be stated as follows:

$$P(C|SL) \leq p_{th}/\lambda_H \quad (1.10)$$

Assuming that the hazard probability λ_H is between $10^{-6}/yr$ and $10^{-7}/yr$, the performance requirement described in (1.13) for the chance of collapse due to local damage is on the order of $10^{-2}/yr$ to $10^{-1}/yr$. This suggests that the reliability index β - additional information will follow concerning its calculation – is of the order of 1.5. This value is much lower with regard to the one anticipated for the final state of new structures, typical usage conditions, that is equal to 3.8, equivalent to a risk of failure of $10^{-4}/year$.

Referring to a *de minimis* risk, which involves an event with an annual occurrence probability of less than $10^{-7}/yr$, this probability becomes on the order of $5 \cdot 10^{-6}/50yr$ when a 50-year-old structure is considered. Since the reliability index for a class 2 building with a theoretical life of 50 years is 3.8, which translates to a $P(C)$ of $7.3 \cdot 10^{-5}/50yr$, the $P(C|SL)$ should be less than $6.9 \cdot 10^{-2}/50yr$ to meet the *de minimis* requirement.

2 Structural Reliability

There is always a degree of unpredictability surrounding natural physical events (and by consequence, structural engineering). This implies that these events are, at least in theory, not completely predictable. The following easy case may be considered: Several "similar" concrete cube specimens are loaded to failure in the lab. For each specimen, the compression failure load would be unique. As a result, these concrete cubes' compressive resistance is a completely arbitrary number (i.e. random variable). In structural engineering, it is common practice to treat all significant factors in the design and evaluation of new and existing structures as uncertain and, thus, as random variables. When discussing risks, the word "reliability" is typically used extremely loosely and has to be defined more precisely. The idea of reliability, at its most basic level, is often taken to be an inviolable characteristic of the building itself. Then, if the structure is reliable, it will never fail, and if it turns out to be unreliable, it will fail without a doubt. As an added bonus, when people hear the phrase "the structure is reliable," they often interpret it to mean that there is zero chance of the structure ever failing. This is an oversimplification that is regrettably both exaggerated and incorrect. The imagined "100% reliability" for structures simply does not exist, and although this may be uncomfortable (or intolerable) for "non-expert" individuals, it is the reality. Despite of assurances to the contrary, even the most "reliable" of structures is subject to the possibility of failure. The field of structural engineering requires the tolerance of a minor failure probability within the expected service life of the structure. Without them, it would be impossible to evaluate current infrastructure or build new civil constructions.

This chapter introduces the limit states approach to structural reliability and explains many types of uncertainty. Methods for assessing structural reliability are listed and Level III is differentiated into its base components. Finally, the most popular safety formats that have been adapted from recent structural codes and standards are outlined and discussed.

2.1 Limit states design, basic principles and uncertainties

International standards like *ISO 2394*, *EN 1990*, and *fib Model Code 2010* report on the fundamentals of *structural reliability*.

Fundamental performance standards for structures should be tied to reliability and economy principles, as stated in the aforementioned regulations. In particular, a building has to be designed and built such that it can withstand every possible action it may get. All of these conditions need to be met with sufficient reliability and cost - effectiveness.

During its service life, a structure's reliability is measured by how well it performs in accordance with specified loading conditions. The chance of a structure failing may be thought of as the quantitative counterpart of the reliability. A structure's service life (sometimes called its design working life for new structures) is the time span throughout which it is expected to serve its intended purpose. Safety, serviceability, durability, and robustness are the primary performance objectives for structural design.

These so-called limit states are identified in order to test these criteria in relation to certain design scenarios. The generic limit state is described as " *the condition beyond which the structure, or a part of it, does no longer satisfy one of its performance requirements* " in the literature and structural codes (e.g. *EN 1990*; *fib Model Code 2010*).

With respect to the aforementioned performance criteria, there are many limit states to choose from:

- *ultimate limit states (ULS)*, are typical situations related with collapse or approaching to structural breakdown. These states are concerned with the safety of people and/or the building. They are as follows: fracture or excessive deformation in important areas of the structural system or within connections; fatigue and time dependent events; instability, divergence of equilibrium; loss of static equilibrium of the structural system or part of it (e.g. buckling, lateral buckling, aero-elastic instability).
- *serviceability limit states (SLS)*, are thresholds beyond which certain factors, such a structure's effectiveness for a certain purpose, become

unacceptable. Damage that affects the appearance, durability, and functionality of the structure; vibrations that affect the comfort of users or limit the functional performance of the structure; and deformations or bending that influence the structure's appearance or cause unacceptable damage to finishes or non-structural elements.

Various structures with different degrees of reliability based on the expected service life should handle these limit states in different ways.

2.1.1 Uncertainties and their classification

It is important to take into consideration a number of potential uncertainties in the procedure designed to assess the structural reliability of new or existing buildings. These doubts may come in many forms:

- *randomness* (or *inherent variability*): it is a measure of the inherent variation included in every physical process or property. Because it is an inherent feature of the physical process or property itself, randomness cannot be controlled or mitigated by human action;
- *model uncertainty*: it refers to the uncertainty that arises as a result of the idealization of mathematical models that are used in order to explain and make predictions about a physical process or characteristic. Therefore, the uncertainty associated with models is due to a combination of ignorance, inherent simplifications, and decisions made throughout the process of defining mathematical models that are intended to explain the actual world. It is possible to bring it down by widening the level of detail and working to improve the models' overall quality.
- *statistical uncertainty*: This form of uncertainty is associated with the method through which the unpredictability of a physical process or attribute is estimated. This is because statistical analyses rely on a small sample of observations, a problem that might be solved by collecting more real-world information (conducting more experiments).
- *measurement error*: is the mistake introduced by the act of measuring or watching the data used to estimate the randomness (and for data methods). It is possible to decrease measurement mistakes by enhancing observation or measuring methods;

- *human errors*: are caused by human mistake in the form of imperfections in the design or evaluation phase. This kind of uncertainty is particularly challenging to evaluate, but it may be mitigated by tightening controls across the whole process.

The reliability analysis of a structural system is influenced by several sources of uncertainty on multiple scales.

If the randomness (i.e. intrinsic variability) of a physical process or characteristic is assumed to be non-negligible, then other sources of uncertainty, such as the quality of tests, measuring methods, and forecasting models, may be decreased. This conclusion often prompts scientists to differentiate between aleatory and epistemic uncertainty in the scientific literature.

When it comes to structural reliability analysis, there are two types of uncertainties: aleatory and epistemic. Aleatory uncertainties relate to the inherent randomness of the variables that govern a specific structural problem, while epistemic uncertainties are primarily related to the "lack of knowledge" in the definition of the structural model. The overall amount of uncertainty in reliability analysis is affected by the decisions made in the beginning. However, this does not imply that simpler models have a higher degree of uncertainty than more complex ones. When comparing highly detailed and complicated non-linear structural models to their simpler counterparts, it is possible that the former will result in more epistemic uncertainty. Different approaches to the same issue may emerge if many feasible modelling hypotheses are at your disposal. Because of this, simpler models are sometimes preferable.

2.1.1.1 Aleatory uncertainties for resistance models

One significant category of factors that affects a structure's reliability is its material properties. Characteristic values, which are nothing more than fractiles of suitable distributions, are used to represent material attributes in design computations.

The JCSS Probabilistic Model Code [3] is used in the following to provide a probabilistic modelling of resistance models in reinforced concrete structures.

Concrete

Compressive strength f_{co} of standard test specimens (cylinder of 300 mm height and 150 mm diameters) measured under normal circumstances and at age 28 days is the concrete's standard property. The following assumptions are made about the distribution of this variable:

- mean value f_{cm} , obtained from testing or code prescription is assumed to be equal to the expected value.
- coefficient of variation V_c equal to 0.15

The other material's variables can be evaluated indirectly

Reinforcement

The yield strength f_y , the ultimate tensile strength f_u , the modulus of elasticity E_s , and the ultimate strain ε_u , are the reference characteristics of structural steel. For the purpose of simplicity, we will merely provide the yield strength distribution. The following assumptions are made about the distribution of this variable:

- mean value f_{ym} determined from testing or code prescription is assumed to be equal to the prescribed value.
- coefficient of variation V_y equal to 0.05

2.1.1.2 Epistemic uncertainties for resistance models

Material models' epistemic uncertainty should be considered together with their aleatory ones. In reality, there is always some degree of uncertainty involved when attempting to represent a material's behaviour through a model, whether that model is physical, semi-empirical, or empirical, because of the simplified assumptions inherent in their definitions or the omission of some parameters that could have been crucial.

The JCSS Probabilistic Model Code [3] has provided a method for quantifying epistemic model uncertainties associated with resistance, but in the initial phase you have to take into account that:

- All of the test parameters and resistance calculation information must be available in the database of experimental observations.

- the bounds of the resistance model are determined by the range of parameters in the set of experimental data.
- In order to perform a goodness-of-fit test, statistical inference for the observed sample must be calculated.

It is possible to represent model uncertainties through the following expression:

$$R(X, Y) \approx \vartheta \cdot R_{Model}(X) \quad (2.1)$$

where:

- $R(X, Y)$ is the actual response of a structure in general
- ϑ is the model uncertainty random variable, due to factors affecting test
- $R_{Model}(X)$ is the response (or the resistance) estimated by the model
- X is a vector of basic variables considered in the resistance model
- Y is a vector of variables that are not considered in the model but may affect the resistance mechanism.

Probabilistic distributions and associated parameters for modelling uncertainty may be defined by statistical inference.

Model uncertainty random variable ϑ follows a lognormal distribution, as specified by the JCSS Probabilistic Model Code [3].

1.1.2 General formulation of the structural reliability problem

When looking at reliability quantitatively, it may be seen as the complement to 1 of the probability of failure P_f . There must be a thorough discussion of how to determine the failure's importance in light of the performance criteria.

Defining the "measure" capable of quantifying the available degree of reliability and providing the mathematical idealization of the limit states conditions is a necessary step in the process of estimating the reliability of a structural system.

2.1.2 Probability of failure

To characterize the behaviour of the structure, a collection of N *basic random variables* X_i is used in reliability analysis:

$$X_i = [X_1, X_2, \dots, X_i, \dots, X_N] \quad (2.2)$$

where the variable X_i may be represented by *material properties*, *actions* (loads), *geometrical properties* and *model uncertainties* (both for actions and resistances).

To define P_f we also to talk about *limit state function* Z (also denoted as *performance function*) which, in general, is defined in the following form as a function of main random variables X_i :

$$Z(X) = g(X_i) = 0 \quad (2.2)$$

The *limit state function* Z is defined, according to Figure 2.1, so that:

$$\begin{cases} Z \geq 0 \rightarrow \text{safe region} \\ Z < 0 \rightarrow \text{failure region} \end{cases}$$

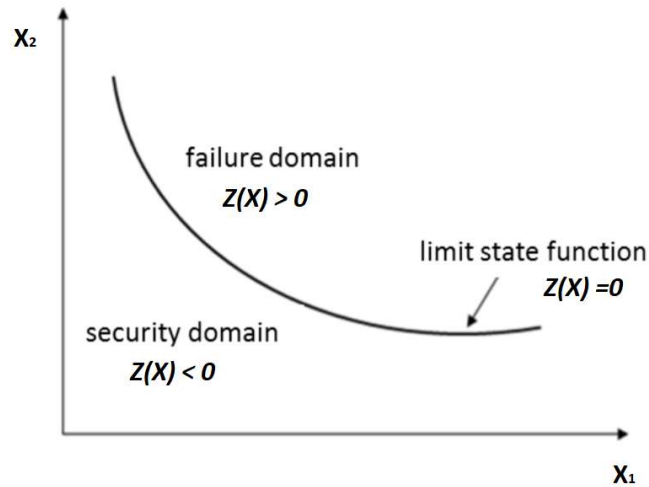


Figure 2.1: Limit state domain with X_1 and X_2 as two random variables.

Using this definition as a starting point, the probability of failure, or P_f , may be determined as follows:

$$P_f = P\{Z(X) < 0\} \quad (2.3)$$

In particular, the probability of failure P_f may be written as an integral by defining the N-dimensional probability density function of the N fundamental variables X as $f_x(x)$:

$$P_f = \int_{Z < 0} f_x(x) dx \quad (2.4)$$

P_f , on the other hand, may be used to calculate the *probability of survival* P_s :

$$P_s = 1 - P_f \quad (2.5)$$

It is also important to note that while estimating the probability of failure P_f , a specified reference period is taken into account, often the design or residual service life, depending on whether we are working with new or old structures.

2.1.3 Reliability index assessment

The reliability index, which may be formalized as the negative value of the inverse of the standard normal variable representing the probability of failure P_f , is another way to quantify the structural reliability.

Mathematically is expressed as:

$$\beta = -\Phi^{-1}(P_f) \quad (2.6)$$

where the quantity Φ^{-1} represents the inverse standardized normal distribution function.

Figure 2.2 shows the numerical relationship between the *reliability index* and the *probability of failure*.

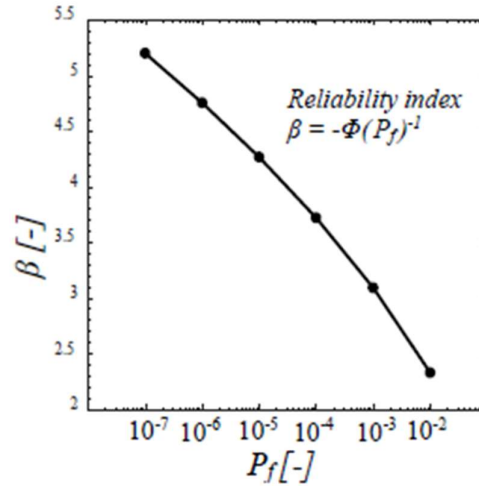


Figure 2.2: Relationship between the probability of failure P_f and reliability index β .

As can be seen, the higher the reliability index, the more reliable the structure is, and therefore the lower the failure probability P_f and the less probable it is to surpass a defined limit state.

2.2 Methods of reliability and theoretical model

Simplified methods or more accurate estimates of the *probability of failure* P_f may be used to quantify structural reliability. The former aim to make reliability considerations more applicable in engineering practice while decreasing the computing work required.

In general, *reliability approaches* are grouped into four levels:

- *level III methods* (probabilistic);
- *level II methods* (probabilistic);
- *level I methods* (semi-probabilistic);
- *level 0 methods* (deterministic).

Probability theory implementation and computing effort for structural reliability estimation both reduce drastically from level III to level 0 approaches.

2.2.1 Methods of Level III

Adopting level III approaches for evaluating structural reliability necessitates an integral expression like Eq.2.5 to precisely calculate the probability of failure P_f (or reliability index β).

Analytical methods, numerical integration, and Monte Carlo simulation are all viable alternatives.

Analytical solutions can only be used in a minority of simple situations, while numerical integration is most practical with a reduced set of variables. The integral given by Eq. 2.5 may therefore be efficiently solved using simulations methods like the Monte Carlo's approach, which are particularly useful when dealing with complicated systems.

The Monte Carlo method and several simplified sampling approaches are outlined here (i.e. Latin Hypercube sampling).

The latter is the method I'll adopt to sample resistance and action basic variables.

2.2.1.1 Monte Carlo's method and sampling techniques

This technique is used to assess the risk or reliability of complex engineering systems (Haldar and Mahadevan [23]).

The following is a summary of the six main components that compose the Monte Carlo simulation method:

- 1) Define all the random variables involved
- 2) Define the probabilistic characteristics of all the random variables in terms of probabilistic distribution and corresponding parameters
- 3) Generate the values of these random variables
- 4) Perform numerical experimentation, which means to evaluate the problem deterministically for each set of realizations of all the random variables
- 5) Extract probabilistic information from these N realizations
- 6) Determine the accuracy and efficiency of the simulation (not explained in this paper)

In the following, this method will be applied in the specific case of computing the failure probability P_f . First of all, according to Eq. **Errore. L'origine riferimento non è stata trovata.**, the probability of failure can be expressed as:

This approach will be used to compute the failure probability P_f that may be represented using:

$$P_f = \int_{g(X_i) < 0} f_{X_i}(x_i) dx_i = \int_{-\infty}^{+\infty} I[g(X_i)] f_{X_i}(x_i) dx_i \quad i = 1, 2, \dots, N \quad (2.8)$$

where $I[g(X_i)]$ is the indicator function defined as:

$$I[g(X_i)] = \begin{cases} 0 & \text{if } g(X_i) \geq 0 \\ 1 & \text{if } g(X_i) < 0 \end{cases} \quad i = 1, 2, \dots, N \quad (2.9)$$

As already mentioned, in order to evaluate if the single realization of the random variables X_i belongs to the safe or to the failure region, it is necessary to define the limit state function. The probability of failure can thus be estimated by the number of samples that gives the structural failure (i.e. for which $g(X_i) < 0$).

As previously indicated, defining the limit state function is required to determine if the single realization of the random variables X_i belongs to the safe or failure zone. The number of samples that produce the structural failure may therefore be used to estimate the probability of failure.

As a result, using n samples, we can estimate the failure probability P_f as:

$$P_f \approx P_f^n = \frac{1}{n} \sum_{j=1}^n I[g(X_i)] \quad i = 1, 2, \dots, N; \quad j = 1, 2, \dots, n \quad (2.10)$$

Several sampling approaches are employed to minimize the computing effort required to execute such a simulation. Common methods of sampling include:

- systematic sampling
- importance sampling
- stratified sampling
- Latin hypercube sampling
- adaptive sampling

- randomization sampling
- conditional expectation

In the following Latin hypercube sampling method (LHS) will be described.

2.2.1.2 Latin hypercube method (LHS)

This thesis demonstrates that the LHS approach is a powerful tool for doing a reliability study using the non-linear finite element technique. In fact, using this technique makes it possible to describe the probabilistic distribution of the structural resistance with less numerical simulations. It has been shown that a sample size of 30–40 is enough for determining the mean, variance, and probability distribution of the examined structural resistance when the coefficient of variation of fundamental variables is less than or equal to 0.2. (Gino, 2019 [22]).

The LHS approach takes samples from the variables according to their probabilistic distribution and then combines them randomly. The method for sampling guarantees that all distribution functions are sampled equally over the range of probabilities (0,1).

The procedure to adopt is the following:

- 1) The probability interval (0,1) is partitioned into n non-overlapping equiprobable sub-intervals (h_{inf}, h_{sup}) for each variable X_i .
- 2) To determine the value of the basic variable X_i , in each of the n intervals, we randomly sample a single value from the interval (h_{inf}, h_{sup}) and we will take the correspondent X_i .
- 3) To generate a random combination of results, we do a random permutation of the n values sampled for each variable X_i . Through this process, we can provide the n sets of input variables that will be used in the simulations.

2.3 Safety formats for reinforced concrete structures

In this Section the basic principles of “levels of approximation approach” are introduced and the different safety formats are commented.

2.3.1 Levels of approximation

The structural analysis is based on representative models, each of which is only a close representation of the real world. It's possible that each model, from the most basic to the most complex, has a varying level of precision when it comes to describing the surrounding world.

To be more specific, a "level of approximation" (LoA) is a design methodology in which the accuracy of an estimation of the response of a structural member or system can be improved by increasing one's knowledge of the involved physical parameters and the complexity of the mathematical model. This can be done in order to achieve a higher level of precision in the estimation of the response.

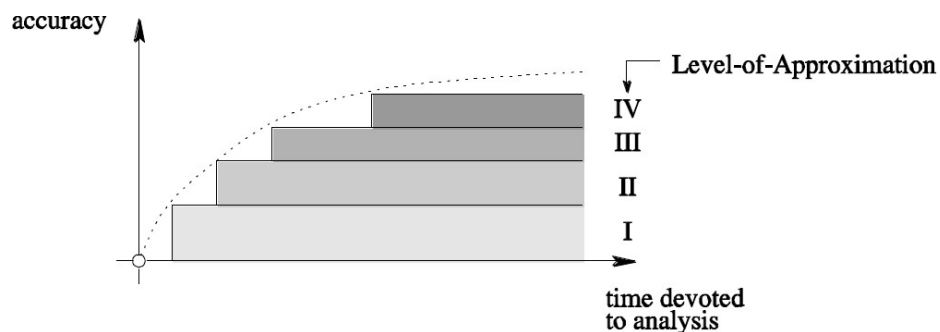


Figure 2.3: The approximation levels approach as outlined by Muttoni and Ruiz, 2012 and fib Model Code 2010.

Once selected the LoA related to the representative model of structural response, the reliability concepts should be introduced by appropriate *safety formats*.

It is up to the designer as well as the practitioners to decide on an appropriate LoA. It is dependent on the sort of analysis that is carried out, the level of the design or evaluation process that is being conducted (either preliminary or executive), and the possible savings that may be offered if a high LoAs is chosen.

After the LoA, that corresponds to the representative model of structural response, has been chosen, the notions of reliability should next be presented using the adequate *safety formats*.

2.3.2 Probabilistic safety format

Full probabilistic analysis in accordance with the procedures defined by the Level III and Level II approaches is now possible with the fib Model Code 2010. Probabilistic safety format may be used to the evaluation of already-built buildings as well.

Estimating the *probability of failure* P_f during a certain reference period is how a structure is checked for proper functionality in a given limit state.

The equation for safety verification may be written in terms of the *probability of failure* P_f :

$$P_f = P[g(X_i) \leq 0] \leq P_{f,T} \quad i = 1, 2, \dots, N \quad (2.117)$$

where $P_{f,T}$ are the target probability of failure indices provided in Section 1.3.6. To analyse P_f and create the probabilistic model for basic variables X_i , use the approaches provided in Subsection 1.3.

2.3.3 Partial factor format

The partial factor format is specified by the Level I methodology and is supported by fib Model Code 2010 and EN 1990. Partial safety factors are used to apply safety precautions to loads and material resistances.

The partial safety factors can be classified:

- *partial safety factors for material properties*:

$$\gamma_M = \gamma_{Rd} \gamma_m \quad (2.12)$$

$$\gamma_{Rd} = \gamma_{Rd1} \gamma_{Rd2} \quad (2.13)$$

where γ_{Rd1} is the model uncertainty partial safety factor, with values of 1.05 for concrete and 1.025 for reinforcement; γ_{Rd2} is the geometric uncertainty factor, also set to 1.05; and γ_m is the material uncertainty factor, calculated using Eq (1.30). The target of reliability is defined by $\beta = 3.8$ if one assumes a normal distribution for material uncertainties, where γ_M is equal to 1.5 for concrete cylinder compressive strength assuming a coefficient of variation equal to 0.15 and equal to 1.15 for bar

reinforcements accounting for a coefficient of variation equal to 0.05.

- *partial safety factors for permanent actions (G) and variable actions (Q):*

$$\gamma_G = \gamma_{sd} \gamma_g \text{ and } \gamma_Q = \gamma_{sd} \gamma_q \quad (2.14)$$

where γ_{sd} is the model uncertainty partial safety factor set equal to 1.05; $\gamma_{G,Q}$ is the partial safety factor for permanent (G) and variable loads (Q) accounting for aleatory variability and reference service life).

where γ_{sd} is the model uncertainty partial safety factor set to 1.05; $\gamma_{G,Q}$ is the partial safety factor for permanent (G) and variable loads (Q) accounting for aleatory variability and reference service life.

The actions for ULS and SLS are correctly combined, allowing for suitable combination factors, to maximize and minimize their influence on the structural response. The *fib Model Code 2010 and EN 1990* both recognize specific values for partial safety factors for activities.

2.3.4 Global resistance format

Incorporating the uncertainties of the structure's behaviour into a global design resistance, which may be stated as a global safety factor, is beneficial. Once again, these values need to be chosen so as to satisfy the prerequisites of the reliability index.

The structural resistance R is an indicator for the overall resistance. The following resistance values represent the range of possible outcomes:

- R_m mean value of resistance
- R_k characteristic value of resistance (corresponding to a probability of failure of 5%)
- R_d design value of resistance

As for the partial safety factor technique, the value of action F is taken into account.

When these conditions are satisfied, we may say that the safety criterion has been met:

$$F_d \leq R_d, \quad R_d = R_m / \gamma_R^* \gamma_{Rd} \quad (2.15)$$

where F_d represents the partial factor definition of the design external action, γ_R^* stands for the global resistance safety factor that takes material aleatory uncertainties into account, and γ_R^* stands for the resistance model uncertainty safety factor.

Values for the model uncertainty factor that are suggested depend on the precision with which the resistance model was formulated.

- $\gamma_{Rd} = 1.0$ for no uncertainties
- $\gamma_{Rd} = 1.06$ for low uncertainties
- $\gamma_{Rd} = 1.1$ for high uncertainties

Differentiating between global and partial safety factors is essential. Partial safety factors only refer to each material property evaluated with its characteristic value for local verification of structural members [22], while global safety factors refer to the overall structural response evaluated by means of mean values of material properties.

3 Design of a multi-storey reinforced concrete frame in a seismic zone

This work of thesis is about the evaluation of reliability for robustness of a real building designed in seismic area. Following previous works of thesis like “Robustness assessment in reliability terms of reinforced concrete structures in seismic zone” by Elena Miceli, I continued these probabilistic studies by comparing the buildings reaction, in terms of structural reliability of two frames having different design criteria with different steel reinforcements.

Following a description of the building's design characteristics in accordance with code requirements (i.e., capacity design), the frame—the focus of this thesis—is next provided as a consequence of the findings from earlier research.

3.1 General description

The building in question is a reinforced concrete structure used for residential purposes in the city of L'Aquila, which is situated in the seismic zone 2 and has an elevation of 714 metres above sea level. This building was designed in a seismic zone in accordance with Italian and European technical standards.

The following regulatory material has been mentioned:

- D.M. 17 Gennaio 2018: Aggiornamento delle “Norme tecniche per le costruzioni” [9]
- EN1990 Eurocode 0: Basis of structural design [5]
- EN1992 Eurocode 2: Design of concrete structures [28]
- EN1998 Eurocode 8: Design of structures for earthquake resistance [29]
- EN206-1 Concrete - Part1: Specification, performance, production and conformity [30]

The construction is newly built; the nominal life is interpreted as the number of years during which the structure must be able to be utilised for the intended

purpose, provided that it is subject to normal maintenance. The standard specifies three forms of construction in Table 2.4.I of DM2018:

Table 3.1: Forms of construction (Table 2.4.I of DM2018)

TIPI DI COSTRUZIONI		Valori minimi di V_N (anni)
1	Costruzioni temporanee e provvisorie	10
2	Costruzioni con livelli di prestazioni ordinari	50
3	Costruzioni con livelli di prestazioni elevati	100

In the present case, the following is assumed:

- Type of construction: Construction with ordinary performance levels;
- Nominal design life: $V_N = 50$ years.

The structure under analysis is considered class II, as described in 2.4.2 of the DM2018: constructions whose use involves normal crowding, without dangerous contents for the environment and without essential public and social functions.

According to table 2.4.II of the aforementioned standard, the usage coefficient C_U for use class II is equal to 1.0:

Table 3.2: Values of the use coefficient C_U

CLASSE D'USO	I	II	III	IV
COEFFICIENTE C_U	0,7	1,0	1,5	2,0

Referring to § 2.4.3 of DM2018 [9], the design period for the seismic action is:

$$V_R = V_N \cdot C_U = 50 \text{ yr} \quad (3.1)$$

3.2 Geometrical properties

The structure consists of four stories plus the roof, with an inter-floor height of 3 metres and a span length of 5 metres; moreover, the effect depth in the transversal direction is 5 metres. The effective span length is 4.4 metres, with the columns of the whole structure having a cross-section of 60x60 cm. The beams have a cross-section of 40x50 centimetres, resulting in an effective inter-floor height of 2.5 metres. A front view (Figure 3.1) and a plan view (Figure 3.2) are given to help visualise these geometrical characteristics.

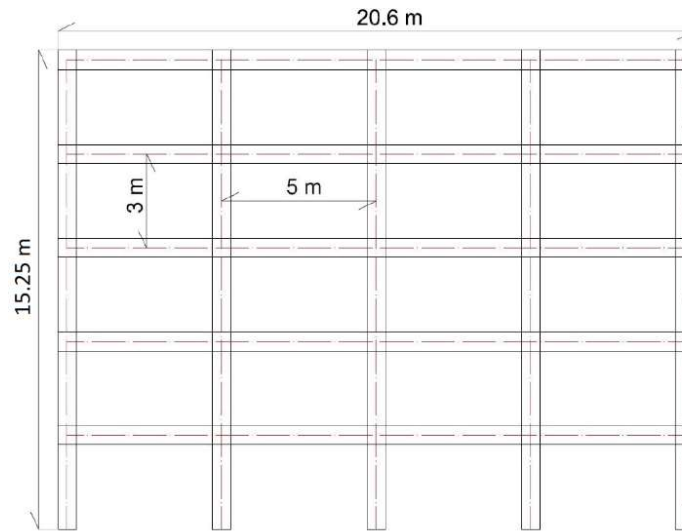


Figure 3.1: Building front view

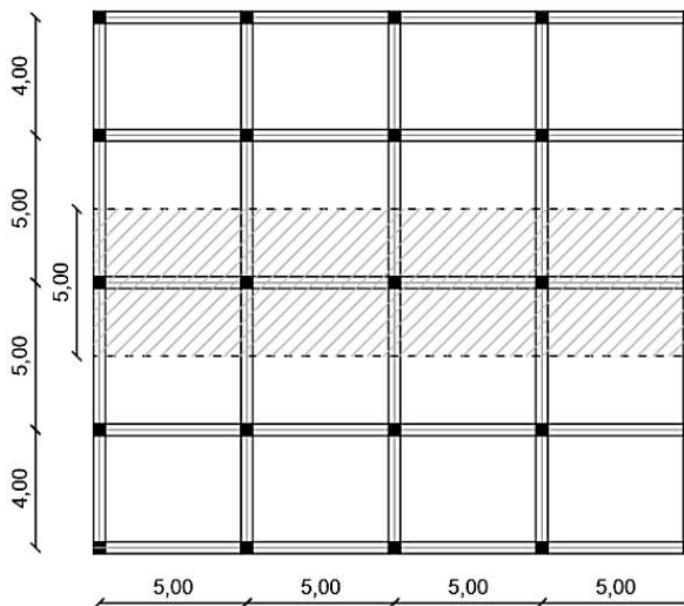


Figure 3.2: Building plan view

3.3 Material properties

3.3.1 Concrete

The concrete used to build columns and beams has the following characteristics:

Table 3.3: Concrete characteristics

Concrete resistance class	C25/30
Cube strength R_{ck}	30 N/mm ²
Cylinder strength f_{ck}	25 N/mm ²
Partial safety coefficient γ_c	1.5 [-]
Long duration load coefficient α_{cc}	0.85 [-]
Design value of compressive strength f_{cd}	14.17 N/mm ²
Mean value of axial tensile strength f_{ctm}	2.56 N/mm ²
Characteristic axial tensile strength f_{ctk}	1.8 N/mm ²
Design value of tensile strength f_{ctd}	1.2 N/mm ²
Ultimate strain at ULS ε_{cu}	3.5 ‰
Specific weight γ	25 kN/m ³
Elastic modulus E_{cm}	31476 N/mm ²
Poisson's coefficient ν	0.2 [-]

3.3.2 Steel

The steel chosen to make the bars and stirrups has the following properties:

Table 3.4: Steel characteristics

Steel class	B450/C
Characteristic tensile strength f_{tk}	540 N/mm ²
Characteristic yield strength f_{yk}	450 N/mm ²
Partial safety coefficient γ_s	1.15 [-]
Design yield strength f_{yd}	391 [-]
Ratio between characteristic tensile and yield strength	1.15 - 1.35 [-]
Characteristic strain at maximum load ε_{uk}	75 ‰
Design yielding strain ε_{syd}	1.96 ‰
Ultimate strain at ULS ε_{ud}	$0.9\varepsilon_{uk} = 63\text{‰}$
Elastic modulus E_s	200000 N/mm ²
Poisson's coefficient ν	0.3 [-]

3.4 Durability

The stability and strength of the structure must be maintained for the whole of the design working life to satisfy the condition of Durability. It is based on the environmental conditions, in particular we mean the chemical and physical conditions in which the structure is exposed in addition to the mechanical actions. Its value is determined by these factors and the reference code rules are defined in EN1992 Eurocode 2: Design of concrete structures [28], at section 4: Durability and cover to reinforcement.

It is possible to determine the **exposure class** of the building by consulting table 4.1-section2 of EC2 [28], which classify buildings in according to the amount of corrosion caused by carbonation (Table 3.5):

Table 3.5: Exposure level for corrosion caused by carbonation

XC1	Dry or permanently wet	Concrete inside buildings with low air humidity Concrete permanently submerged in water
XC2	Wet, rarely dry	Concrete surfaces subject to long-term water contact Many foundations
XC3	Moderate humidity	Concrete inside buildings with moderate or high air humidity External concrete sheltered from rain
XC4	Cyclic wet and dry	Concrete surfaces subject to water contact, not within exposure class XC2

The environmental factors to which the case study is subjected may be described as "wet, rarely dry," resulting in an exposure class of XC2 for the case study.

The following proposed limiting values for the composition and qualities of concrete are specified in EN 206-1 [30], table F.1, based on the class that was previously established (Table 3.6):

Table 3.6: Limiting parameters for the composition and characteristics of concrete are prescribed

	Exposure classes																		
	No risk of corrosion or attack	Carbonation-induced corrosion					Chloride-induced corrosion						Freeze/thaw attack				Aggressive chemical environments		
							Sea water			Chloride other than from sea water									
		X0	XC 1	XC 2	XC 3	XC 4	XS 1	XS 2	XS 3	XD 1	XD 2	XD 3	XF 1	XF 2	XF 3	XF 4	XA 1	XA 2	XA 3
Maximum w/c	---	0,65	0,60	0,55	0,50	0,50	0,45	0,45	0,55	0,55	0,45	0,55	0,55	0,50	0,45	0,55	0,50	0,45	
Minimum strength class	C12/15	C20/25	C25/30	C30/37	C30/37	C30/37	C35/45	C35/45	C30/37	C30/37	C35/45	C30/37	C25/30	C30/37	C30/37	C30/37	C30/37	C35/45	
Minimum cement content (kg/m³)	---	260	280	280	300	300	320	340	300	300	320	300	300	320	340	300	320	360	
Minimum air content (%)	---	---	---	---	---	---	---	---	---	---	---	---	4,0 ^a	4,0 ^a	4,0 ^a	---	---	---	
Other requirements													Aggregate in accordance with prEN 12620:2000 with sufficient freeze/thaw resistance				Sulfate-resisting cement ^b		

^a Where the concrete is not air entrained, the performance of concrete should be tested according to an appropriate test method in comparison with a concrete for which freeze/thaw resistance for the relevant exposure class is proven.

^b When SO₄²⁻ leads to exposure classes XA2 and XA3, it is essential to use sulfate-resisting cement. Where cement is classified with respect to sulfate resistance, moderate or high sulfate-resisting cement should be used in exposure class XA2 (and in exposure class XA1 when applicable) and high sulfate-resisting cement should be used in exposure class XA3.

When the design working life is intended to be 50 years, such as in the case study, the Eurocode 2 [28], at 4.4.1.2(5) advises beginning with a structural class S4 as a starting point. There are suggested values for structural categorization included in table 4.3N of the previously described normative. These recommended values change depending on the exposure class (Table 3.7):

Table 3.7: According to exposure class XC, the recommended structural categorization

Structural Class							
Criterion	Exposure Class according to Table 4.1						
	X0	XC1	XC2 / XC3	XC4	XD1	XD2 / XS1	XD3 / XS2 / XS3
Design Working Life of 100 years	increase class by 2	increase class by 2	increase class by 2	increase class by 2	increase class by 2	increase class by 2	increase class by 2
Strength Class ^{1/2)}	≥ C30/37 reduce class by 1	≥ C30/37 reduce class by 1	≥ C35/45 reduce class by 1	≥ C40/50 reduce class by 1	≥ C40/50 reduce class by 1	≥ C40/50 reduce class by 1	≥ C45/55 reduce class by 1
Member with slab geometry (position of reinforcement not affected by construction process)	reduce class by 1	reduce class by 1	reduce class by 1	reduce class by 1	reduce class by 1	reduce class by 1	reduce class by 1
Special Quality Control of the concrete production ensured	reduce class by 1	reduce class by 1	reduce class by 1	reduce class by 1	reduce class by 1	reduce class by 1	reduce class by 1

Due to the fact that the case study has an exposure class of XC2 and a concrete class minor than C35/45, the structural class is still the same as the value that was first recommended, which is S4.

Referring again to Eurocode 2 [28], **concrete cover** is defined as the minimum possible distance between the surface of the reinforcement and the nearest concrete surface. The nominal concrete cover is calculated as the sum of a minimal component known as c_{min} and a design deviation known as c_{dev} :

$$c_{nom} = c_{min} + \Delta c_{dev} \quad (3.2)$$

The bare minimum of concrete coverage is required to provide the reliable transfer of bond forces, to protect the steel from corrosion (for reasons of durability), and to provide sufficient confidence of resistance to fire. The following formula is used to determine its value:

$$c_{min} = \max \{ c_{min,b} ; c_{min,dur} + \Delta c_{dur,\gamma} - \Delta c_{dur,st} - \Delta c_{dur,add} ; 10 \} \quad (3.2)$$

where:

- $c_{min,b}$ is the minimum cover for bond requirement, according to table 4.2 of [28] (here):

Table 3.8: In terms of bonds, the minimal cover needed

Bond Requirement	
Arrangement of bars	Minimum cover $c_{min,b}^*$
Separated	Diameter of bar
Bundled	Equivalent diameter (ϕ_e)(see 8.9.1)
*: If the nominal maximum aggregate size is greater than 32 mm, $c_{min,b}$ should be increased by 5 mm.	

- $c_{min,dur}$ is the minimum cover due to environmental conditions, according to table 4.4N of [28] (here):

Table 3.9: In terms of durability, the minimum cover needed

Environmental Requirement for $c_{min,dur}$ (mm)							
Structural Class	Exposure Class according to Table 4.1						
	X0	XC1	XC2 / XC3	XC4	XD1 / XS1	XD2 / XS2	XD3 / XS3
S1	10	10	10	15	20	25	30
S2	10	10	15	20	25	30	35
S3	10	10	20	25	30	35	40
S4	10	15	25	30	35	40	45
S5	15	20	30	35	40	45	50
S6	20	25	35	40	45	50	55

$\Delta c_{dur,\gamma}$ is the additive safety element, whose recommended value according to Eurocode 2 [28], at §4.4.1.2(6), is 0 mm;

- $\Delta c_{dur,st}$ is the reduction of minimum cover for use of stainless steel, whose recommended value according to Eurocode 2 [28], at § 4.4.1.2(7), is 0 mm;
- $\Delta c_{dur,add}$ is the reduction of minimum cover for use of additional protection, whose recommended value according to Eurocode 2 [28], at §4.4.1.2(8), is 0 mm;

Taking into account all the previous suggestions, the assumed values are:

- $c_{min,b} = 18 \text{ mm}$ for the beams and $c_{min,b} = 20 \text{ mm}$ for the columns, according to the design bars' diameter (i.e. $\phi 18$ for the beams and $\phi 20$ for the columns);
- $c_{min,dur} = 25 \text{ mm}$, being the structural class S4 and the exposure coefficient XC2;
- $\Delta c_{dur,\gamma} = \Delta c_{dur,st} = \Delta c_{dur,st} = 0 \text{ mm}$
- Thus, according to (3.2), the minimum concrete cover is

$$c_{min} = \max\{20; 25; 10\} = 25 \text{ mm}.$$

In conclusion, considering that the recommended value of Δc_{dev} is 10 mm according to §4.4.1.2 of Eurocode 2 [28], referring to equation **Errore. L'origine riferimento non è stata trovata.**)

$$c_{nom} = c_{min} + \Delta c_{dev} = 25 + 10 = 35 \text{ mm},$$

used both for columns and beams.

3.5 Actions

In § 2.5 of the DM2018, an action is defined as any consequence or set of consequences capable of inducing limit states in a structure. Loads can be classified according to the variation of their intensity over time as (definitions are taken from Eurocode 0 [5]):

- Permanent loads (G): “action that is likely to act throughout a given reference period and for which the variation in magnitude with time is negligible, or for which the variation is always in the same direction (monotonic) until the action attains a certain limit value”
- Variable loads (Q): “action for which the variation in magnitude with time is neither negligible nor monotonic”
- Accidental (exceptional) loads (A): “action, usually of short duration but of significant magnitude, that is unlikely to occur on a given structure during the design working life”
- Seismic actions (E): “action that arises due to earthquake ground motions”

Depending on the limit states to be considered, actions can be combined as follows:

- Fundamental combination, usually assumed for Ultimate Limit State (ULS):

$$\gamma_{G1}G_1 + \gamma_{G2}G_2 + \gamma_P P + \gamma_{Q1}Q_{k1} + \gamma_{Q2}\Psi_{02}Q_{k2} + \gamma_{Q3}\Psi_{03}Q_{k3} + \dots \quad (3.3)$$

- Rare combination, usually assumed for irreversible Serviceability Limit State (SLS):

$$G_1 + G_2 + P + Q_{k1} + \Psi_{02}Q_{k2} + \Psi_{03}Q_{k3} + \dots \quad (3.4)$$

- Frequent combination, usually assumed for reversible Serviceability Limit State (SLS):

$$G_1 + G_2 + P + \Psi_{11}Q_{k1} + \Psi_{22}Q_{k2} + \Psi_{23}Q_{k3} + \dots \quad (3.5)$$

- Quasi-permanent combination (SLS), usually assumed for reversible long term effects:

$$G_1 + G_2 + P + \Psi_{21}Q_{k1} + \Psi_{22}Q_{k2} + \Psi_{23}Q_{k3} + \dots \quad (3.6)$$

- Accidental combination, usually assumed for Serviceability Limit State (SLS) and long-term effects:

$$G_1 + G_2 + P + A_d + \Psi_{21}Q_{k1} + \Psi_{22}Q_{k2} + \Psi_{23}Q_{k3} + \dots \quad (3.7)$$

- Seismic combination, usually assumed for both SLS and ULS, when considering seismic actions:

$$G_1 + G_2 + P + \Psi_{21}Q_{k1} + \Psi_{22}Q_{k2} + \dots \quad (3.8)$$

where:

- γ_{G1} partial coefficient of structural standing loads;
- γ_{G2} partial coefficient of non-structural standing loads;
- γ_Q partial coefficient of variable shares;
- Ψ_{ij} coefficients of combinations relative to the j-th variable action; the values of the combination factors T depend on the type of action considered, the intended use of the structure and the

design situation, as reported in Table 2.5.I of DM2018:

Table 3.10: Coefficients of combination

Action	ψ_0	ψ_1	ψ_2
Imposed loads in buildings, category (see EN 1991-1-1)			
Category A : domestic, residential areas	0,7	0,5	0,3
Category B : office areas	0,7	0,5	0,3
Category C : congregation areas	0,7	0,7	0,6
Category D : shopping areas	0,7	0,7	0,6
Category E : storage areas	1,0	0,9	0,8
Category F : traffic area, vehicle weight $\leq 30\text{kN}$	0,7	0,7	0,6
Category G : traffic area, $30\text{kN} < \text{vehicle weight} \leq 160\text{kN}$	0,7	0,5	0,3
Category H : roofs	0	0	0
Snow loads on buildings (see EN 1991-1-3)*			
Finland, Iceland, Norway, Sweden	0,70	0,50	0,20
Remainder of CEN Member States, for sites located at altitude $H > 1000\text{ m a.s.l.}$	0,70	0,50	0,20
Remainder of CEN Member States, for sites located at altitude $H \leq 1000\text{ m a.s.l.}$	0,50	0,20	0
Wind loads on buildings (see EN 1991-1-4)	0,6	0,2	0
Temperature (non-fire) in buildings (see EN 1991-1-5)	0,6	0,5	0
NOTE The ψ values may be set by the National annex.			
* For countries not mentioned below, see relevant local conditions.			

3.5.1 Permanent actions

Permanent structural actions (G1) are represented by the proper weight of pillars and beams, which is taken into account by the calculation software, which receives as input the dimensions and specific weight, as well as the weight of the latero-cement floor, with load-bearing joists in reinforced concrete and interposed brick lighting blocks, the geometry of which is shown in Figure 3.4:

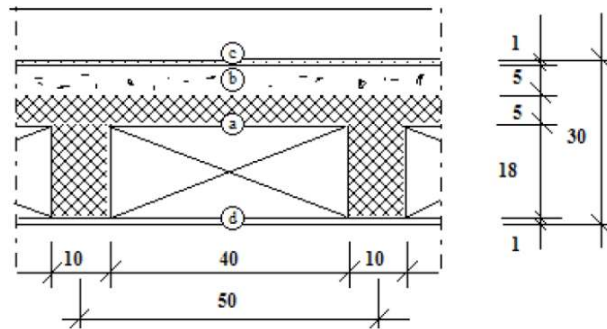


Figure 3.3: Slab design

The fraction of permanent structural load of the floor is calculated taking into account the various contributions, and is equal to 3.20 kN/m², as indicated in Table 3.11:

Table 3.11: Permanent structural load of the slab

	<i>Width [m]</i>	<i>Thickness[m]</i>	<i>Weight [kN/m³]</i>	<i>g₁ [kN/m²]</i>
Slab	1.00	0.05	25	1.25
Rib	2x0.10	0.18	25	0.90
Brick	2x0.40	0.18	7.3	1.05
				3.20

The **permanent non-structural loads (G_2)** are given by the non-structural parts of the slabs (screed, floor and plaster) and the inner walls. The former is equal to 1.40 kN/m², as Table 3.12 shows:

Table 3.12: Slab's permanent non-structural load

	<i>Width [m]</i>	<i>Thickness[m]</i>	<i>Weight [kN/m³]</i>	<i>g₂ [kN/m²]</i>
Screed	1.00	0.05	16.0	0.8
Floor	-	-	-	0.20
Plaster	1.00	0.02	20.0	0.40
				1.40

The other part of G_2 , related to the internal walls, can be computed considering the Figure 3.4

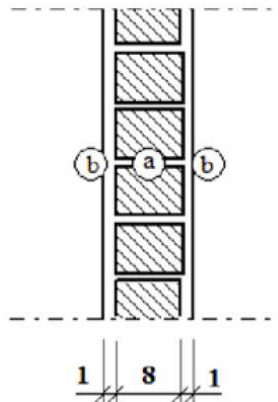


Figure 3.4: Design for the interior walls

From the values of the weight per unit volume of the following materials and the thickness, the weight per unit of area of the internal masonry is

obtained (Table 3.13):

Table 3.13: Weight of internal walls

	Width [m]	Weight [kN/m³]	g_2 [kN/m²]
Brick	0.08	6.0	0.48
Plaster	0.01	20.0	0.40
			0.88

To determine the G_2 value connected to the internal walls, code guidelines recommend referring to loads per m², beginning with the load per metre. This amount may be simply calculated for the current situation by multiplying the previous load by the floor height, as shown below:

$$G_2 = 2.65 \cdot 0.88 = 2.33 \text{ kN/m} \quad (3.10)$$

The DM2018 standard in § 3.1.3, with regard to internal partition elements, suggests ordinary surface load values to refer to: partitions and light systems of residential and office buildings can generally be assumed as equivalent distributed loads, provided that the floors have adequate transverse distribution capacity. The uniformly distributed load g_2 may be correlated to the own weight per unit length G_2 of the partitions as follows:

- for dividing elements with $G_2 \leq 1.00 \text{ kN/m} \rightarrow g_2 = 0.40 \text{ kN/m}^2$
- for dividing elements with $1.00 < G_2 \leq 2.00 \text{ kN/m} \rightarrow g_2 = 0.80 \text{ kN/m}^2$
- for dividing elements with $2.00 < G_2 \leq 3.00 \text{ kN/m} \rightarrow g_2 = 1.20 \text{ kN/m}^2$
- for dividing elements with $3.00 < G_2 \leq 4.00 \text{ kN/m} \rightarrow g_2 = 1.60 \text{ kN/m}^2$
- for dividing elements with $4.00 < G_2 \leq 5.00 \text{ kN/m} \rightarrow g_2 = 2.00 \text{ kN/m}^2$

In this situation, given the load of 2.33 kN/m, the surface load to be considered is 1.20 kN/m².

Surface loads are appropriately multiplied by the area of influence's depth of 5 metres and treated as linear loads acting on the beams.

The total permanent non-structural load is then equal to **$g_2 = 2.60 \text{ kN/m}^2$** .

3.5.2 Variable actions

The variable overload due to use, according to Table 3.1.II of DM2018 [9], is equal to 2.00 kN/m² for intermediate floors and 0.50 kN/m² for roofing.

The action of the wind is calculated according to the indications of § 3.3 of the DM2018:

$$p = q_r \cdot c_e \cdot c_p \cdot c_d \quad (3.9)$$

where:

- q_r is kinetic wind pressure

The kinetic wind pressure q_r is computed using the following formula:

$$q_r = \frac{1}{2} \rho v_r^2 \quad (3.10)$$

Considering an air density $\rho = 1,25 \text{ kg/m}^3$ and a reference wind velocity $v_r = 31.3 \text{ m/s}$ for L'Aquila city. Thus, by plug in these values on (3.10), it results $q_r = 612,3 \text{ N/m}^2$.

- c_e is the exposure factor

The exposure coefficient c_e is given by the following formulae:

$$c_e(z) = k_r^2 c_t \ln(z/z_0) [7 + c_t \ln(z/z_0)] \quad \text{for } z \geq z_{min} \quad (3.11)$$

$$c_e(z) = c_e(z_{min}) \quad \text{for } z < z_{min} \quad (3.12)$$

where:

- k_r, z_0, z_{min} are given in table 3.3.II of DM2018 [9] depending on the exposure category of the site. Since the category is V, it results: $k_r = 0.23$, $z_0 = 0,70\text{m}$, $z_{min} = 12\text{m}$

- c_t is the topography coefficient and the normative suggests $c_t = 1$

Thus, it is possible to define the exposure coefficient as function of the height z , expressed in meters:

Table 3.14: Exposure coefficient c_e , as function of the height

z [m]	0	3	6	9	12	15
c_e [-]	1.48	1.48	1.48	1.48	1.48	1.63

- c_p is the shape coefficient (or aerodynamic) and it is assumed equal to 0.80 for the upwind surface and -0.45 for the downwind surface
- c_d is the dynamic factor, the normative suggests to assume $c_d = 1$

In conclusion, by plug in all these coefficients and taking into account an influence area of 5 meters, it is possible to obtain the distribution of the wind pressure along the height:

Table 3.15: Relationship between wind pressure and height

z [m]	p_{up} [kN/m]	p_{down} [kN/m]
0	3.60	- 1.80
3	3.60	- 1.80
6	3.60	- 1.80
9	3.60	- 1.80
12	3.60	- 1.80
15	4.00	- 2.00

The snow load is determined by the following expression (§ 3.4 of the DM2018):

$$q_s = \mu_i * q_{sk} * C_E * C_t \quad (3.13)$$

where:

- q_{sk} is the characteristic ground snow load and it depends on the location of the city (L'Aquila is in zone III) and on the elevation of the site (714 meters over the sea level for L'Aquila). Thus, referring to § 3.4.2, it results $q_{sk} = 2.72 \text{ kN/m}^2$
- μ_i is the shape coefficient and depends on the inclination angle of the roofing. For the specific case, the roof is planar, thus referring to table 3.4.II of DM2018 [9], $\mu_i = 0.8$
- C_E is the exposure coefficient, suggested unitary in § 3.4.4
- C_t is the thermal coefficient, suggested unitary in § 3.4.5

In conclusion, the snow load is $q_s = 2.17 \text{ kN/m}^2$ for the case study.

3.5.3 Seismic action

This action is specified in section 3.2 of DM2018 [9], where the design seismic action is determined as a function of the seismic hazard of the site, as well as the morphological and stratigraphic characteristics of the ground on which the building is built:

$$S_e(T) = f(a_g, F_0, T_c^*)$$

where:

- a_g is the design ground acceleration on ground type A
- F_0 is the maximum horizontal amplification factor
- T_c^* is the corner period at the upper limit of the constant acceleration region of the elastic spectrum

The abovementioned variables are assessed in respect to a VR of 50 years and computed using the equation (3.1).

The Excel file released by the Ministry of Infrastructure and Transport was used to create the response spectrum. The elastic response spectrum was obtained by entering the geographical coordinates of the region under investigation in phase 1, the nominal life and coefficient of utilization in phase 2, the soil category and topographic one in phase 3. The parameters entered are summarised as follows:

Nominal life $V_N = 50$ years;

- Coefficient of use $C_U = 1$;
- Soil category: B (soft rocks and deposits of very thickened coarse-grained soils or very consistent fine-grained soils);
- Topographic class: T3

The spectrum was also analysed in relation to the reinforced concrete structure with conventional damping =5%.

An extra parameter, the structural factor q , must be defined for the inelastic design response spectrum. Taking into account the structural typology, ductility class, elevation regularity, and number of floors, the structure factor is calculated using the method shown in 7.3.1 of the

DM2018:

$$q = q_0 K_R \quad (3.16)$$

Because the structure is regular, the parameter K_R , which is a reductive factor that depends on the characteristics of regularity in height of the buildings, is assumed to be equal to 1; q_0 is the base value of the structure factor, which depends on the expected ductility level, the structural type, and the ratio u_1 . Using the high ductility class "A," the value of q_0 is calculated using the following relation:

$$q_0 = 4.5 \cdot \frac{\alpha_u}{\alpha_1} = 4.5 \cdot 1.3 = 5.85$$

having chosen a ductility class A and $\alpha_u/\alpha_1 = 1.3$ for multi-storey frames

Ultimately q will be equal to:

$$q = q_0 K_R = 5.85 \cdot 1 = 5.85$$

The response spectrum at the ultimate limit state (Figure 3.5) and the serviceability limit state (Figure 3.6) are shown below.

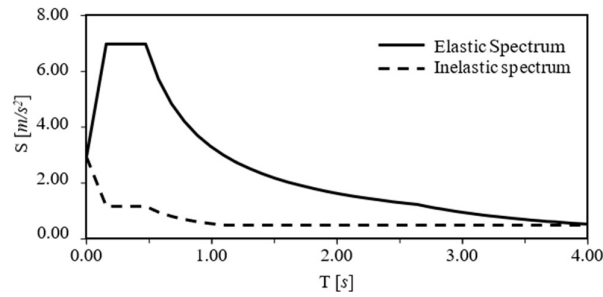


Figure 3.5: Response spectrum at ULS

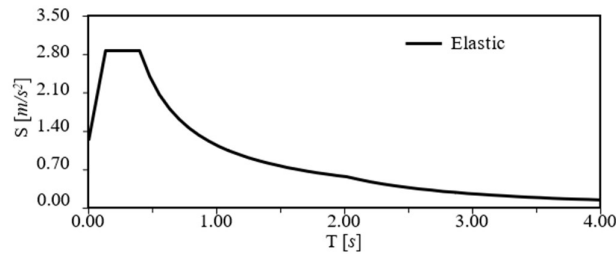


Figure 3.6: Response spectrum at SLS

3.6 Modal analysis

While taking into consideration the DM2018, it is required to consider all of the eigenvalues and eigenvectors that have the potential to contribute significantly to the response of a structure when seen from a global perspective. In particular, it is essential to make sure that:

- The sum of the modal masses of the considered vibration modes should represent the 85% of the total mass of the structure
- The examined modes must have a modal more than 5% of the structure's overall mass.

In this particular instance, the building is distinguished by regularity both in plan and in elevation; hence, it is feasible to carry out the modal analysis using a linear strategy. This is because the building is symmetrical in both planes.

The following table presents the periods that are involved, along with the corresponding modal masses:

Table 3.16: 12 initial vibration modes of modal analysis

Mode	Period	Mass mobilized along X	
		For each mode	Sum
[–]	[s]	[%]	[%]
1	0.45	82.223	82.223
2	0.14	10.792	93.015
3	0.08	4.320	97.335
4	0.05	0.000	97.335
5	0.05	2.041	99.376
6	0.05	1E-04	99.376
7	0.05	4E-18	99.376
8	0.04	0.617	99.994
9	0.04	3E-18	99.994
10	0.04	2E-03	99.996
11	0.03	2E-18	99.996
12	0.03	5E-17	99.996

It can be observed that the 85% threshold has already been met with the first two modes, as well as the fact that the 5% threshold has been crossed for them. Hence, the suggestion indicated by the provisions of the code are respected.

Another factor to consider is the fact that the modal mass was determined by using the formula below, which was again recommended by the code rules:

$$G_1 + G_2 + \sum \Psi_{2j} Q_{kj} \quad (3.14)$$

3.7 Dimensioning and verification

As a result of taking into consideration the criticalities associated to the seismicity of the location, the capacity design of the building is the primary criterion. According to this, the structural components should be built in a given sequence, taking into consideration the significance that they take, in order to favour ductile mechanisms (bending) rather than fragile ones (shearing). Since beams are ductile components, it is the beams themselves that must first reach plasticization in order to be able to absorb and dissipate the energy during an earthquake. This indicates that the longitudinal reinforcement of the beams is calculated first, and then, as a result of it, the shear reinforcement of the beams as well as the bars and stirrups of the columns are designed.

The procedures used for the verification of the structural elements at the ultimate limit and serviceability state are illustrated below, suitable to comply with all the checks.

3.7.1 Beam design: bending at ULS

The geometry of the beams is reported in Table 3.17:

Table 3.17: Peculiarities of beams' geometry

<i>B</i> [mm]	<i>H</i> [mm]	<i>c</i> [mm]	<i>d'</i> [mm]	<i>d</i> [mm]
400	500	35	52	448

The value of M_{Ed} acting on the beam must be compared with that of $M_{Rd,lim}$, obtained as:

$$M_{Rd,lim} = 0.2961 B d^2 f_{cd} = 503.9 \text{ kNm}$$

Two different cases can occur:

- if $M_{Ed} < M_{Rd,lim}$ the reinforcement is simply in tension

- if $M_{Ed} > M_{Rd,lim}$ also the compressive reinforcement is needed

It has been shown that the value of the moment acting on the beam in the different spans is always less than $M_{Rd,lim}$, equal to 503.9 kNm. Although, for regulatory reasons, the compression reinforcement will always be designed so that robustness will be increased.

Being aware of the characteristics of steel and concrete, as well as of the filling coefficients β_1 and β_2 actively equal to 0.8095 and 0.4160, it was possible to determine a first design value of x_U , identified by the binomial formula, whose constituent terms are:

$$a = \beta_1 \beta_2 B f_{cd} \quad (3.18)$$

$$b = \beta_1 B f_{cd} d \quad (3.19)$$

$$c = M_{Ed} \quad (3.20)$$

Determined x_U , it is possible to derive the value of the minimum reinforcement needed in the tensile zone by the formula:

$$A_{s,min}[mm^2] = \frac{\beta_1 B f_{cd} x_U}{f_{yd}} \quad (3.21)$$

Having chosen the bar diameters, it is necessary to respect what it is recommended by code rules (DM2018 § 7.4.6.2.1):

at least two bars with a diameter of less than 14 mm shall be present above and below along the entire length of the beam;

- in correspondence of the critical zones (i.e. at both extremities of the beam), the reinforcement in compression should be not less than half of the one in tension, such that:

$\rho'_s \geq 0.5\rho_s$. In the other sections, it should be guaranteed that $\rho'_s \geq 0.25\rho_s$, where:

$$\rho'_s = \frac{A'_s}{BH} \quad (3.15)$$

$$\rho_s = \frac{A_s}{BH} \quad (3.16)$$

- in each section, the limits of the geometrical reinforcement ρ_s are:

$$\frac{1.4}{f_{yk}} \leq \rho_s \leq \rho'_s + \frac{3.5}{f_{yk}} \quad (3.17)$$

When the reinforcement in compression and tension have been specified, it is important to assess whether or not these values are enough to provide an adequate level of resistance. To start, the depth of the neutral axis position may be determined using the following formula:

$$x_U = \frac{f_{yd}(A_s - A'_s)}{\beta_1 f_{cd} B} \quad (3.18)$$

To validate the original assumption about the material's strengths (field 3, where $\varepsilon_{cd} = 0.35\%$ and $\varepsilon_s > 0.196\%$), an x_U value is computed, solving the equation:

$$C + S' - S = 0 \quad (3.19)$$

where $C = \beta_1 f_{cd} B x_U$, $S = f_{yd} A_s$ and $S' = f_{yd} A'_s = \varepsilon'_s E_s A'_s$

Once x_U is computed, the verifications are:

- Ductility: $x_U < 0.45d$
- Resistant moment: $M_{Ed} < M_{Rd}$ with M_{Rd} calculated by balance around the tense armor:

$$M_{Rd} = \beta_1 f_{cd} B x_U (d - \beta_2 x_U) + A'_s f_{yd} (d - d') \quad (3.20)$$

To simplify the arrangement of the longitudinal reinforcement of the beams, only bars with a diameter of 18 mm were used.

The assessments (ULS for bending and construction details) require the adoption of the following disposition:

- 3 continuous bars in the lower part for all the beams and for the entire length of the same, suitable to support the positive moments in the span;
- 2 bars in the upper part for all the beams, which crossing each other, such that on the nodes beam-column the total amount of bars is 4;
- from 1 to 3 additional bars in the upper part in correspondence of the nodes, to obtain a reinforcement used to retain the peaks of negative applied bending moment.

3.7.2 Beams – shear at ULS

For load-bearing beams, the reference legislation prescribes to design the structure with an appropriate shear reinforcement.

The brackets are arranged with variable s_w pitch along the beam in order to meet the regulatory requirements in terms of strength and minimum quantity of transverse reinforcement.

The shear action should be determined in accordance with the resistance hierarchy criteria, beginning with the bending moments at the ends of the beams at the time of the creation of the plastic hinges and taking into consideration the contribution due to gravity loads, as follows:

$$V_{Ed} = \gamma_{Rd} \frac{M_{Rb,1} + M_{Rb,2}}{l_c} + \frac{1}{2}(G + \psi_2 Q)l_c \quad (3.21)$$

where:

- l_c is the length of the simply supported beam
- $M_{Rb,1}$ is the resistant bending moment of the first support
- $M_{Rb,2}$ is the resistant bending moment of the second support
- γ_{Rd} overstrength factor, taken equal to 1.0 for $q \leq 3$, or to 1.2 otherwise
- $G + \psi_2 Q$ gravitational load

Calculated the shear action, we proceed with the classic shear reinforcement design, indicated in § 4.1.2.3.5.2 of the DM2018.

The calculation model is based on the Ritter-Morsch model, an ideal isostatic lattice that is formed due to the combined effect of bending and cutting, consisting of an upper current of compressed concrete, a tense lower current represented by the longitudinal reinforcement, concrete struts inclined by θ with respect to the longitudinal direction and tie rods with inclination α with respect to the longitudinal direction represented by stirrups, in this case vertical, therefore $\alpha = 90^\circ$.

Assuming this behavior, with reference to concrete struts, the design resistance to "compression shear" is calculated with:

$$V_{Rcd} = 0.9db_w\alpha_c v f_{cd} \frac{\cot\alpha + \cot\theta}{1 + \cot^2\theta} \quad (3.22)$$

On the other hand, the design resistant shear, referred to the steel stirrups, is:

$$V_{Rsd} = 0.9d \frac{A_{sw}}{s} f_{yd} (\cot\alpha + \cot\theta) \sin\alpha \quad (3.23)$$

where:

- d is the effective height of the cross-section
- b_w is the width of the cross-section
- α_c is a coefficient that considers the tension state of the compressive chord, for this case equal to 1
- $v f_{cd}$ design value of compressive strength, reduced with a quantity $v = 0.5$
- α stirrups inclination with respect to the longitudinal reinforcement direction (i.e. horizontal)
- θ strut inclination, value that should respect the limits: $1 \leq \cot\theta \leq 2.5$ and $\cot\theta = 1$ for CD "A"
- A_{sw} is the area of the transversal reinforcement
- s is the distance between consecutive transversal stirrups

The verifications consist of guaranteeing that:

- $V'_{Ed} < V_{Rcd}$ where V'_{Ed} is the shear value in correspondence of the joint with the column
- $V''_{Ed} < V_{Rsd}$ where V''_{Ed} is the shear value at a distance d from the joint with the column

- $V_{Rsd} > V_{Rcd}$ for ductility reasons

For the definition of the construction details, the dissipative zone is distinguished from the non-dissipative one. The dissipative zone, with a length equal to 1.5 and 1.0 times the height of the beam, respectively for CD "A" and CD "B", is the area at the end of the beam, where the formation of plastic hinges is expected.

There are limitations regarding both the dissipative and non-dissipative areas, defined at DM2018 § 4.1.6.1.1 and § 7.4.6.2.1. In particular:

In the dissipative area the stirrups should have a step s that is the minimum among:

- a quarter of the effective height d of the cross-section
- 175 mm and 225 mm respectively for CD "A" and CD "B"
- 6 times and 8 times the minimum diameter of the longitudinal bars respectively for CD "A" and CD "B"
- 24 times the diameter of the transversal reinforcement

In the non-dissipative zone, i.e. the one between the two dissipative zones of the beams, the stirrups must comply with the following limitations:

- The cross-section of the stirrups should be at least $A_{st} = 1.5b \text{ mm}^2/\text{m}$ where b is the minimum width of the web
- At least there should be 3 stirrups per meter
- The step should be not larger than 0.8 times the effective height d of the cross-section

In order to comply with the checks and limitations mentioned above, it was decided to use an equal arrangement of the transverse reinforcements for all the beams of the frame, which includes two-arm stirrups, a diameter of 8 mm and the following inter-axes:

- 7.5 cm in the dissipative zones;
- 15 cm in non-dissipative zones.

3.7.3 Beams – SLS

STRESS LIMITATION

These restrictions are outlined in Section 7.2 of EC2 [28], where it is advised to keep the concrete's compressive stress within safe limits to prevent longitudinal fractures, microcracks, or significant levels of creep.

Limit values:

- $\sigma_c < 0.6 f_{ck}$ for the characteristic combination
- $\sigma_c < 0.45 f_{ck}$ for the quasi-permanent combination
- $\sigma_s < 0.8 f_{yk}$ for the characteristic combination

Stresses in concrete and steel are computed using Navier formula:

$$\sigma_c = \frac{M}{I_{om,x}} y \quad (3.24)$$

$$\sigma_s = n \frac{M}{I_{om,x}} y \quad (3.25)$$

where x is the position of the neutral axis (found through the cancellation of the static moment of the section), n indicates the homogenization coefficient (in order to calculate the homogenized moment of inertia of the section) and y value indicates the distance from the neutral axis of the considered fiber (i.e. y is taken as the distance of the longitudinal bars for the steel stresses calculation while for the concrete stresses computation is the extremity of the cross-section because it is the most stressed part).

By calculating the stresses in the most stressed points, all the cross-sections of the beams result verified.

CRACKING

It is necessary to limit the width of the cracks in order not to compromise the functionality, durability and aesthetics of the structure.

The EC2 allows the use of limit values for the opening of the w_{max} slots, indicated in Table 7.1N of the same standard, depending on the load combination

and the environmental exposure class; the verification can be carried out through the analytical calculation of the amplitude of the slits:

$$w_k = s_{r,max}(\varepsilon_{sm} - \varepsilon_{cm}) \quad (3.26)$$

where:

- $s_{r,max} = k_3c + k_1k_2k_4\Phi/\rho_{eff}$ is the maximum crack distance
- c is the concrete cover
- k_1 coefficient taking into account the adhesion properties of the reinforcement (0.8 for bars with improved adhesion; 1.6 for smooth bars);
- k_2 coefficient taking into account the distribution of deformations (0,5 for bending; 1.0 for pure traction);
- $k_3 = 0.4$
- $k_4 = 0.425$
- ε_{sm} the average deformation of the reinforcement, taking into account the deformations imprinted and the effect of "tension stiffening";
- ε_{cm} average deformation of the concrete between the cracks.

The difference between the two strains in formula (3.26) is computed as follow:

$$\varepsilon_{sm} - \varepsilon_{cm} = \frac{\sigma_{s,max} - \frac{k_t f_{ctm}}{\rho} (1 + \alpha_e \rho_{eff})}{E_s} \quad (3.27)$$

Where:

- k_t is a factor that is function of load duration (0.6 for short duration and 0.4 for long duration)
- $\alpha_e = E_s/E_c$
- $\rho_{eff} = A_s/B h_{c,eff}$

Moreover, the difference at should be larger or equal to $0.6 \sigma_{s,max}/E_s$.

All the cross-sections of the beams result verified.

DEFLECTION

The functionality of the structure must be guaranteed by establishing appropriate deformation limit values. In general we have that:

- The appearance and functionality of the structure can be compromised if the deflection of a beam, slab or cantilever subjected to quasi-permanent loads is greater than 1/250 of the span;
- For the elements brought, such as partitions, walls, fixtures, windows, the inflection must not exceed 1/500 of the span.

According to the circular to DM2018, for beams and floors with lights not exceeding 10 m it is possible to omit the verification of inflections, considering it implicitly satisfied, if the ratio of slenderness $\lambda = l/h$ between light and height complies with the limitation:

$$\lambda \leq K \left(\frac{11 + 0.0015f_{ck}}{\rho + \rho'} \right) \left(\frac{500A_{s,eff}}{f_{yk}A_{s,calc}} \right) \quad (3.28)$$

where f_{ck} is the characteristic compressive strength of concrete, ρ and ρ' are the ratios of tense and compressed reinforcement, respectively, $A_{s,eff}$ and $A_{s,calc}$ are respectively the tension reinforcement effectively present on the most stressed cross-section and the corresponding reinforcement that has been calculated, f_{yk} is the yield strength characteristic of the armature (in MPa) and K is a corrective coefficient, which depends on the structural scheme. All the beams result verified.

3.7.4 Column: bending and compression at ULS

The DM2018 [9] at § 4.1.6.1.2 and 7.4.6.2.2 contain the reference code rules, which prescribe limitations on the longitudinal reinforcement as follows:

- The diameter of longitudinal bars should be greater than or equal to 12 mm, and the distance between the bars should not exceed 300 mm.
- The reinforcement area should be at least equal to $0.10N_{Ed}/f_{yd}$ and not less than $0.003A_c$, where N_{Ed} is the design axial force acting on the column,

f_{yd} is the design yield strength of the reinforcement, and A_c is the cross-sectional area of the column.

- The ratio ρ between the area of the longitudinal reinforcement and the gross concrete cross-section should be within the limits of $1\% \leq \rho \leq 4\%$.

For this particular case study, all columns have a cross-section of $600 \times 600 = 3600 \text{ mm}^2$, and 12 bars of 20 mm diameter each have been selected. Among these, 4 are located on the sides and 8 are in the intermediate position, resulting in a total area of 3770 mm^2 .

Following the criteria of hierarchy of resistances (capacity design), for each direction and each seismic action directions of application, the column must be protected from premature plasticization by adopting appropriate design bending moments: this condition is achieved if, for each beam-column node and for each direction and seismic action direction, the overall resistance of the columns is greater than the overall strength of the beams amplified by a coefficient γ_{Rd} , in accordance with § 7.4.4.2.1 of the DM2018.

$$\sum M_{c,Rd} \geq \gamma_{Rd} \sum M_{b,Rd} \quad (3.29)$$

where:

- γ_{Rd} coefficient of overstrength, equal to 1.30 for CD "A" and "B";
- $M_{c,Rd}$ resistant moment of the generic column converging in the node, computed for the levels of axial stress present in the seismic combinations of the actions;
- $M_{b,Rd}$ resistant moment of the generic beam that converges in the node.

3.7.5 Column: shear at ULS

In order to exclude the formation of inelastic mechanism due to shear, the criterion of the hierarchy of resistances provides that the shear stresses to be used for checks and reinforcements dimensioning are obtained from the columns equilibrium condition, subject to the action of resistant moments in the upper end sections $M_{c,Rd}^s$ and lower $M_{c,Rd}^i$, according to the expression given by DM2018 in § 7.4.4.2.1:

$$V_{Ed} = \gamma_{Rd} \frac{M_{c,Rd}^s + M_{c,Rd}^i}{l_p} \quad (3.30)$$

where:

- γ_{Rd} overstrength coefficient equal to 1.30 for CD "A" and 1.10 for CD "B";
- l_p length of the pillar.

Computed the stressful shear, we proceed with the classic shear design, indicated in § 4.1.2.3.5.2 of the DM2018.

As described for the beams, the calculation model is based on the Ritter-Morsch model. Assuming this behavior, with reference to concrete core, the design resistance to "compression shear" is calculated with:

$$V_{Rcd} = 0.9db_w\alpha_c v f_{cd} \frac{\cot\alpha + \cot\vartheta}{1 + \cot\alpha\cot\vartheta}$$

With reference to the transverse reinforcement, the design resistance to "tensile shear" is calculated with:

$$V_{Rsd} = 0.9d \frac{A_{sw}}{s} f_{yd} (\cot\alpha + \cot\vartheta) \sin\alpha \quad (3.36)$$

where:

- d is the effective height of the cross-section
- b_w is the width of the cross-section
- α_c is a coefficient that considers the tension state of the compressive chord, for this case equal to 1
- $v f_{cd}$ design value of compressive strength, reduced with a quantity $v = 0.5$
- α stirrups inclination with respect to the longitudinal reinforcement direction (i.e. horizontal)
- ϑ strut inclination, value that should respect the limits: $1 \leq \cot\alpha\cot\vartheta \leq 2.5$ and $\cot\alpha\cot\vartheta = 1$ for CD "A"
- A_{sw} is the area of the transversal reinforcement
- s is the distance between consecutive transversal stirrups

It should also be verified, for reasons ductility reasons, that V_{Rsd} is greater than V_{Rcd} .

According to § 7.4.6.1.2 of the DM2018, in the absence of more accurate analysis, it can be assumed that the length of the dissipative zone is the maximum of:

- the height of the cross section;
- $1/6$ of the effective height of the column;
- 45 cm;
- the free height of the column, if this is less than 3 times the height of the cross section.

According to § 7.4.6.2.2 of the DM2018, the following conditions must be guaranteed in dissipative zones:

- the bars at the corners of the cross-section have to be retained by the stirrups
- at least one bar over two, among the ones located at the sides, should be retained by the stirrups
- the non-retained bars should be located at less than 20 cm from the adjacent retained one for CD "A" and 15 cm for CD "B"

The diameter of the containment stirrups should be not less than 6 mm and their step must be no higher than the lesser of the following quantities:

- $1/3$ or $1/2$ of the minimum side of the cross section for CD "A" and CD "B";
- 175 mm for CD "B" or 125 mm for CD "A";
- 6 or 8 times the diameter of the longitudinal bars for CD "A" and CD "B".

In each column and across the entire length, two stirrups with two arms have been placed, for a total of four. The diameter of each stirrup is 8 mm with a step of 10 cm.

With this reinforcement value, all columns are verified.

3.7.6 Joints

The portion of the column where the latter connects the beam is known as a joint. It is crucial for the capacity design that the connection does not reach collapse before the surrounding beams and columns do. The

verifications mandate that the joint's maximal compression and tension do not exceed the concrete's strength.

The horizontal shear occurring on a joint, for each seismic direction, is calculated as follows according to DM2018's section 7.4.4.3.1:

- For internal joints

$$V_{jbd} = \gamma_{Rd}(A_{s1} + A_{s2})f_{yd} - V_c \quad (3.317)$$

- For external joints

$$V_{jbd} = \gamma_{Rd}A_{s1}f_{yd} - V_c \quad (3.38)$$

where:

- A_{s1} is the beam reinforcement in the upper chord
- A_{s2} is the beam reinforcement in the lower chord
- V_c is the shear that acts on top of the joint, at the level of the column
- γ_{Rd} overstrength factor, taken equal to 1.2 for CD “A” and 1.1 for CD “B”

The diagonal compression induced in the joint by the lattice mechanism must not be higher than the compressive strength of concrete; in the absence of a more accurate model, this requirement can be verified by the use of the following rule:

$$V_{jbd} \leq \eta f_{cd} b_j h_{jc} \sqrt{1 - v_d/\eta} \quad (3.39)$$

where:

- $\eta = \alpha_j(1 - f_{ck}/250)$ and α_j equal to 0.48 for external joints and 0.60 for internal
- $v_d = N_{Ed}/(A_c f_{cd})$ normalized compressive stress, acting in the column above the joint
- h_{jc} distance from the more external bars of the column
- b_j effective width of the joint, equal to the minimum between:
 - the maximum among the sides of column and beam cross-sections
 - the minimum between the sides of column and beam cross-section, both increased to half of the column's cross-section height

Due to the existence of transversal reinforcement it is possible to prevent diagonal cracking of the joint, however it is important to ensure that:

- For internal joints

$$A_{sh}f_{ywd} \geq \gamma_{Rd}(A_{s1} + A_{s2})f_{yd}(1 - 0.8v_d) \quad (3.40)$$

- For external joints

$$A_{sh}f_{ywd} \geq \gamma_{Rd}A_{s2}f_{yd}(1 - 0.8v_d) \quad (3.41)$$

There are a total of 4 stirrups, each with 2 arms, which have been incorporated in each joint. For all stirrups, the diameter is 8 mm, and the step is 5 cm.

All of the columns' results are validated using this reinforcement value.

3.7.7 Capacity design - Design solutions' summary

Below are summarized the main characteristics of the frame designed according to the method at the ultimate limit state, in compliance with the hierarchy of the resistances and the constructive limitations of Eurocodes and DM2018:

- Columns' cross section: 60 x 60 cm
- Beams cross section: 40x50 cm
- Columns reinforcement: transversal: stirrups with 4 arms, diameter 8 mm, steps 10 cm longitudinal: 12 bars with diameter 20 mm
- Beams reinforcement: transversal (dissipative zone): stirrups with 2 arms, diameter 8 mm, steps 7.5 cm transversal (non-dissipative zone): stirrups with 2 arms, diameter 8 mm, steps 15 cm longitudinal (dissipative zone): 3 bars with diameter 18 mm in the lower chord, 5 bars with diameter 18 mm in the upper chord longitudinal (non-dissipative zone): 3 bars with diameter 18 mm in the lower chord, 2 bars with diameter 18 mm in the upper chord
- Joints transversal reinforcement: stirrups with 4 arms, diameter 8 mm, steps 5 cm
- Concrete cover: 35 mm

3.7.8 Design characteristics of the improved frame

As was previously indicated, the second frame under examination does not have the same structural features as the original structure as has been previously explained. This is due to the fact that in earlier works of thesis, several design approaches were tested in an effort to improve the robustness of the same structure.

The various approaches are examined in the sections that follow, accompanied by a summary of the improved frame's structural properties.

3.7.9 Previous robustness evaluation's summary

Several analyses have indicated that the behavior of the frame as designed according to seismic capacity design is insufficient to prevent disproportionate collapse in the event of column removal. Particularly, the discontinuity between the dissipative and non-dissipative zones, in terms of reinforcement and concrete confinement, leads to the formation of plastic hinges in locations where they should not occur and the rupture of the longitudinal rebars, which is the most important factor in ensuring robustness.

Three key details have considerably enhanced the performance of the frame in response to column removal:

- **Continuity** of longitudinal bars along beams, which enhances ultimate displacement
- **Symmetry** of longitudinal beam bars between the upper and lower chords, which promotes flexural and membrane strength.
- **Equality** of longitudinal reinforcement between floors, which enhances flexural and membrane strength

The presence of these three circumstances necessitates the usage of 5Φ18 not only in the upper chord but also in the lower chord, continuously along the beams, and uniformly throughout all the floors. Hence, an increase of 10% in the column's longitudinal reinforcement will decide a 30% rise in

the column's resistance against removal.

After this, another test was conducted to examine the effects of increasing the number of bars to 7 Φ 18, continuing to follow to the aforementioned three requirements. This has led to an increase in the bending peak, but a decrease in the final displacement; as a consequence, the behaviour is now more fragile.

Another strategy has included the centralization of the bars, which was accomplished by lowering the effective height and increasing the concrete cover. This has revealed that there is a decline in resistance immediately after the bending peak, but that there is a delay in the resistance-fall in correspondence of the maximum displacement.

3.7.10 Robustness analysis - Design solutions' summary

The design solution chosen for the second frame in this project of thesis will be stated in the sections that follow, starting with the basic design feature and taking into account the findings of the research conducted on the same structure:

Columns cross section: 60 x 60 cm

Beams cross section: 40x50 cm

Column reinforcement:

transversal: stirrups with 4 arms, diameter 8 mm, steps 10 cm

longitudinal: 12 bars with diameter 20 mm

Beams reinforcement:

transversal (dissipative): stirrups with 2 arms, diameter 8mm, steps 7.5cm

transversal (non-dissipative): stirrups with 2 arms, diameter 8mm, steps 15cm

longitudinal: 5 bars with diameter 18 mm both in the upper and lower chord

Joints transversal reinforcement: stirrups with 4 arms, diameter 8 mm, steps 5cm

Concrete cover: 53 mm

Additionally, because the geometrical and material features, as well as the usage behavior of the structure, stay invariant, the loading characteristics do not vary in relation to the initial design. The distribution of the loads along beams is resumed as follows:

Permanent structural load G_1 for the slabs: 16 kN/m

Permanent non-structural load G_2 13 kN/m

Variable loads Q_p for the floors: 7.28 kN/m

Variable loads Q_c for the roofing: 1.82 kN/m

4 ATENA 2D

The ATENA software was utilized in two phases: first, for a pushdown analysis to evaluate the dynamic effect involved in the structure in the event of a sudden column loss; and second, for a reliability analysis.

4.1 The Software

ATENA 2D is a finite element software program designed for the analysis of reinforced concrete and masonry structures. It is widely used in civil engineering and construction for the assessment, design, and analysis of such structures.

ATENA 2D employs a range of advanced material models to accurately simulate the behavior of concrete and masonry structures, including material nonlinearity, cracking, and shear deformation. The software is capable of modeling different reinforcement types, including rebar, prestressing tendons, and fiber-reinforced polymers (FRP).

One of the key features of ATENA 2D is its ability to simulate the nonlinear behavior of concrete and masonry structures. The software uses advanced material models to simulate the behavior of these materials under various loading conditions. This allows users to simulate the behavior of concrete and masonry structures during seismic events, for example, or under other extreme conditions.

ATENA 2D also includes advanced modeling capabilities for analyzing the behavior of reinforced concrete and masonry walls, slabs, and beams.

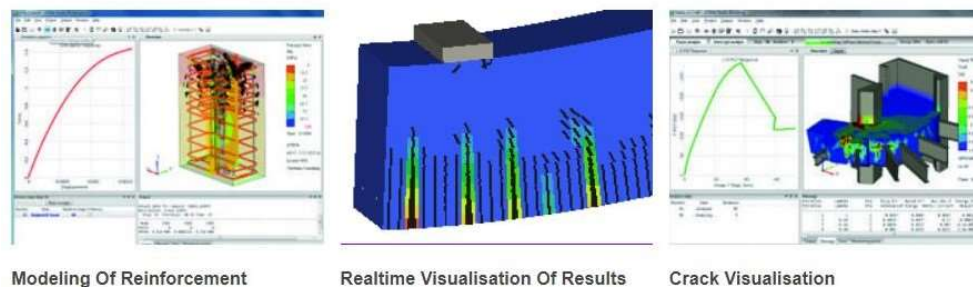


Figure 4.1: Main features of Athena 2D (www.cervenka.cz)

The software can model complex geometries and perform 2D simulations of structures subjected to different types of loading, such as point loads, distributed loads, and thermal loads.

ATENA is implemented to perform both two-dimensional and three-dimensional analysis; in the present case, the analysis was carried out using a flat model, for which the section of the ATENA 2D software was used.

The software is divided in two different interfaces: pre-processing, in which materials, geometry, loads, and analysis settings are configured, and post-processing, in which the structure's deformation, cracking condition, tensions, and deformations of the materials can be observed.

One advantage of ATENA 2D is the ability to manage the software without using a graphical interface but by writing a CCT file that can be imported. This file, which may be viewed using a text editor, includes alphanumeric instructions that define all of the input required by the program to perform the analysis. This method of progressing is very helpful for this thesis work since dealing with a sample of 100 distinct mechanical characteristic combinations is difficult when you have to input all of the various 100 combinations using a graphical interface.

Both techniques will be detailed in the following sections: by graphical interface and via CCT file.

4.2 Pre-processing

The pre-processing phase is the phase before the analysis in which all of the structural model's characteristics must be specified, which are represented by the materials, geometry, load cases, and analysis settings.

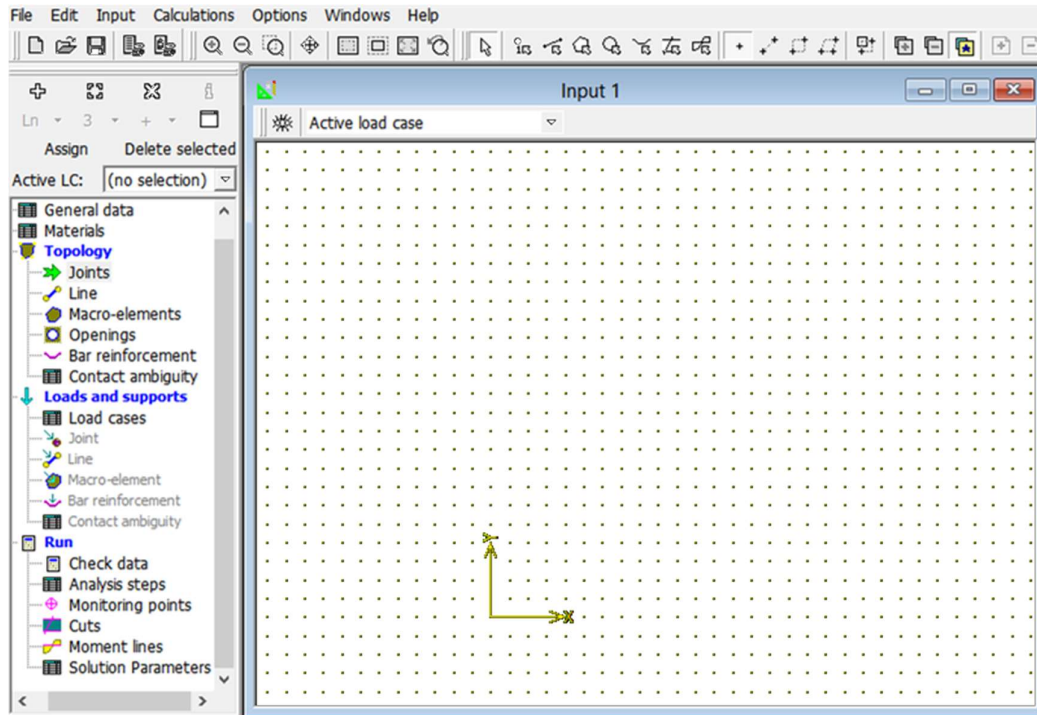


Figure 4.2: Atena 2D

4.2.1 Graphical interface

As was just said, the designer is able to operate inside a graphical environment that is easily accessible to users while using ATENA 2D. (Figure 4.2). You have the possibility to save, construct the mesh, perform the analysis, zoom in or out, choose points, lines, or macro parts, and a variety of other functions thanks to the icons that are organized horizontally on the upper portion of the interface. You have access to all of the instructions through a sliding bar on the left-hand side of the screen. This gives you the opportunity to specify in a logical order all of the input that is to be delivered to the software. The symbol that looks like an eye may be used to switch the visibility of many aspects of the design, including the points, the nodes, the lines, and the labels associated with them, among other elements.

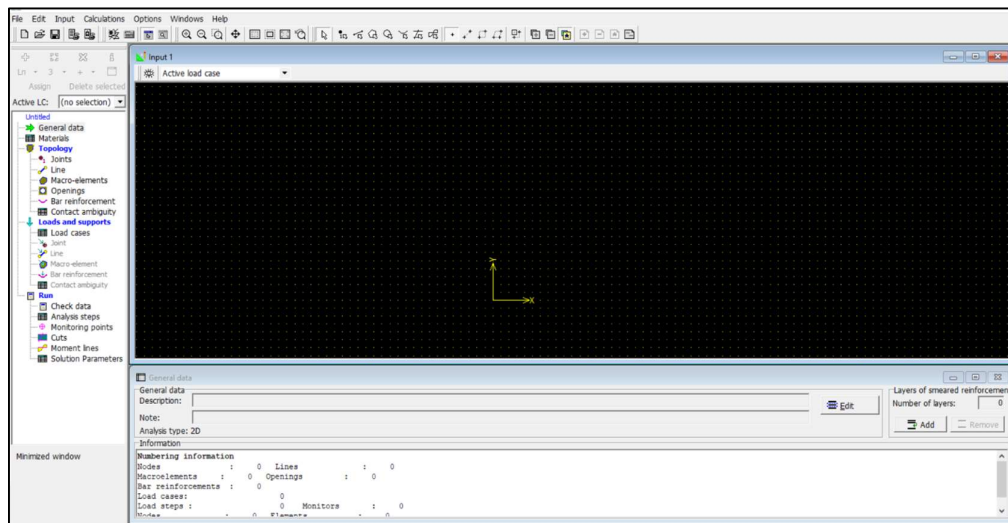


Figure 4.3: Graphical interface

Last but not least, the general data command enables users to give the project a name, add comments, specify the number of decimal points that will be applied, and obtain information regarding the number of nodes, lines, bar reinforcements, load cases.

4.2.2 Materials definition

In the *Materials* section it is possible to define the following types of materials:

- *Plane Stress Elastic Isotropic;*
- *Plane Strain Elastic Isotropic;*
- *3D Non Linear Cementitious;*
- *SBeta Material;*
- *Microplane4 Material;*
- *3D BiLinear Steel Von Mises;*
- *2D Interface |*
- *Reinforcement;*
- *Spring;*
- *Bond for Reinforcement;*
- *3D Drucker-Prager Plasticity;*
- *Material with Random Fields.*

Concrete, which is described with SBeta Material, and steel from reinforcing bars, which is defined with Reinforcement, are the materials that are used in the modelling of a structure made of reinforced concrete.

The term SBeta comes from the software in which this kind of material was initially utilised. It is an acronym for StahlBETonAnalyse, which translates to "analysis of reinforced concrete" from the German language. The SBeta material has the following concrete behaviour effects:

- Non-linear behaviour in compression including hardening and softening
- Fracture of concrete in tension
- Biaxial strength failure criterion
- Reduction of compressive strength and shear stiffness after cracking
- Tension stiffening effect
- Two crack models: fixed crack direction and rotated crack direction

Figure 4.4: Definition of the fundamental concrete characteristics

Material characterization in ATENA 2D is done by defining parameters in five different sections:

- *Basic*, in which the tangent elastic modulus E , the Poisson coefficient μ , the tensile strength f_t and the compressive strength must be defined f_c .
- *Tensile*, where it is possible to choose the traction model of concrete between exponential, linear and local deformation; there is also to define the softening parameter c_3 and the slit model, which can be fixed

or rotated.

Figure 4.5: Concrete's traction model definition

- *Compression*, in which is required the definition of the compression deformation value at the compressive strength (uniaxial test), the coefficient of reduction of the compressive strength due to cracking, the type of *softening* law, and the *softening* parameter c_d .

Figure 4.6: Concrete's compression law definition

- *Shear*, where you have to choose a reduction model of the fixed or variable shear modulus, and the type of compression-tension interaction, which can be linear or described by two different hyperbolic laws.

Name:

Basic | Tensile | Compressive | **Shear** | Miscellaneous

Shear retention factor :

Tension-compression interaction:

Variable shear retention

Material #: f_cu- = 3.000E+01 [MPa]

Figure 4.7: Concrete's shear behaviour definition

- *Miscellaneous*, in which you have to introduce the specific material gravity ρ and the thermal expansion coefficient α .

Name:

Basic | Tensile | Compressive | Shear | **Miscellaneous**

Specific material weight ρ : [MN/m³]

Coefficient of thermal expansion α : [1/K]

Material #: f_cu- = 3.000E+01 [MPa]

Figure 4.8: Concrete's specific gravity and thermal expansion coefficient definition

There are two different ways to describe the type of reinforcement material: discretely or diffusely. Discrete armour is made of reinforcing bars that are shaped by placing the start and end points. Diffuse reinforcement is thought of as a part of the composite material it is made of.

In both situations, the software takes into account the "constitutive law" of the monoaxial test, which is used for all types of steel and can be modelled as linear, bilinear, multilinear, or bilinear with hardening. In the Basic section, four parameters—the elastic modulus E , the yield stress σ_y , the breaking voltage t , and

the *limit deformation* ϵ_{lim} —are needed to define the latter

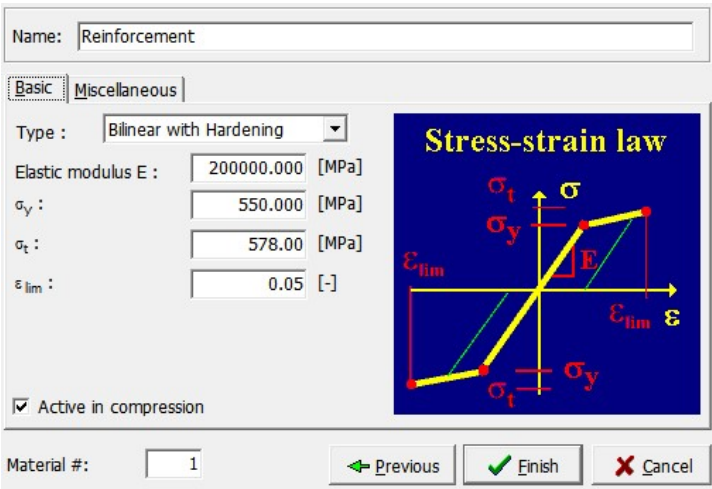


Figure 4.9: Steel's fundamental parameters definition

In the *Miscellaneous* section, the specific gravity of the material ρ and the coefficient of thermal expansion α must be defined.

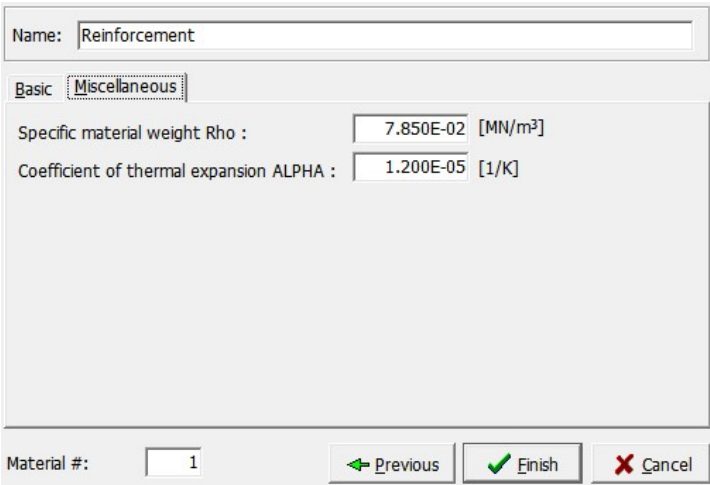


Figure 4.10: Steel's specific gravity and thermal coefficient definition

4.2.3 CCT material description

In addition to the methods previously described, it is also possible to specify the properties and behaviour of the materials by writing a CCT file, which can be read by any text reader. The CCTs for the seven new materials in the model are listed below.

BEG_MAT 1	BEG_MAT 2	BEG_MAT 3	BEG_MAT 4
VER_MAT 0	VER_MAT 0	VER_MAT 0	VER_MAT 0
NAME "Travi D"	NAME "Travi ND"	NAME "Pilastro"	NAME "Nodi"
TYPE "CCSBETAMaterial"	TYPE "CCSBETAMaterial"	TYPE "CCSBETAMaterial"	TYPE "CCSBETAMaterial"
E 3.400E+04	E 3.364E+04	E 3.527E+04	E 3.700E+04
Mu 0.200	Mu 0.200	Mu 0.200	Mu 0.200
Ft 2.560E+00	Ft 2.560E+00	Ft 2.560E+00	Ft 2.560E+00
Fc -3.626E+01	Fc -3.501E+01	Fc -4.099E+01	Fc -4.809E+01
ISOFT 3.0	ISOFT 3.0	ISOFT 3.0	ISOFT 3.0
C3 7.524E-04	C3 7.604E-04	C3 7.253E-04	C3 6.913E-04
Eps_C -3.380E-03	Eps_C -2.990E-03	Eps_C -4.860E-03	Eps_C -7.090E-03
CompRed 0.800	CompRed 0.800	CompRed 0.800	CompRed 0.800
CSOFT 2.0	CSOFT 2.0	CSOFT 2.0	CSOFT 2.0
Cd 0.072	Cd 0.089	Cd 0.050	Cd 0.018
Shear Variable	Shear Variable	Shear Variable	Shear Variable
CS 0.6	CS 0.6	CS 0.6	CS 0.6
Rho 2.500E-02	Rho 2.500E-02	Rho 2.500E-02	Rho 2.500E-02
Alpha 1.200E-05	Alpha 1.200E-05	Alpha 1.200E-05	Alpha 1.200E-05
END_MAT 1	END_MAT 2	END_MAT 3	END_MAT 4

Figure 4.11: Material's CCT command description

BEG_MAT 5	BEG_MAT 6
VER_MAT 0	VER_MAT 0
NAME "CLS-NC"	Func_Type 4
TYPE "CCSBETAMaterial"	xvalues 0.000E+00 2.445E-03 2.000E-01 2.020E-01
E 3.271E+04	yvalues 0.000E+00 4.890E+02 5.620E+02 0.000E+00
Mu 0.200	NAME "ACC-B450C"
Ft 2.560E+00	TYPE "CCReinforcement"
Fc -3.187E+01	RHO 0.000E+00
ISOFT 3.0	ALPHA 1.200E-05
C3 7.822E-04	COMPRESSION 1
Eps_C -2.000E-03	END_MAT 6
CompRed 0.800	BEG_MAT 7
CSOFT 2.0	VER_MAT 0
Cd 0.097	NAME "Piastra"
Shear Variable	TYPE "CCPlaneStressElastIsotropic"
CS 0.6	E 5.000E+05
Rho 2.400E-02	Mu 0.300
Alpha 1.200E-05	Rho 0.000E+00
END_MAT 5	Alpha 1.200E-05
	END_MAT 7

Figure 4.12: Material's CCT command description

4.2.4 Geometrical definition

In ATENA 2D, the geometry of reinforced concrete parts is described in the Topology section by joints, lines connecting the different joints, and macro-elements between many lines.

4.2.4.1 Joints

The points are specified in the Joints portion, where the X and Y coordinate values are requested, as shown in Figure 4.13; there is also the option to insert

springs at each designated point.

Topology

X-coordinate: [m]

Y-coordinate: [m]

Mesh refinement

Refinement type:

Springs

Direction	Material

Joint # :

Figure 4.13: Joints definition

Working on the CCT file, as seen in Figure 4.14, is a much simpler method for inserting all the joints than repeatedly clicking on the joints tab.

BEG_JOINTS		
COUNT	20	
1	0.0000	0.0000
2	0.0530	0.0000
3	0.3000	0.0000
4	0.5470	0.0000
5	0.6000	0.0000
6	0.0000	0.6000
7	0.0530	0.6000
8	0.3000	0.6000
9	0.5470	0.6000
10	0.6000	0.6000
11	0.0000	2.1000
12	0.0530	2.1000
13	0.3000	2.1000
14	0.5470	2.1000
15	0.6000	2.1000
16	0.0000	2.7500
17	0.0530	2.7500
18	0.3000	2.7500
19	0.5470	2.7500
20	0.6000	2.7500
END_JOINTS		

Figure 4.14: CCT command for joint definition

4.2.4.2 Lines

Even for the lines, it is possible to make springs that function on the full length of the lines themselves. The lines are established in the Line subsection, which is where the markers of the start and finish points are inserted (Figure 4.15).

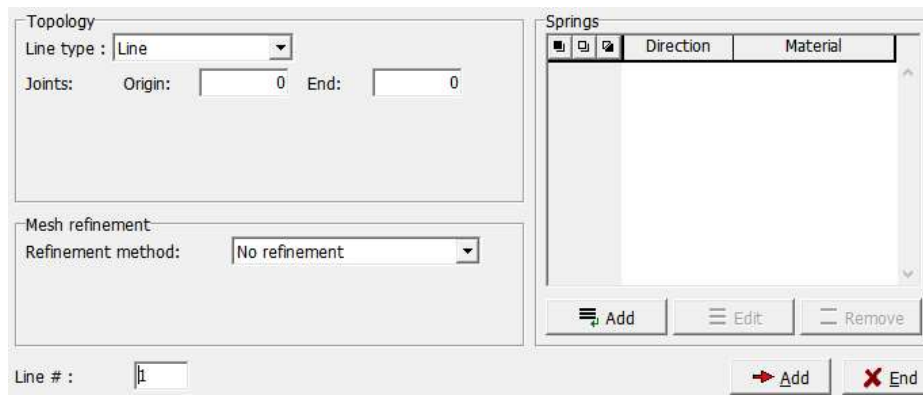


Figure 4.15: Lines' definition

Acting on the CCT file:

```

BEG_LINES
COUNT 10
  1 LI      1      2
  2 LI      2      3
  3 LI      3      4
  4 LI      4      5
  5 LI      1      6
  6 LI      2      7
  7 LI      3      8
  8 LI      4      9
  9 LI      5     10
 10 LI      6      7
END_LINES

```

Figure 4.16: CCT command for line definition

4.2.4.3 Macro-elements

In the Macro-elements subsection, macro-elements are generated through the following steps: the request of a Boundary list, which is the list of markers of the lines that enclose the element; the selection of the type of mesh, which can be triangular, quadrilateral, or mixed; the selection of the size of the mesh; the selection of the material; and the selection of the thickness. Figure 4.17 illustrates these steps.

Topology
Boundary list:

FE mesh
Mesh type:
Element size: [m]
☒ Smooth element shapes

Properties
Material:
Thickness: [m]
Quadrilateral elements:
☒ Geometrically nonlinear

Layers of smeared reinforcement

Layer	Material of reinf. layer

No. of smeared reinf. layers should be entered within general data.

Macro-element #:

Figure 4.17: Definition of macro-elements

A further illustration of a CCT format is provided here (Figure 4.18). On the left and side, the definition of the macro-element is presented as follows: the first number is the marker of the macro-element, the second number is the marker of the material, the third number is the thickness, the remaining four numbers are the Boundary List lines, and the final NON LINEAR stands for the geometrically non-linearity. The properties of the mesh are specified on the right-hand side of the image; the first number indicates the mark of the macro-element, and the numbers 0–100 denote the mesh size

BEG_MACROELEMENTS					BEG_MACROELEMENTS				
COUNT	10				COUNT	10			
1	5	0.6000	1,5-6,10	NONLINEAR	1	QUAD	0.1000	REFINE	ISOQUAD
2	3	0.6000	2,6-7,11	NONLINEAR	2	QUAD	0.1000	REFINE	ISOQUAD
3	3	0.6000	3,7-8,12	NONLINEAR	3	QUAD	0.1000	REFINE	ISOQUAD
4	5	0.6000	4,8-9,13	NONLINEAR	4	QUAD	0.1000	REFINE	ISOQUAD
5	5	0.6000	10,14-15,19	NONLINEAR	5	QUAD	0.1000	REFINE	ISOQUAD
6	3	0.6000	11,15-16,20	NONLINEAR	6	QUAD	0.1000	REFINE	ISOQUAD
7	3	0.6000	12,16-17,21	NONLINEAR	7	QUAD	0.1000	REFINE	ISOQUAD
8	5	0.6000	13,17-18,22	NONLINEAR	8	QUAD	0.1000	REFINE	ISOQUAD
9	5	0.6000	19,23-24,28	NONLINEAR	9	QUAD	0.1000	REFINE	ISOQUAD
10	3	0.6000	20,24-25,29	NONLINEAR	10	QUAD	0.1000	REFINE	ISOQUAD
END_MACROELEMENTS					END_MACROELEMENTS				

Figure 4.18: CCT command for Macro-elements definition and mesh characteristics

4.2.4.4 Bar Reinforcements

At this point, diffuse reinforcements may be defined by using the Layers of smeared reinforcement sub-window.

In contrast to this, discrete reinforcing bars are described in the Reinforcement part by the material, the coordinates of the start and end points (Figure 4.20), the area of the bar section, and the interaction between steel and concrete, which may be regarded to be of complete adherence, or you can model

are via a specific bond (Figure 4.19).

Reinforcement: Normal

Topology: Properties

Basic parameters

Material: (undefined)

Area: 0.000E+00 [m²] Calculate section area

☒ Geometrically nonlinear

Reinforcement bond

Connection to the material: perfect connection

Bar perimeter: 0.000E+00 [m]

Bond material: (undefined)

☐ Disable slip at bar beginning

☐ Disable slip at bar end

Reinforcement bar: 1

Add End

Figure 4.19: Definition of the reinforcement area and the interaction with concrete

Reinforcement: Normal

Topology: Properties

Segment type: Polyline of straight segments

Seg.#	Segment type	Point		Center		Radius	Dir
		X [m]	Y [m]	X [m]	Y [m]	Rs [m]	Dir.
1	Origin	0.0000	0.0000				
2	Line	0.0000	1.0000				

Add

Insert

Edit

Remove

Items: 2

Reinforcement bar: 1

Add End

Figure 4.20 Defining the position of the reinforcing bars

4.2.5 Loads and supports

Within this chapter, it is possible to design a new load case and apply it to all of the components, including Joints, Line, Macro-element, Bar reinforcement, and Contact ambiguity.

It is possible to add seven distinct kinds of load cases when using Atena 2D. These load cases include body force, forces, supports, prescribed deformation,

temperature, shrinkage, and pre-stressing.

The overall process of defining the load cases will be discussed in the following paragraphs.

4.2.5.1 Supports

It is important to establish a new load case called Supports to fix the columns' bases (Figure 4.21).

The lines that work as the foundation of the columns must then be assigned to them, which requires that you first click on the load case's set active button and then choose the Line tab located in the Loads and supports area of the software's main interface.

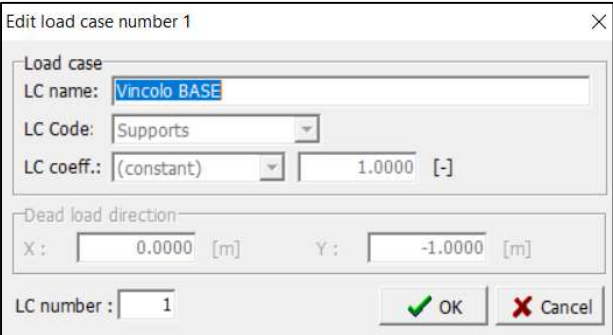


Figure 4.21: Fixed support load case definition

Defining the fixed directions in this window is required (both X and Y for the specific case of a fixed support).

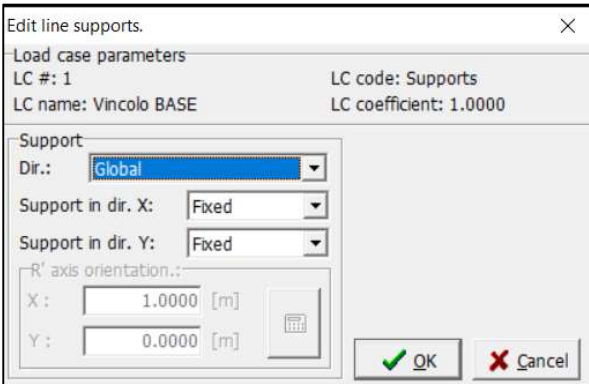


Figure 4.22: Supports load case application

Writing on the CCT file works almost in the same way. The line mark (1736 in this example) and fixed direction must be defined (both X and Y).

```

BEG_LOADCASE
NO 1
NAME "Vincolo BASE"
CODE SU
COEFTYPE CONST
COEFFICIENT 1.0000
BEG_JOINTLOAD
COUNT 0
END_JOINTLOAD
BEG_LINELOAD
COUNT 1|
1736 -1 GLOB FIXD FIXD
END_LINELOAD
END_LOADCASE

```

Figure 4.23: CCT command for Supports load case definition

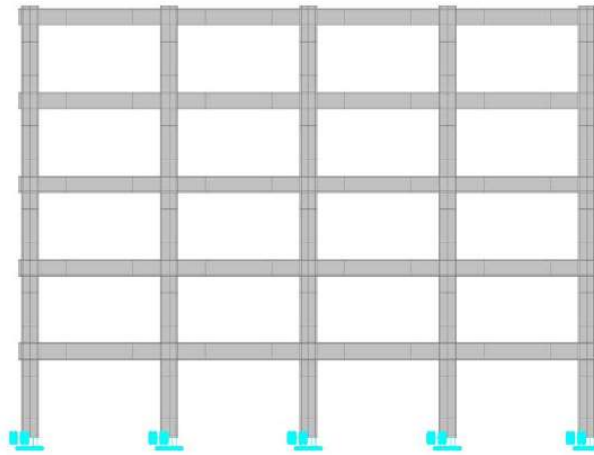


Figure 4.24: 2D frame illustration

4.2.5.2 Body force

This load case is absolutely necessary in order to determine the structure's self-weight. The information that need to be provided are the load case name, the load case code and the direction in which the dead load should be applied. In contrast to the earlier scenario, it is not necessary to apply this load case to elements of the structure such as joints, lines, or macro-elements because the software already identifies its application to the entire structure.

Figure 4.25: *Body force load case* introduction

```

BEG_LOADCASE
NO 2
NAME "Peso proprio"
CODE SW
COEFTYPE CONST
COEFFICIENT 0.0000
DIRECTION 0.0000 -1.0000
END_LOADCASE

```

Figure 4.26: CCT commands for *Body force load case* introduction

4.2.5.3 Forces

This load case includes distributed loads such permanent structural and non-structural loads, live loads, and column response before removal.

To assign the load case to lines, press the set active button again, pick the lines, and fill out the Edit line loading window. Choose from Continuous whole length, Point load, Partial, and Quadrilateral line forces. Choose the load direction (global Y along line) and value with the proper sign.

Figure 4.27: *Forces load case* introduction

Edit line loading.

Load case parameters
 LC #: 3
 LC name: Perm strutt
 LC code: Forces
 LC coefficient: 0.0000

Line forces
 Type: Continuous full length Dir.: Global Y, along line
 Value f: -1.600E-02 [MN/m]
 Force orientation:
 X: 0.0000 [m]
 Y: 0.0000 [m]

The length of the shortest selected line: 2.4000 [m]

OK Cancel

Figure 4.28: Forces load case allocation

Another option is to write the load to the CCT file:

```

BEG_LOADCASE
NO 3
NAME "Perm strutt"
CODE F0
COEFTYPE CONST
COEFFICIENT 0.0000
BEG_JOINTLOAD
COUNT 0
END_JOINTLOAD
BEG_LINELOAD
COUNT 120
278 -1 COFL GLYA -1.600E-02
END_LINELOAD
END_LOADCASE

```

Figure 4.29: CCT commands Forces load case allocation

Finally, it is possible to display the chosen load condition:

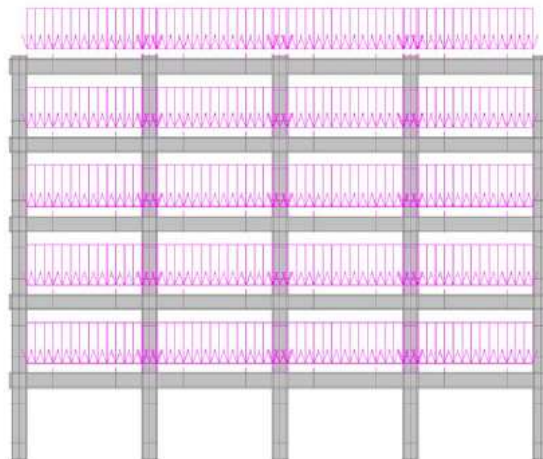


Figure 4.30: distributed line loads applied to 2D frame

4.2.5.4 Prescribed deformation

For the objectives of this thesis study, the specified deformation load scenario has been employed to conduct the pushover analysis. In the Edit prescribed displacements window, you can specify the entity of the prescribed deformation.

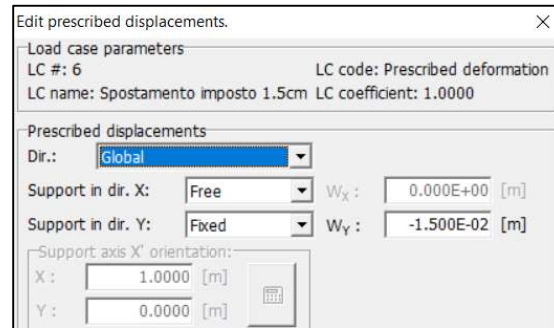


Figure 4.31: *Prescribed deformation load case* allocation to the junction above the main column

Lastly, Figure 4.32 shows the command to be used in the CCT file:

```
BEG_LOADCASE
NO 6
NAME "Spostamento imposto 1.5cm"
CODE DF
COEFTYPE CONST
COEFFICIENT 1.0000
BEG_JOINTLOAD
COUNT 1
963 -1 GLOB FREE FIXD -1.500E-02
END_JOINTLOAD
BEG_LINELOAD
COUNT 0
END_LINELOAD
END_LOADCASE
```

Figure 4.32: CCT command for allocation of *Prescribed deformation load case*

4.2.6 Analysis settings

The analysis settings are defined in the *Run* section; in particular, the main subsections are represented by the *Check data*, *Analysis steps* and the *Monitoring points*.

The *Check data* tab is a tool that enables you to conduct a quick check of the model to see if there are any problems, as detailed in the other subsections (materials, topology, load and supports and load steps).

The individual steps of the analysis are created by clicking on *Add* in the *Analysis steps* subsection; here the list of *Load cases* to be considered in the analysis and the type of nonlinear calculation, which can be *Standard Newton-Raphson* and *Standard arc length*, is requested: in Figure4.33 a possible sequence of steps of the analysis is illustrated:

Number	Load case list	Coefficient [-]	Parameters analysis	Save results	Calculated results
1	1,6,8	1.0000	Standart Newton	Yes	Not analyzed
2	1,6,8	1.0000	Standart Newton-R	Yes	Not analyzed
3	1,6,8	1.0000	Standart Newton-R	Yes	Not analyzed
4	1,6,8	1.0000	Standart Newton-R	Yes	Not analyzed
5	1,6,8	1.0000	Standart Newton-R	Yes	Not analyzed
6	1,6,8	1.0000	Standart Newton-R	Yes	Not analyzed
7	1,6,8	1.0000	Standart Newton-R	Yes	Not analyzed
8	1,6,8	1.0000	Standart Newton-R	Yes	Not analyzed
9	1,6,8	1.0000	Standart Newton-R	Yes	Not analyzed

Figure 4.33: Examples of analysis steps

Figure 4.39 shows how a CCT can be built to describe the load steps. In that example, LC 1 and LC2 are applied in 5 load steps with a multiplier of 0.2, so that the complete entity of both load cases is applied at the fifth load step. The first number represents the load step marker, the second the multiplier, the third the kind of solution parameter, and the final two the load case markers.

```

BEG_CALCSTEPS
COUNT 5
  1 0.2000 1 F T 1,2
  2 0.2000 1 F T 1,2
  3 0.2000 1 F T 1,2
  4 0.2000 1 F T 1,2
  5 0.2000 1 F T 1,2
END_CALCSTEPS

```

Figure 4.34: CCT commands for Analysis steps implementation

The monitoring points are specific points of the model, where you want to know for example the displacement or the nodal reaction

With the setting of the monitoring points, any curves to be checked in the *post-processing* phase are automatically chosen: each component will have a value for each step in the analysis, which can be related to all the other components in the form of graphs, which can be for example force-displacement curves or curves displacement-displacement.

4.2.7Parameters

This last significant option essentially indicates the procedures and settings for the iterative nonlinear solution of the equilibrium equations at each load step.

Two essential solution approaches are available: Newton-Raphson and Arc Length. The latter should be used for force loading up to near peak load or in post peak, meanwhile the former should be utilized in all other instances. The error tolerances, or limitations for different criteria, are shown in the final four rows of the General tab. If these restrictions are respected, the iteration ends and the computation proceeds to the next phase.

The screenshot shows the 'New solution parameters' dialog box with the 'General' tab selected. The 'Line Search' tab is also visible. The 'Conditional Break Criteria' tab is not selected. The 'Title' field is 'Solution Parameters'. The 'Solution method' is 'Newton-Raphson'. The 'Optimize node numbers' is 'Sloan'. The 'Update Stiffness' is 'Each iteration'. The 'Stiffness Type' is 'Tangent'. The 'Iteration number limit' is '40'. The 'Displacement error tolerance' is '0.010000 [-]'. The 'Residual error tolerance' is '0.010000 [-]'. The 'Absolute residual error tolerance' is '0.010000 [-]'. The 'Energy error tolerance' is '0.000100 [-]'. There is a checked box for 'Line search'.

Figure 4.35: Solution parameters (General solution)

Both methods may have conditional break conditions specified to terminate the calculation if an error exceeds the given tolerance multiplied by the prescribed factor shown in Figure 4.36.

The screenshot shows the 'New solution parameters' dialog box with the 'Conditional Break Criteria' tab selected. The 'General' and 'Line Search' tabs are also visible. The table below shows the break criteria for different error types.

	Break immediately	Break after step	
Displacement error multiple:	10000.0	1000.0	[-]
Residual error multiple:	10000.0	1000.0	[-]
Absolute residual error multiple:	10000.0	1000.0	[-]
Energy error multiple:	1000000.0	10000.0	[-]

Figure 4.36: Solution parameters (Conditional Break-Criteria section)

4.3 Post-processing

After providing the software all of the inputs required to do the fem analysis, the next stages are mesh generation and finite element analysis.

They must be completed, necessarily in that sequence, by clicking on the corresponding Menu Calculations icons. As the analysis begins, post-processing is enabled, and only tools for graphical post-processing are available. Furthermore, ATENA 2D enables the graphically solution visualisation not only at the analysis conclusion but also in real time at the end of each load step.

Figure 4.37 shows all of the available tools in the post-processing phase. It is possible to pick a particular load step and visually observe all the potential outcomes in terms of Springs, Forces MNQ, Cracks, Bar reinf., Interfaces, Scalars, Vectors, and Tensors.

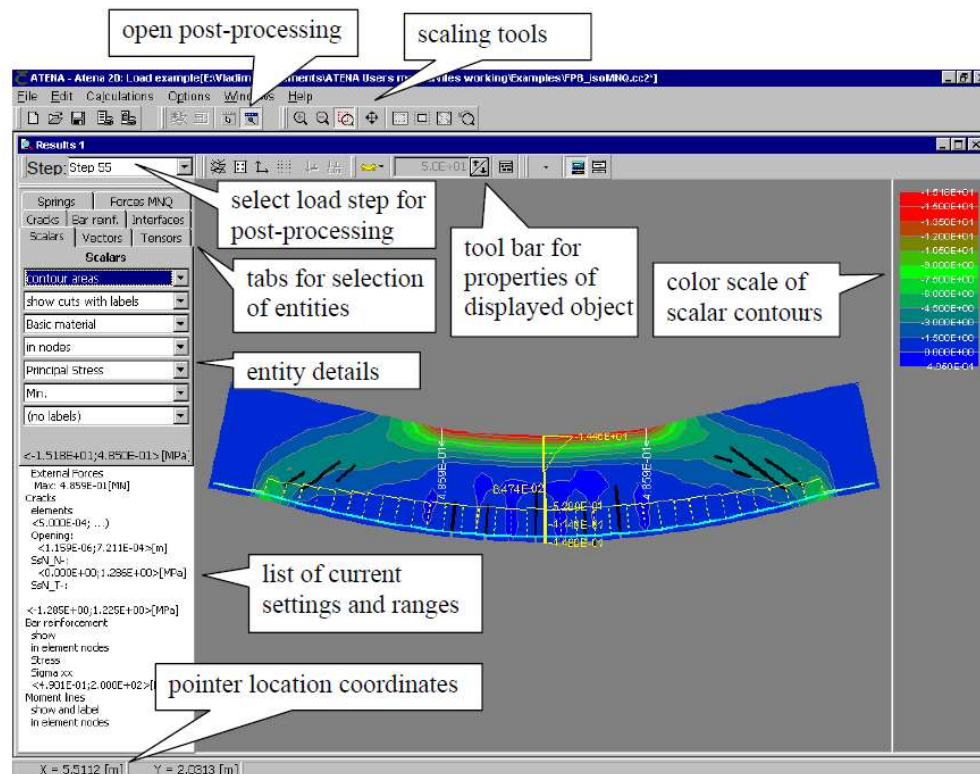


Figure 4.37: Post processing visualization

4.3.1 Outputs

When you click on the Text printout button, a data tree structure appears, allowing you to generate a significant quantity of output data. Another option is to export a CCO file containing the results of all the step of monitoring points specified in the pre-processing phase.

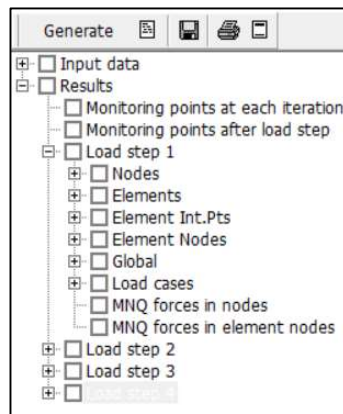


Figure 4.38: Text printout button

5 Fundamental variables sampling

The JCSS – Probabilistic Model Code [3] and the fib Model Code 2010 [2] are the reference code guidelines that must be followed in order to successfully complete the sampling of the fundamental variables. In addition, a method known as the Probabilistic Method, which was described in fib MC 2010 [8], was used. This method involves conducting a number of non-linear finite element analyses (NLFEAs) while using a sampling strategy, such as the Latin Hypercube Sampling used here. In summary, this method involves selecting a random data point from each of the N divisions that result from splitting the cumulative density function associated with a standard distribution into an equal number of parts.

The resistance basic variables that has been sampled are:

- Concrete compressive strength f_c
- Reinforcement yield strength f_y
- Reinforcement ultimate strength f_u
- Reinforcement ultimate strain ε_{su}
- Reinforcement elastic modulus E_s

The action basic variables that has been sampled are:

- Reinforced concrete specific-weight ρ
- Permanent structural load G_1
- Permanent non-structural load G_2
- Floor variable loads Q_p
- Roofing variable loads Q_c

Using the MATLAB command "X_LHS=*lhsnorm*(MU,C,N)," the LHS was calculated for each of the $n=10$ variables in the dataset. This function requires the following data inputs in order to operate properly:

- MU is a vector ($1 \times n$) which contains the mean values (or the logarithmic mean or 0) for each variable. More details will be followingly explained.
- $[C]_{n \times n} = [D * Ro * D]_{n \times n}$ is a matrix ($n \times n$), where $[D]_{n \times n}$ is a diagonal matrix ($n \times n$) which contains on the diagonal the variances (or the

logarithm of the variances or 1) for each basic variable and $[Ro]_{n \times n}$ is the covariance matrix. More details are followingly explained.

- N is the number of samples for each basic variable, chosen equal to 100.
- $[X_{LHS}]_{N \times n}$ is a $(N \times n)$ matrix which contains in each column the $[X_{LHS,i}]_{N \times 1}$ vector coming as an output from the sampling and $i = 1, 2, 3, \dots, 10$, since ten are the basic variables.

Based on the analysed fundamental variable, three kinds of distributions have been utilised:

- **Normal distribution:** as the LHS approach works on a Normal CDF, the mean and variance values to enter in the MU vector and D matrix are the same as the distribution. Hence, the output of the generic basic variable $[X_{LHS,i}]_{N \times 1}$ corresponds to the sample vector $[X_{sam,i}]_{N \times 1}$ of the generic basic variable X_i
- **Lognormal distribution:** the logarithm of the mean and variance of the generic basic variable X_i must be computed in accordance with the following formula, where $X_{m,i}$ is the mean of the generic basic variable and V_i is its coefficient of variation:

$$MU_i = \ln(X_{m,i}) - \log(V_i^2) \quad (5.1)$$

$$D_{ii} = \sqrt{\log(V_i^2 + 1)} \quad (5.2)$$

When the LHS sampling generates the $[X_{LHS,i}]_{N \times 1}$ vector, the exponential function must be applied to the generic basic variable X_i to connect the LHS output, which is normally distributed, to the lognormally distributed basic variable.

- **Gumbel distribution:** the values for the mean and variance that are supposed to be entered into the MU vector and the D matrix are assumed to be equal to 0 and 1 respectively, considering the distribution as a standardised normal

distribution. Following that, in order to return to a Gumbel distribution, the vector that includes the samplings of the generic basic variable X_i is generated from the output of the LHS sampling in the following manner:

$$X_{sam,i} = -\ln(-\ln(\Phi^{-1}(X_{LHS,i}) * \vartheta_2) \quad (5.3)$$

where Φ^{-1} is the cumulative density function of the standard normal distribution and $\vartheta_{1,i}$ and $\vartheta_{2,i}$ are the two parameters of the Gumbel distribution that may be obtained as follows:

$$\vartheta_{2,i} = \sigma_i * \sqrt{6}/\pi \quad (5.4)$$

$$\vartheta_{1,i} = X_{m,i} - 0.5772 * \sigma_i * \sqrt{6}/\pi \quad (5.5)$$

with $X_{m,i}$ being the mean value of the generic basic variable and σ_i being its variance.

Last but not least, the covariance matrix C includes every correlation coefficient that exists between the variables that were sampled. If the coefficient is 0, there is no correlation between the two variables; if it is 1, the correlation is as high as it can be (i.e. between the same variable). The table that follows presents the results of a correlation analysis between the following variables:

Table 5.1: Correlation coefficients [-]

	f_c	f_y	f_u	ε_{su}	E_s	ρ	G_1	G_2	Q_p	Q_c
f_c	1	0	0	0	0	0	0	0	0	0
f_y	0	1	0.75	-0.45	0	0	0	0	0	0
f_u	0	0.75	1	-0.6	0	0	0	0	0	0
ε_{su}	0	-0.45	-0.6	1	0	0	0	0	0	0
E_s	0	0	0	0	1	0	0	0	0	0
ρ	0	0	0	0	0	1	0	0	0	0
G_1	0	0	0	0	0	0	1	0	0	0
G_2	0	0	0	0	0	0	0	1	0	0
Q_p	0	0	0	0	0	0	0	0	1	0
Q_c	0	0	0	0	0	0	0	0	0	1

It is worthwhile to note that, in accordance with the Fb Model Code 2010 [8], there is a positive correlation between the yielding of steel and its ultimate strength, whilst there is a negative association between the ultimate strain and the ultimate strength. It can be also noticed that when there is no correlation—that is, when one is working with variables that are not related to one another—the coefficient is equal to zero.

In the following, particulars relating to the distribution, mean value, and variance of each fundamental variable will be discussed.

5.1 Action fundamental variables

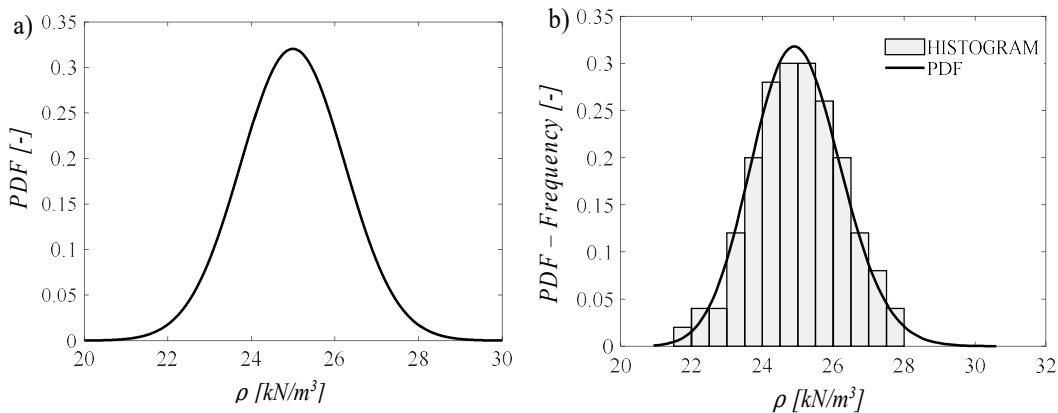
5.1.1 Reinforced-concrete specific-weight ρ

The specific weight of reinforced concrete is a normal distribution, as stated by the JCSS – Probabilistic Model Code [3], and it has the following characteristics:

$$\rho \sim N(\rho_m, V_\rho) \quad (5.66)$$

where $\rho_m = 25 \text{ kN/m}^3$ is the mean value of the normal distribution for reinforced-concrete specific-weight, according to EC2, while $V_\rho = \sigma_\rho / \rho_m = 0.05$ is the coefficient of variation.

The concrete specific-weight, that is the part occupying the concrete cover, is taken as the value assumed by the sampled reinforced concrete specific-weight minus one, since it is a dependent variable.



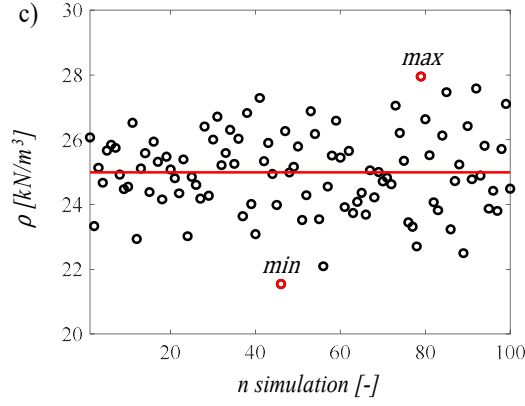


Figure 5.1: Reinforced concrete specific-weight - Normal distribution: a) Probability density function; b) Histogram and Distribution fit; c) Scatter plot

The dependence relationship between the reinforced concrete self-weight (independent variable) and the concrete self-weight (dependent variable) is shown in the following image.

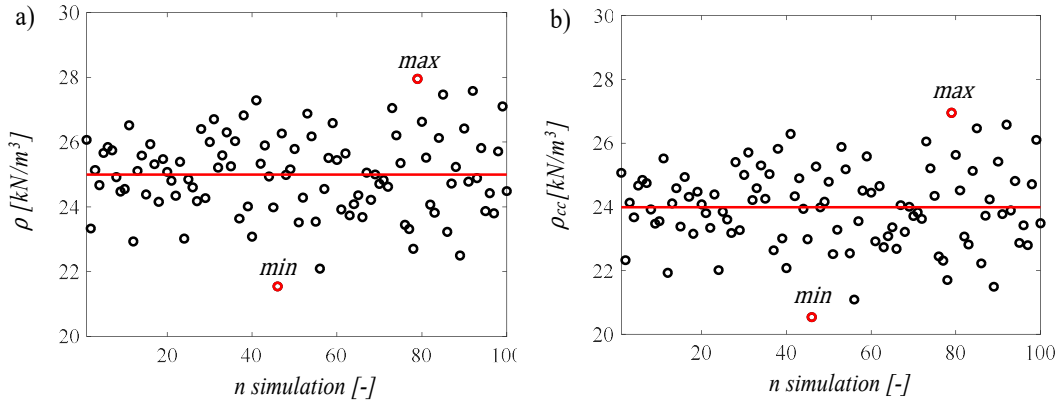


Figure 5.2: Scatterplots for specific weight: a) reinforced concrete (independent sampled variable); b) concrete cover (dependent variable)

5.1.2 Permanent structural load of the slab G_1

The permanent structural load is described as a normal distribution with the following parameters by the JCSS – Probabilistic Model Code [3], which may be considered here:

$$G_1 \sim N(G_{1m}, V_{G_1}) \quad (5.7)$$

The normal distribution for the permanent structural load of the slab is

assumed to have a mean value of $G_{1m} = 16 \text{ kN/m}$, with a coefficient of variation of $V_{G_1} = \sigma_{G_1}/G_{1m} = 0.05$.

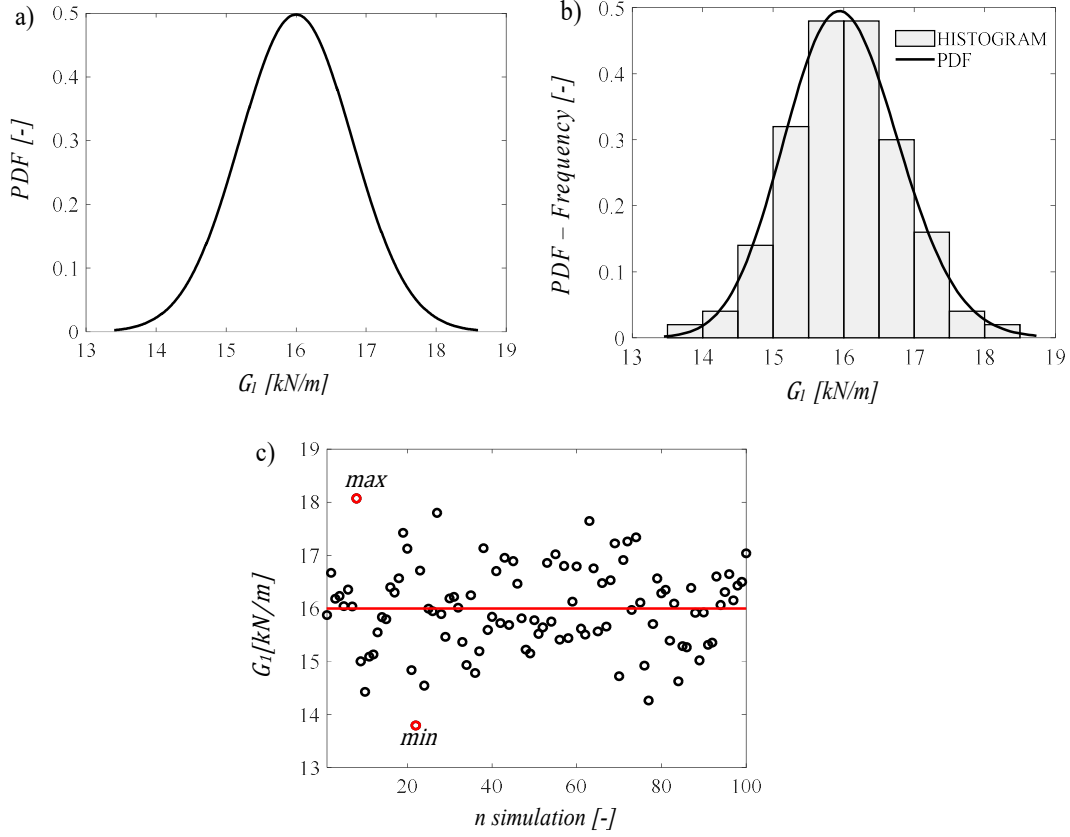


Figure 5.3: Permanent structural load - Normal distribution: a) Probability density function; b) Histogram and Distribution fit; c) Scatter plot

5.1.2.1 Permanent non-structural load G_2

The permanent non-structural load is a normal distribution with the following parameters, as described by JCSS - Probabilistic Model Code [3]:

$$G_2 \sim N(G_{2m}, V_{G_2}) \quad (5.8)$$

The normal distribution for the permanent structural load of the slab is assumed to have a mean value of $G_{2m} = 13 \text{ kN/m}$, with a coefficient of variation of $V_{G_2} = \sigma_{G_2}/G_{2m} = 0.05$

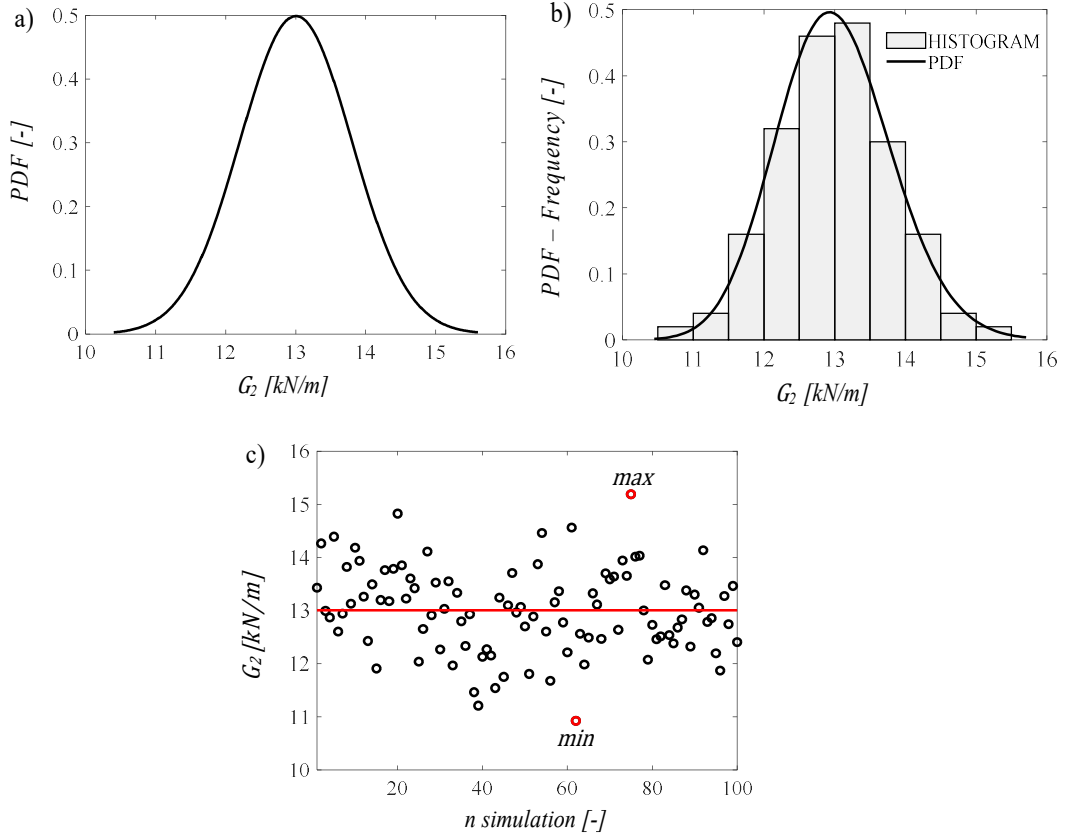


Figure 5.4: Permanent non-structural load - Normal distribution: a) Probability density function; b) Histogram and Distribution fit; c) Scatter plot

5.1.3 Floor variable loads Q_p

The floor's fluctuating loads follow the next Gumbel distribution, as described by the JCSS - Probabilistic Model Code [3]:

$$Q_p \sim \text{Gumbel}(Q_{p_m}, V_{Q_p}, \vartheta_{1Q_p}, \vartheta_{2Q_p}) \quad (5.9)$$

In this case, the mean value of the Gumbel distribution for the variable floor loads is $Q_{p_m} = 7.28 \text{ kN/m}$.

In addition, Q_{c_m} represents also the characteristic value (i.e. fractile 98 percent) of the design value equal to 10 kN/m. The coefficient of variation $V_{Q_p} = \sigma_{Q_p}/Q_{p_m} = 0.20$, and the parameters of the Gumbel distribution $\vartheta_{2Q_p} = 1.0136$ and $\vartheta_{1Q_p} = 5.91$, are calculated using Equations (5.4) and (5.5), respectively.

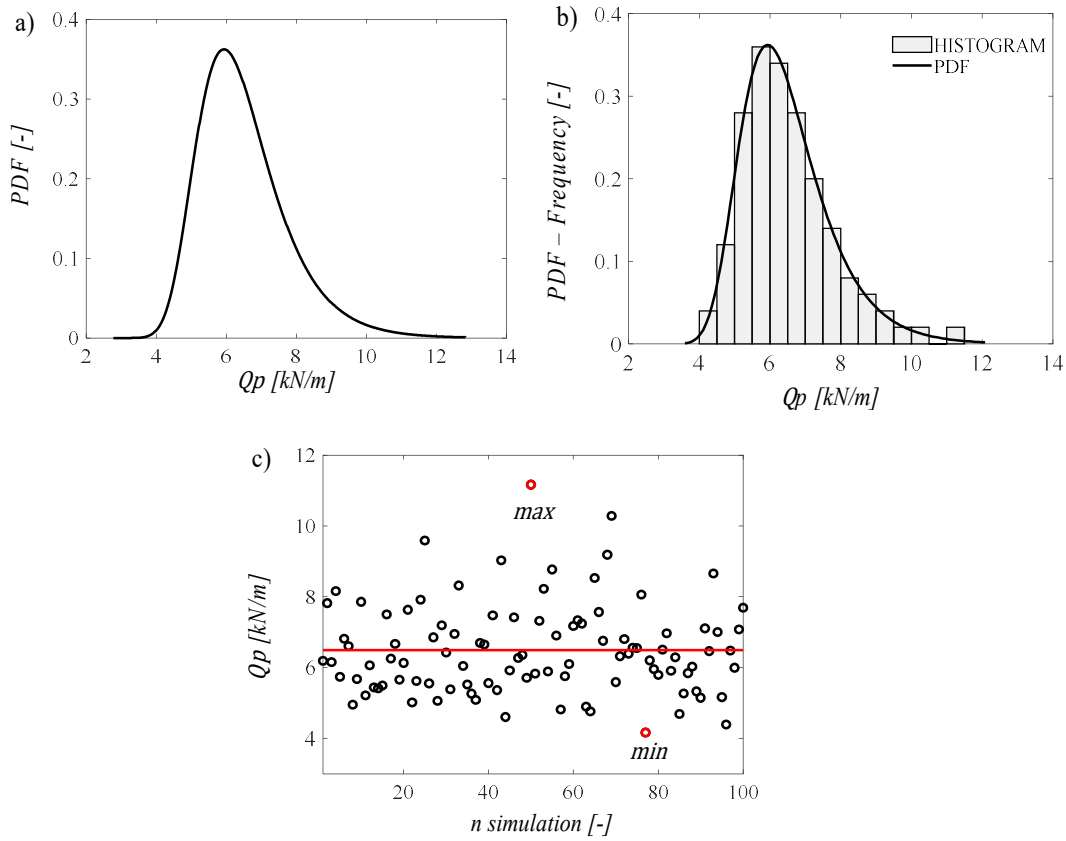


Figure 5.5: Floor variable load - Gumbel distribution: a) Probability density function; b) Histogram and Distribution fit; c) Scatter plot

5.1.4 Roofing variable loads Q_c

The roofing variable loads follow the next Gumbel distribution, as described by the JCSS - Probabilistic Model Code [3]:

$$Q_c \sim \text{Gumbel}(Q_{c_m}, V_{Q_c}, \vartheta_{1_{Q_c}}, \vartheta_{2_{Q_c}}) \quad (5.10)$$

In this case, the mean value of the Gumbel distribution for the variable floor loads is $Q_{c_m} = 1.82 \text{ kN/m}$. In addition, Q_{c_m} represents also the characteristic value (i.e. fractile 98 percent) of the design value equal to 2.5 kN/m . The coefficient of variation $V_{Q_p} = \sigma_{Q_p} / Q_{p_m} = 0.20$, and the parameters of the Gumbel distribution $\vartheta_{2_{Q_c}} = 0.249$ and $\vartheta_{1_{Q_c}} = 1.46$, are calculated using Equations (5.4) and (5.5), respectively.

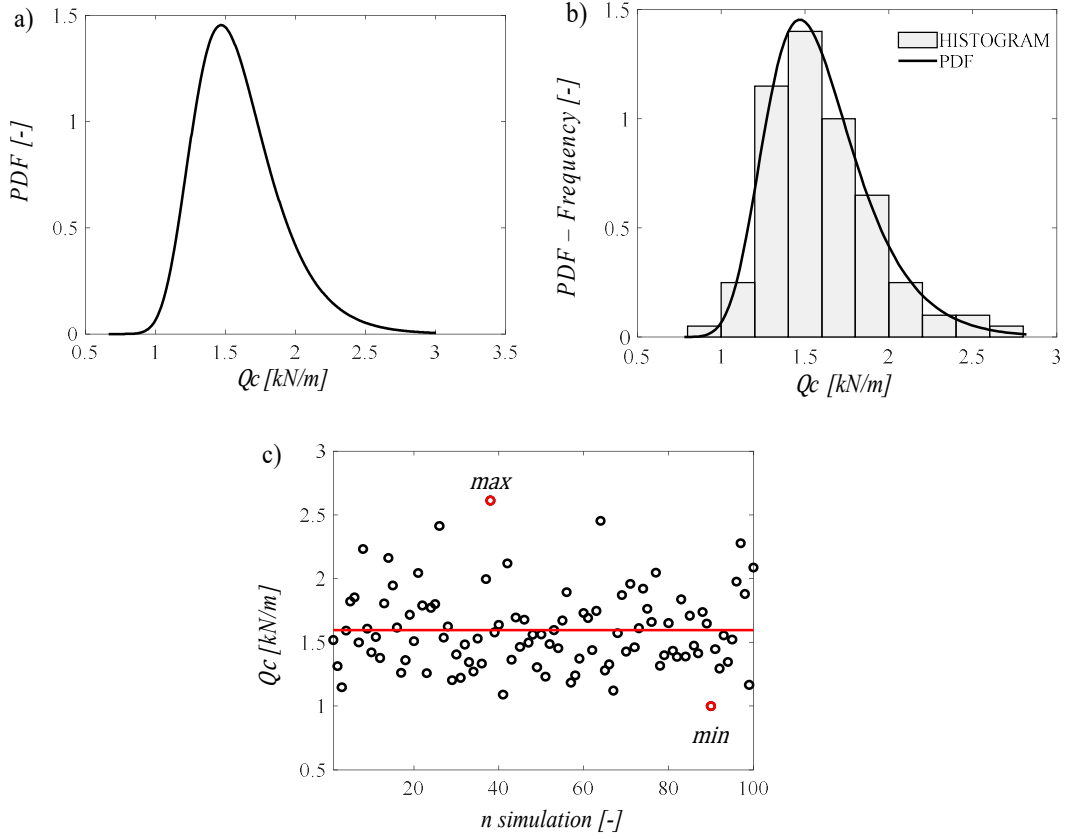


Figure 5.6: Roofing variable load - Gumbel distribution: a) Probability density function; b) Histogram and Distribution fit; c) Scatter plot

5.2 Resistance basic variables

5.2.1 Concrete compressive strength f_c

The concrete compressive strength is a lognormal distribution with the following properties, as described by JCSS - Probabilistic Model Code [3]:

$$f_c \sim \text{LN}(f_{cm}, V_c) \quad (5.11)$$

where f_{cm} is the mean value for the lognormal distribution of concrete cylinder compressive strength determined in accordance with EC2 [28] and, $V_c = \sigma_c / f_{cm} = 0.15$ is the coefficient of variation:

$$f_{cm} = f_{ck} \exp(1.645 V_c) \quad (5.12)$$

$f_{ck} = 0.83 * R_{ck}$ is the characteristic compressive cylinder strength of concrete after 28 days, where R_{ck} is the characteristic compressive cube strength, which is equivalent to 30 MPa for C25/30. As a consequence of this, we may deduce that $f_{ck} = 24.9 \text{ MPa}$ and $f_{cm} = 31.87 \text{ MPa}$ respectively.

In terms of everything else that has to do with concrete, such as its elastic modulus, E_c , its tensile concrete strength, f_{ct} , its compressive strain at the peak stress, ϵ_{co} , and its ultimate compressive strain, ϵ_{cu} , etc., these are all examples of aleatory dependent variables. Since the values of these variables are related to the independent fundamental variable, f_c , there is no need to take samples of them at this point of the process.

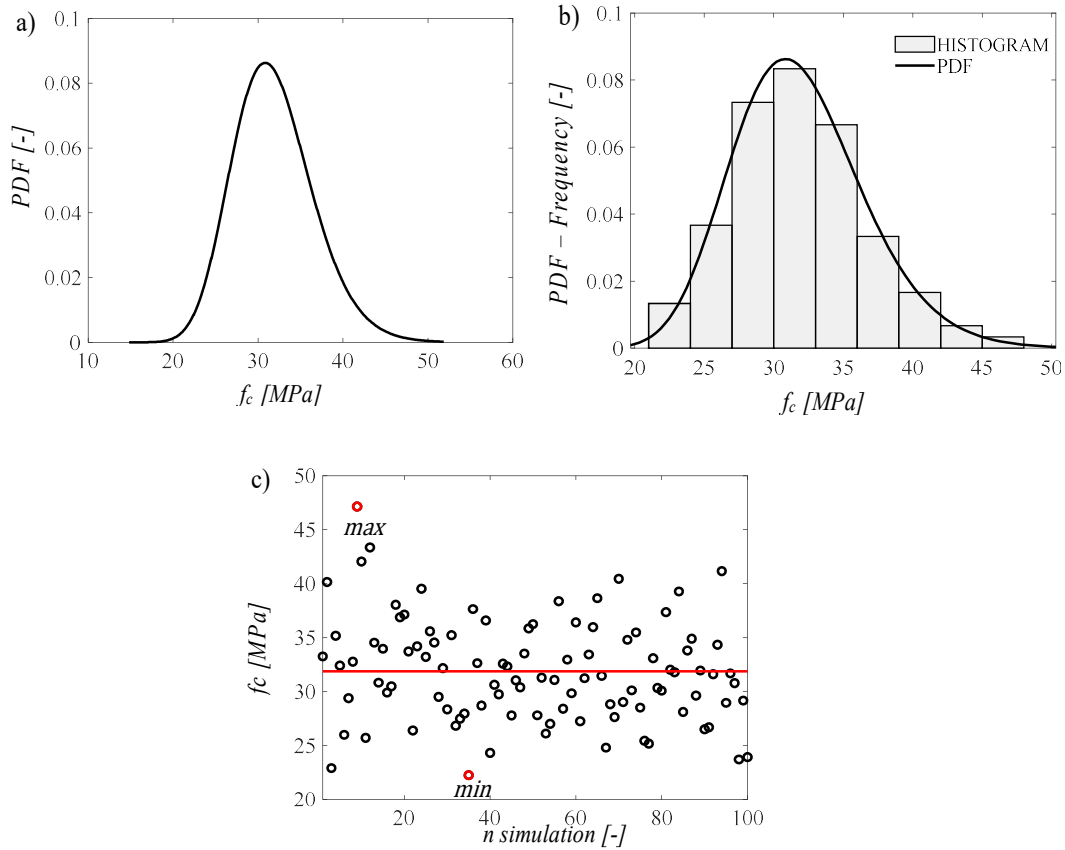


Figure 5.7: Concrete compressive strength - Lognormal distribution: a) Probability density function; b) Histogram and Distribution fit; c) Scatter plot

5.2.2 Reinforcement yield strength f_y

The reinforcement yielding strength is a lognormal distribution with the

following properties, as described by JCSS - Probabilistic Model Code [3]:

$$f_y \sim \text{LN}(f_{ym}, V_{sy}) \quad (5.13)$$

where f_{ym} is the mean value determined in accordance with EC2 [28] and, $V_{sy} = \sigma_{sy}/f_{ym} = 0.05$ is the coefficient of variation:

$$f_{ym} = f_{yk} \exp(1.645 V_{sy}) \quad (5.14)$$

with f_{yk} the characteristic yield strength of reinforcement, equal to 450 MPa for steel B450C. Thus, it results that $f_{ym} = 488.58$ MPa.

f_{yk} . Is the reinforcement's typical yield strength, equivalent to 450 MPa for steel B450C. So we can obtain $f_{ym} = 488.58$ MPa.

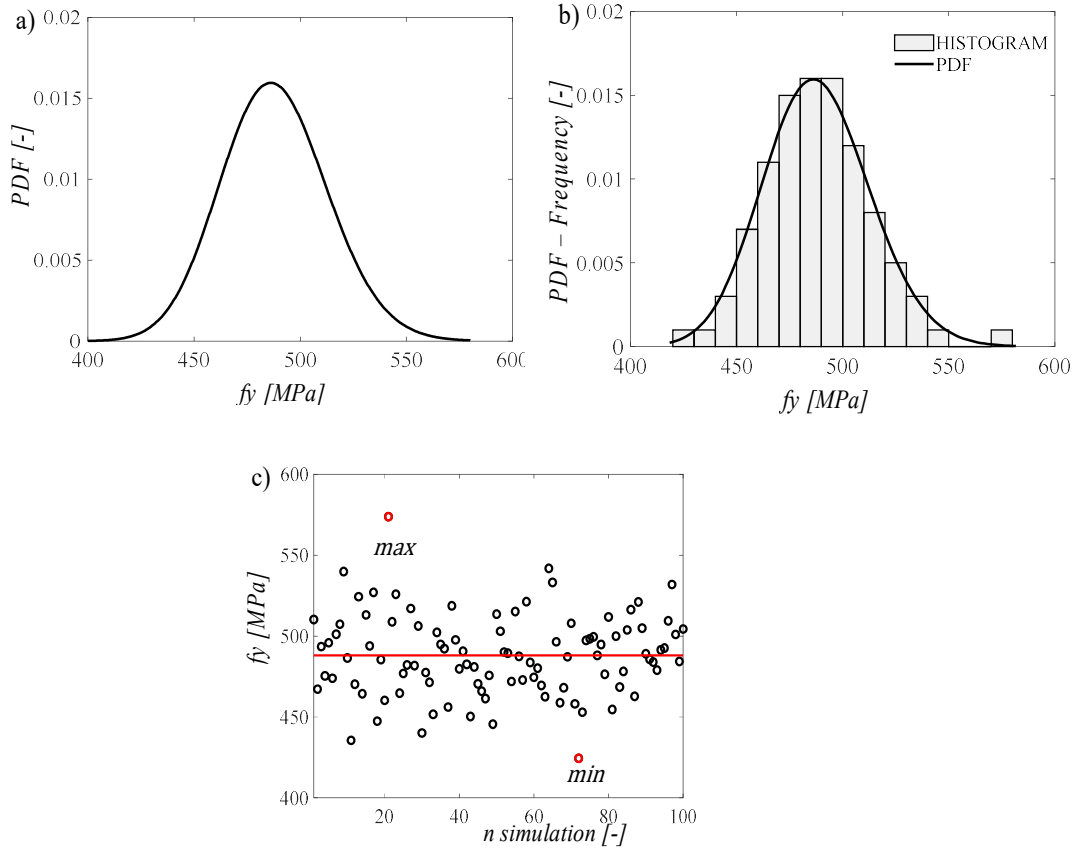


Figure 5.8: Steel yield strength - Lognormal distribution: a) Probability density function; b) Histogram and Distribution fit; c) Scatter plot

5.2.3 Reinforcement ultimate strength f_u

The reinforcement ultimate strength is a lognormal distribution with the following properties, as described by JCSS - Probabilistic Model Code [3]:

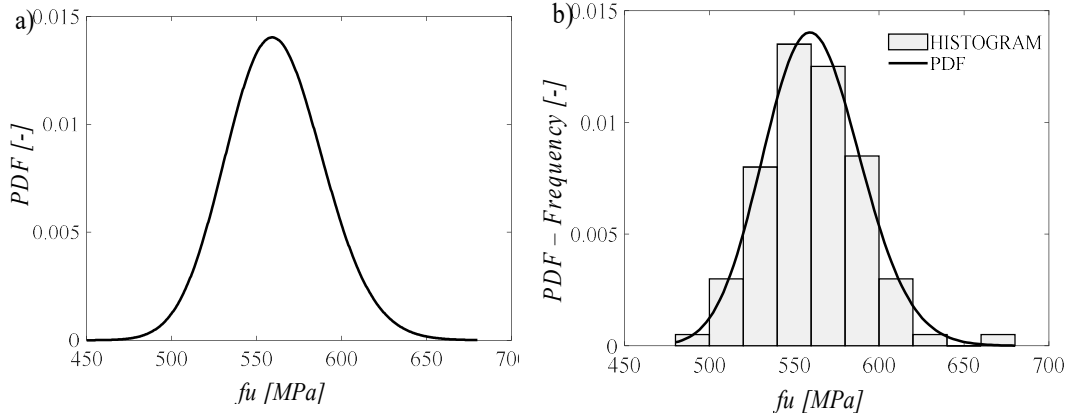
$$f_u \sim \text{LN}(f_{um}, V_{su}) \quad (5.15)$$

where f_{um} is the mean value determined with the following expression and $V_{su} = \sigma_{su}/f_{um} = 0.05$ is the coefficient of variation:

$$f_{um} = f_{ym}(1 + k) \quad (5.76)$$

with f_{ym} the mean value for the yield strength of reinforcement and $k = 0.15$ is a coefficient that determines the relation between the yield and the ultimate strength of concrete. Thus, it results that $f_{um} = 561.86 \text{ MPa}$.

with $k = 0.15$ being a coefficient that defines the link between the yield and the ultimate strength of concrete, and f_{ym} being the mean value for the yield strength of reinforcement. As a consequence of this, we may deduce that f_{um} equals 561.86 MPa.



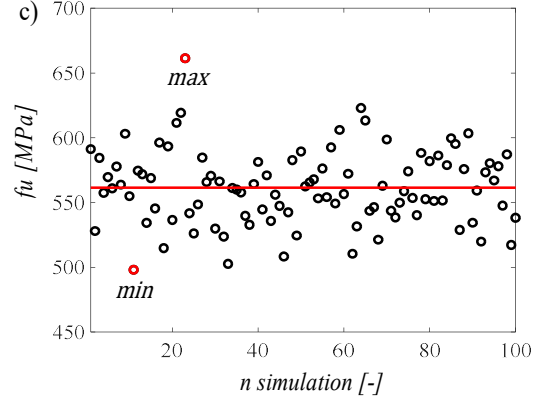


Figure 5.9: Steel ultimate strength - Lognormal distribution: a) Probability density function; b) Histogram and Distribution fit c) Scatter plot

5.2.4 Reinforcement ultimate strain ϵ_{su}

The ultimate strain for reinforcement is a lognormal distribution with the following properties, as described by JCSS - Probabilistic Model Code [3]:

$$\epsilon_{su} \sim \text{LN}(\epsilon_{sum}, V_{su}) \quad (5.16)$$

The coefficient of variation, $V_{su} = \sigma_{su}/\epsilon_{sum} = 0.09$, is obtained from many papers in the literature ([35], [36], [37], [38], and [39]), where studies on steel samples were performed. Furthermore, the ultimate strain is assumed to $\epsilon_{sum} = 0.14$, contradicting the specified value in Eurocodes (i.e. 7.5 percent). This is because the structure was created using robustness criteria, hence a greater, more realistic number should be used.

Caprili and Salvatore [40] give results from a large experimental test campaign conducted on several types of steel reinforcing bars, providing support for the 14% result. We give table 4 from the aforementioned study, which contains the ultimate strain experimental results for B450C $\phi 16$ (represented by the symbol A_{gt} [%]):

Table 5.2: Mechanical properties of tested rebars (monotonic tensile tests).

Steel grade/diameter/process/producer	R_m [MPa]	σ_{Rm}	R_e [MPa]	σ_{Re}	R_m/R_e	$\sigma_{Rm/Re}$	A [%]	σ_A	A_{gt} [%]	σ_{Agt}
B450C-16-TEMP-R Prod.1(1)	640.5	32.2	537.3	27.1	1.19	0.01	23.9	1.3	8.9	1.10
B450C-16-TEMP-R Prod.1(2)	542.7	3.10	446.7	1.90	1.21	0.00	30.3	2.4	15.4	1.70
B450C-16-TEMP-R Prod.1(3)	615.4	2.50	517.8	5.60	1.19	0.01	25.4	0.2	13.8	1.50
B450C-16-TEMP-R Prod.2	601.1	4.80	479.3	14.6	1.25	0.03	28.8	0.5	17.5	1.62

The average may be calculated using data from Table 5.2:

$$\varepsilon_{sum} = \frac{\sum A_{gt}}{4} = \frac{8.9+15.4+13.8+17.5}{4} = 13.9\% \cong 14\% \quad (5.17)$$

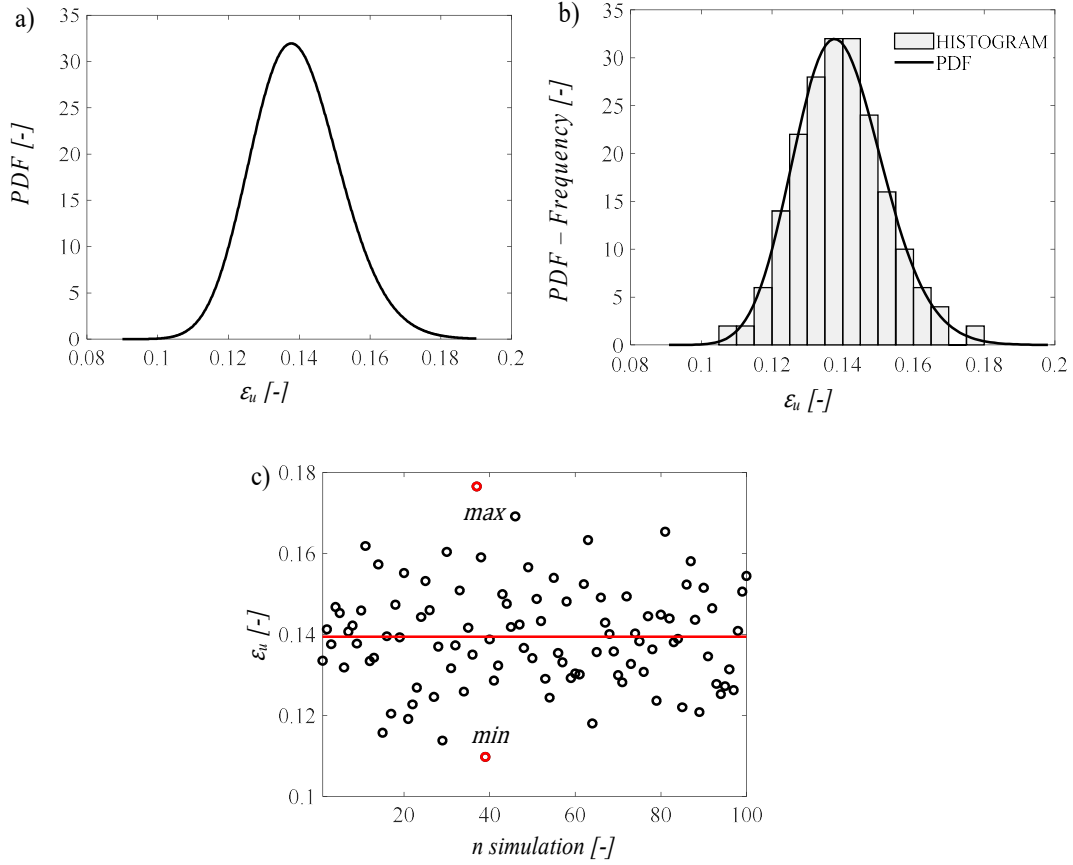


Figure 5.10: Steel ultimate strain - Lognormal distribution: a) Probability density function; b) Histogram and Distribution fit; c) Scatter plot

5.2.5 Reinforcement Elastic Modulus E_s

The Elastic Modulus for reinforcement is a lognormal distribution with the following properties, as described by JCSS - Probabilistic Model Code [3]:

$$E_s \sim \text{LN}(E_{sm}, V_{E_s}) \quad (5.18)$$

where $E_{sm} = 210000 \text{ MPa}$ is the mean value of the lognormal distribution for the Elastic Modulus, according to EC2, while $V_{E_s} = \sigma_{E_s}/E_{sm} = 0.03$ is the

coefficient of variation.

Where $V_{E_s} = \sigma_{E_s}/E_{sm} = 0.03$ is the coefficient of variation and $E_{sm} = 210000 \text{ MPa}$ is the mean value determined in accordance with EC2 [28].

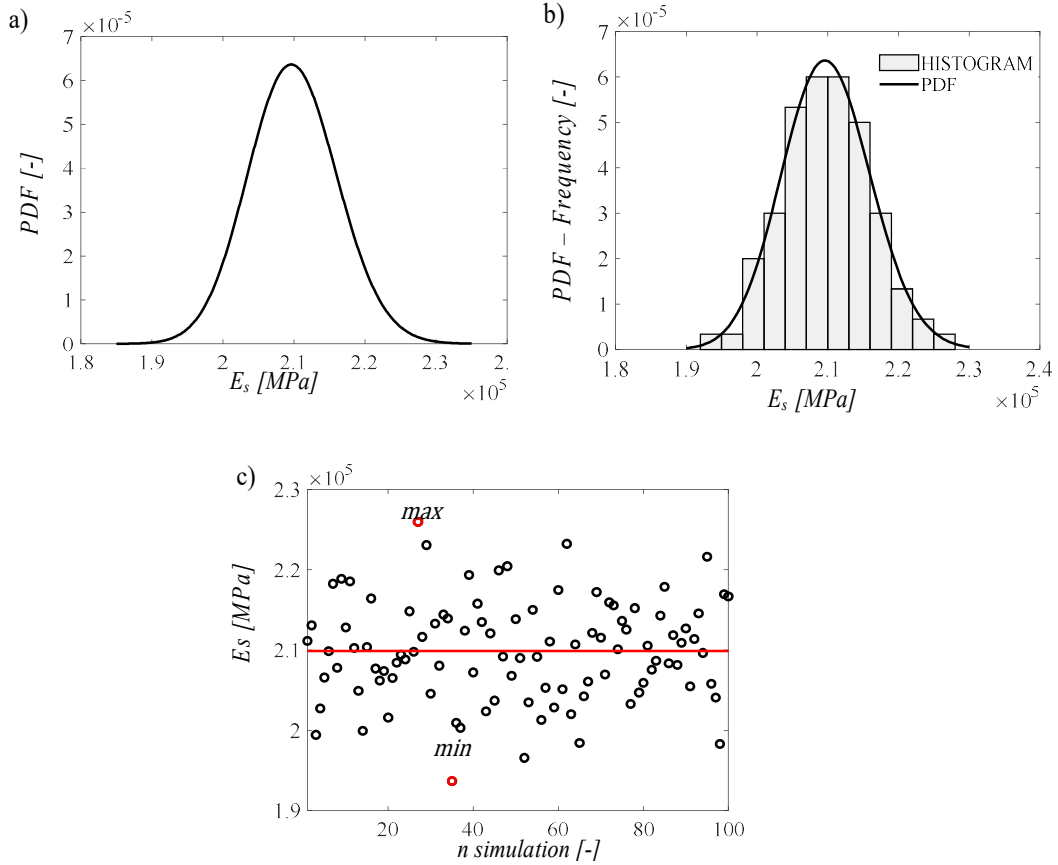


Figure 5.11: Steel Elastic Modulus - Lognormal distribution: a) Probability density function; b) Histogram and Distribution fit; c) Scatter plot

5.3 Correlation coefficients

The correlation coefficients between the four fundamental of reinforcement characteristics are examined more below. Following the Fib Model Code 2010, here there are the parameters that, for the particular scenario, demonstrate a correlation that is not equal to zero. The correlation coefficients are shown in the table below:

Table 5.3: Correlation coefficients [-]

	f_y	f_u	ε_{su}	E_s
f_y	1	0.75	-0.45	0
f_u	0.75	1	-0.6	0
ε_{su}	-0.45	-0.6	1	0
E_s	0	0	0	1

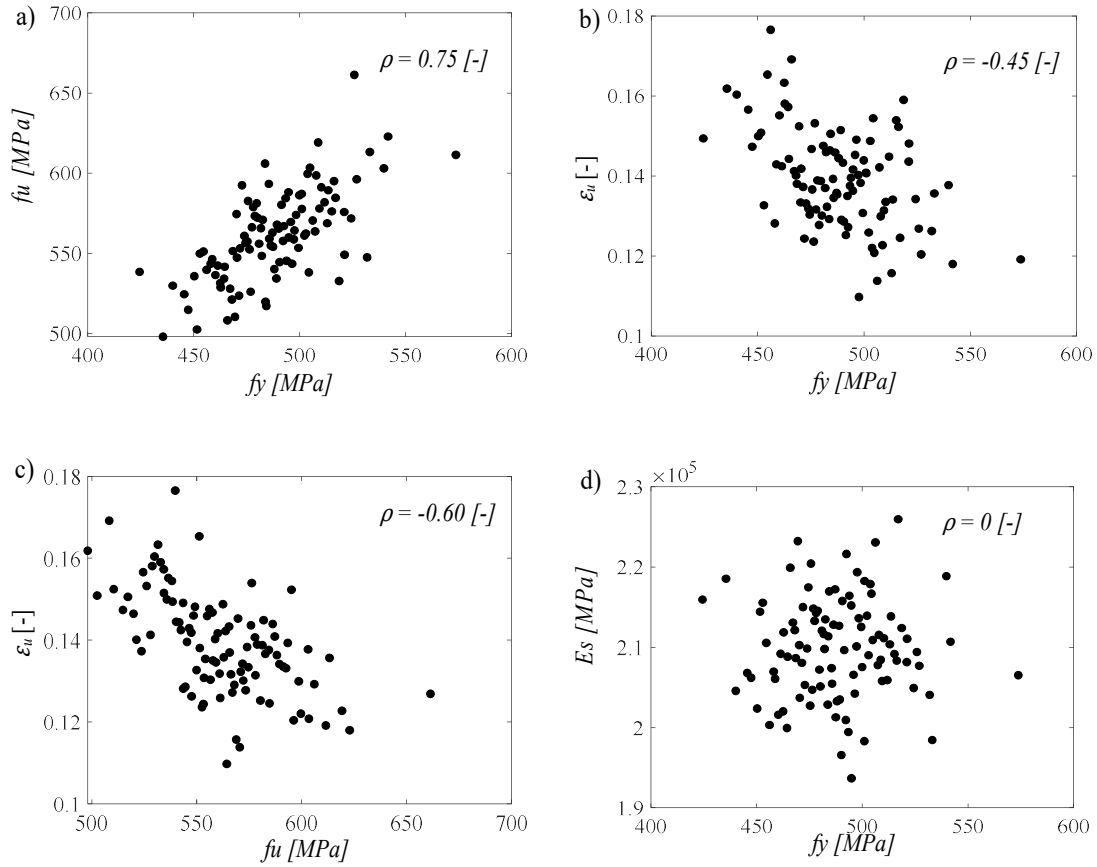


Figure 5.12: Reinforcement basic variables correlation: a) correlation between f_y and f_u ; b) correlation between f_y and ε_u ; c) correlation between f_u and ε_u ; d) correlation between f_y and E_s

The following provides a concise summary of all the assumptions that have been made about distribution type, mean value, and coefficient of variation:

Table 5.4: Sampled basic variables summary

	Distribution type	Mean value	Coefficient of Variation
Concrete compressive strength f_c	LN	31.87 MPa	0.15 [-]
Reinforcement ultimate strength f_u	LN	589.77 MPa	0.05 [-]
Reinforcement yield strength f_y	LN	488.57 MPa	0.05 [-]
Reinforcement ultimate strain ε_{su}	LN	0.14 [-]	0.09 [-]
Reinforcement elastic modulus E_s	LN	210000 MPa	0.03 [-]
Reinforced concrete specific-weight ρ	N	25 kN/m ³	0.05 [-]
Permanent structural load G_1	N	16 kN/m	0.05 [-]
Permanent non-structural load G_2	N	13 kN/m	0.05 [-]
Floor variable loads Q_p	GUMBEL	7.28 kN/m	0.20 [-]
Roofing variable loads Q_c	GUMBEL	1.82 kN/m	0.20 [-]

6 Reliability analysis by using FEM models

The FEM properties of the static non-linear finite element model used to conduct the reliability analysis are examined in this chapter. The two procedures required to do the reliability analysis are described here. The choosing of fundamental variables, i.e. material and geometrical features, is next explained using the Latin Hypercube Sampling technique. The assumptions, geometry, and mesh features of the FEM material constitutive law are then analysed. Finally, the chapter reviews the two aforementioned studies in terms of conclusions and the objective of this thesis, i.e. local and global reliability factor.

6.1 Introduction

In order to carry out the analysis, which involves simulating the removal of the centre column as a result of an unintentional event, prior non-linear studies are required. ATENA 2D does not permit the removal of geometrical components from one analysis step to the next. As a result, the simulation of the column removal is carried out by constructing a model in which the centre column is missing and then, in the course of the preliminary analysis stages, applying a force in the nodes of the beam that are adjacent to the column that isn't present. This force is proportional to the reaction that occurs at the base of the column, without the weight of the column itself; this is done so that the effect may be analogous to the real existence of the column. The column is then eliminated in the followings analysis phases (that is, the reaction in the previously stated nodes is set equal to zero), and the loads of the central spans are increased to replicate the dynamic behaviour of the incident. In order to achieve this objective, two separate analyses need be carried out in sequence:

Analysis 1 - Pushdown analysis (i.e. performed in a model without the central column), needed to calculate the amplification coefficients according to Izzuddin et al. [1]. The software used is ATENA 2D

Analysis 2 -Reliability analysis, simulation of the removal of the column and amplification of the loads in the central span. The software used is ATENA 2D

In terms of geometrical parameters, mesh sizes, material and mechanical qualities, these studies are equivalent. The only difference is in the analysis steps, how the analysis is carried out.

Moreover, in order to perform a reliability assessment in accordance with what was described in Chapter 2 (i.e. Method of Level III for reliability analysis), a statistical sample of the fundamental variables must be done. Consequently, the aforementioned analyses have been performed N times, where N is the sample dimension for all of the fundamental variables, which is fixed to 100.

6.2 Constitutive laws

The building is made up of two different materials: concrete and steel reinforcement. The confinement effect that the reinforcement has on the concrete varies according to the location (i.e. beam, column, joint, dissipative, non-dissipative zone), which is why the stirrups' reinforcement varies inside the structure.

Six distinct materials have been modelled in ATENA 2D, as indicated in the preceding chapter:

- Material 1: Beam D. It is referred to as an SBeta Material, and it describes the constrained concrete of the beam that is located in the dissipative zone (D stands for dissipative).
- Material 2: Beam ND. It is a Sbeta Material, it corresponds to the constrained concrete of the beam in the non-dissipative zone (ND).
- Material 3: Column. It is another example of a Sbeta Material and it describes the constrained concrete column
- Material 4: Joints. It is referred to as Sbeta Material and it describes the constrained concrete that may be found in the joints between beams and columns
- Material 5: NC Concrete. Again a Sbeta material, is used to define the concrete cover, the material used to distinguish the NC, or non-confined,

concrete region, which is the portion of the concrete that is not surrounded by reinforcing bars.

- Material 6: Steel B450C: type B450C steel was utilized for both the longitudinal and transverse reinforcements.

In what follows, a schematic representation of the bulk of the Materials that have been used will be shown. The longitudinal and transversal reinforcements, also known as Material 6, are denoted by horizontal and vertical green lines, respectively.

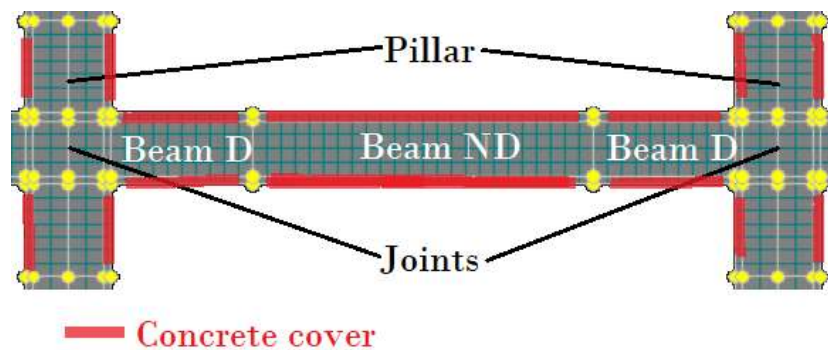


Figure 6.1: Scheme for Material 1 (Beam D), Material 2 (Beam ND), Material 3 (Column) and Material 4 (Joints) and Material 5 (NC Concrete)

6.2.1 Concrete (Model by Saatcioglu and Razvi, 1992)

Due to the presence of internal microcracks caused by stress concentrations at the interface between cement paste and aggregates, concrete, being a composite material, often exhibits non-linear behavior.

Beams and columns of reinforced concrete buildings benefit from lateral confinement made possible by transverse stirrups, which significantly influence the shape of the concrete's resistance curve σ - ϵ .

In this research, the model of Saatcioglu and Razvi (1992) (Figure 6.2) was used to characterize the nonlinear behaviour of confined and unconfined concrete, providing considerations of diverse behaviours with the confinement variations.

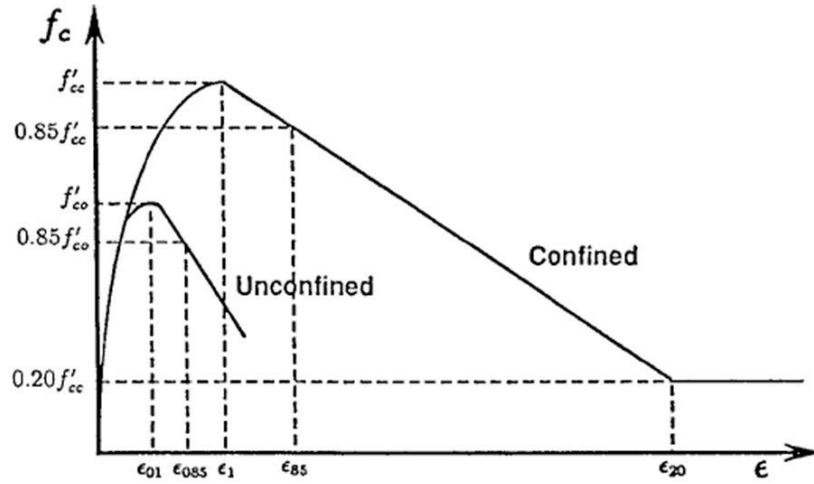


Figure 6.2: Model of Saatcioglu and Razvi (1992)

The model has been implemented in an Excel spreadsheet, which requires the average strength of the concrete f_{cm} , the section geometry, the iron cover, the average yield strength of the steel used, the diameter of the four side bars enclosed by the brackets, the diameter, the number of arms, and the pitch of the stirrups to be entered.

As discussed in the previous section, the material used for the construction was C25/30, where the first term represents the characteristic cylindrical compressive strength f_{ck} and the second term represents the characteristic cubic compressive strength R_{ck} .

Five distinct concrete strength curves (Figure 6.3) were generated by using the Saatcioglu and Razvi model, reflecting the differences in geometry and bars used.

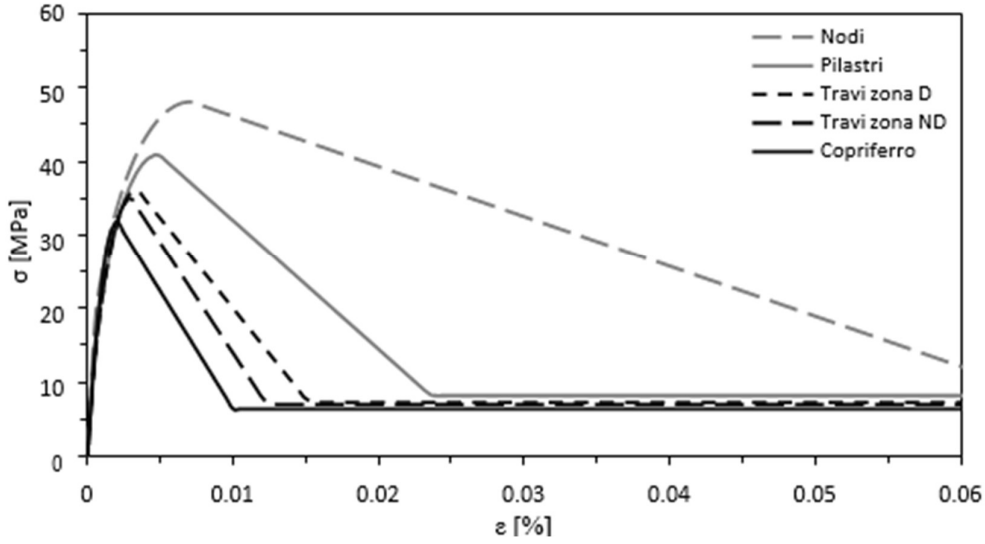


Figure 6.3: Concrete strength curves according to confinement

Here are illustrated assumptions have been made in ATENA 2D:

- in *Tensile*, the traction law of local deformation and the fixed crack model were chosen;
- in *Compressive*, a law of the *Softening Modulus* type has been adopted;
- in *Shear*, a law of reduction of the variable shear modulus was chosen, and in type of linear compression-tension interaction;

All the input parameters utilized by ATENA 2D for the various concrete components are shown in tables below:

Table 6.1: SBeta Material inputs

	BASIC			
	f_{cc} [MPa]	f_{ctm} [MPa]	$E_{cm,TG}$ [MPa]	ν [—]
1) Beam D	37.45	2.56	34328	0.2
2) Beam ND	35.01	2.56	33641	0.2
3) Column	41.00	2.56	35272	0.2
4) Joint	48.09	2.56	37003	0.2
5) NC Concr	31.87	2.56	32706	0.2

Table 6.2: Tensile, Compressive, Shear and Miscellaneous inputs for SBeta Material

	TENSILE	COMPRESSIVE			SHEAR	MISCELLANEOUS	
	C_3 [-]	ε_{cc} [-]	$R.C.S.$ [-]	$C.S.P.$ [-]	$F.S.F.$ [-]	ρ [kN/m ³]	α [1/K]
1) Beam D	0.000745	0.00375	0.8	0.0575	0.2	25	0.000012
2) Beam ND	0.000760	0.00298	0.8	0.0893	0.2	25	0.000012
3) Column	0.000725	0.00486	0.8	0.0497	0.2	25	0.000012
4) Joint	0.000691	0.00709	0.8	0.0184	0.2	25	0.000012
5) NC Concr	0.000782	0.002	0.8	0.0974	0.2	24	0.000012

6.2.2 Steel

The modeling of steel reinforcing bars is an essential part of this research because it has a considerable impact on the degree to which the beam is predisposed to exhibit membrane behavior and, as a result, the evolution of the catenary mechanism.

The kind of steel that was used was B450C, which had a ductility class of C (hot rolled steels) and a typical yield strength of 450 MPa.

The bilinear law with hardening was utilized for nonlinear analysis; more specifically for these studies average stresses were employed, namely yield strength and break tension, which were derived using the following formulas:

$$\sigma_y = f_{yk} * e^{1.645*0.05} \quad (6.1)$$

$$\sigma_t = 1.15 \sigma_y$$

The literature's experimental models were used to estimate an ultimate deformation of $\varepsilon_{lim} = 0.14$; lastly, a specific gravity of zero was assumed since the mass of the steel was thought to be included in the mass of the concrete.

The ATENA 2D steel characteristics are listed in Table 6.3.

Table 6.3: Steel characterization

BASIC				MISCELLANEOUS	
σ_y [MPa]	σ_t [MPa]	E [MPa]	ε_{lim} [-]	ρ [kN/m ³]	ALPHA [1/K]
489	562	200000	0.14	0	1.20E-05

6.2.3 Geometry

The geometry was defined in the ATENA 2D by first creating the points, then the lines, then the macro-elements, and lastly the reinforcing bars, as shown in previously design drawings;

The chosen model allowed for the subdivision of beams, columns, and nodes in a way that is in accord with the several confinement-related requirements composing concrete:

- the pillars have been divided into four vertical bands, two external ones represented by the iron cover and two internal ones dividing the barycentric axis, for horizontal rows of five points have been inserted, and three regions in height representing the two dissipative zones and the non-dissipative zone.
- the beams have been divided into three vertical bands, two external represented by the iron cover and one internal, for which vertical rows of four points have been inserted for each beam, and three regions in the longitudinal direction representing the two dissipative zones and the non-dissipative zone.

The geometry remains constant in all the analyses in the two cases under study, the standard design frame and the improved one, called for simplicity respectively frame 1 and frame 2.

The joints are the basic elements of the model, to which the lines and macro-elements are then linked, their total number was 1025 and 1005 regarding respectively the model with and without the central column:



Figure 6.4: Joints representation: left model with column, right model without column

Figure 5.17 shows final model lines. The model with and without the middle column utilizes 1890 and 1854 lines, respectively.

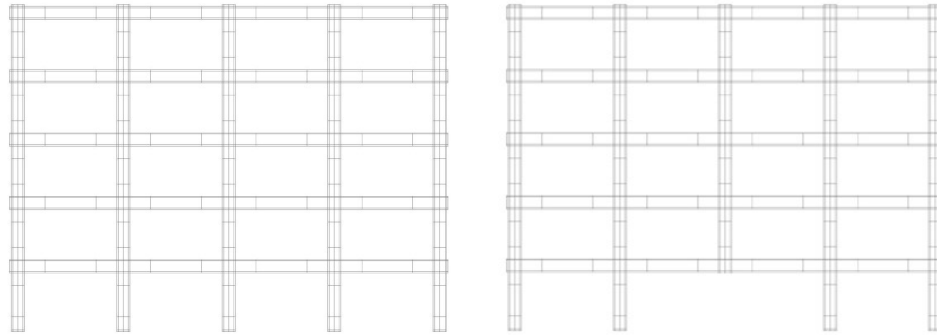


Figure 6.5: Lines representation: left model with column, right model without column

The overall number of macro-elements in the model with the center column is 850, whereas the number of macro-elements in the model without the central column is 834. At the conclusion of this procedure, the model will look exactly like what is shown in Figure 6.6:

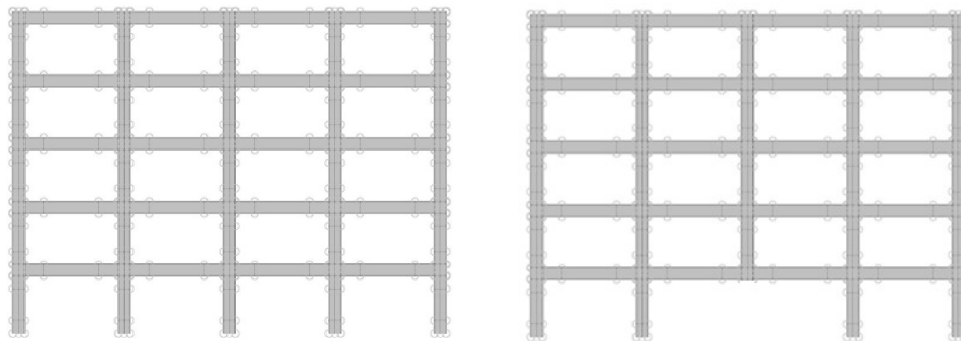


Figure 6.6: Representation with joints, lines and macro-elements: left model with column, right model without the column

Including all, the Reinforcements type lines used in the model with and without the centre column are 1825 and 1796, respectively.

Figure 6.7 shows the arrangement of the bars in the models:

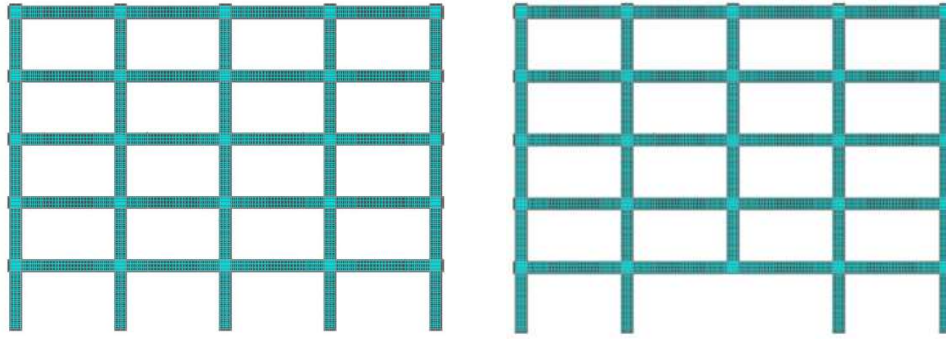


Figure 6.7: Representation of longitudinal and transversal reinforcement: left model with column, right model without the column

6.3 Analysis 1 - Pushdown analysis

6.3.1 Introduction

As a result of the coupling between concrete and steel, reinforced concrete exhibits a non-linear constitutive bond, which is particularly apparent after the cracking of the concrete and the yield strength of the reinforcing bars.

Additionally, when there are significant displacements, as when a column is removed, a phenomenon known as geometric non-linearity emerges, which must be considered when assessing the balance of the structure in its deformed shape.

Therefore, the composition of a reinforced concrete frame seems to have highly non-linear properties, particularly when a structural element is lost, implying that linear theory is unable to provide adequately accurate outcomes.

After the central column is removed, non-linear static analyses of the flat frame are conducted. This analysis involves the static imposition of an increasing vertical displacement of the point at the top of the central column (Figure 61), as a result the force that the rest of the structure is able to provide itself can be obtained at each step.

Pushdown curves, also known as force-displacement capacity curves, are the resultant curves.

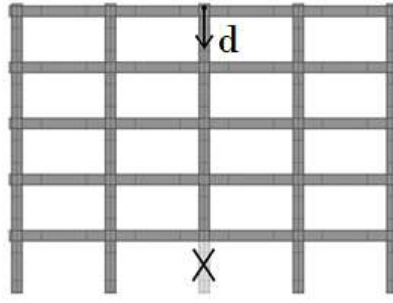


Figure 6.8: Pushdown analysis's scheme

The following are some of the characteristics that may be found in the approach selected to carry out the research on the flat frame's robustness:

- it is a *direct design* method, In fact, the structure's capacity is explicitly assessed in terms of the progression of disproportionate collapse, with the goal of identifying a structural solution capable of not collapsing even if the fundamental center column is lost.
- it is an *alternative load paths* method, because it aims to avoid excessive collapse by redistributing the loads carried by the collapsing element to the remaining components;
- uses *non-linear constituent models* of materials, both for steel and concrete, taking into consideration the production of inelastic deformations and plasticization, which are essential in energy dissipation and action redistribution;
- performs *nonlinear static analysis*, since they allow for the real understanding of essential effects such as geometric and mechanical nonlinearities and hence the catenary effect, but dynamic effects are not addressed, thus an adequate dynamic amplification coefficient is required.

The behaviour of the frame constructed according to the requirements of the Italian and European standards is presented first in this chapter, then the impact of the continuity and symmetry of the longitudinal reinforcing bars of the beams is studied.

6.3.2 Load cases in Atena

The load cases examined for this study are shown in the table below:

Table 6.4: Pushdown analysis's load cases

Load case number	Description
1	Base support
2	Imposed displacement of 1 cm

The base support is a fixity that was produced in accordance with sub-section 4.2.4.1 of the previous chapter and is applied to the lines that form the foundation of the four columns. The forced displacements are generated using ATENA 2D, according to chapter 4.2.4.4 they are called "Prescribed Deformation". They have been assigned to the node of the central column's centerline, in particular to the top of the frame as shown in figure 6.9

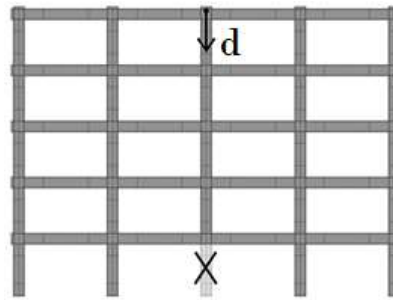


Figure 6.9: Pushdown analysis' scheme

6.3.3 Steps of the analysis and results

In these analyses imposed displacements have been applied by steps of 1.00 centimetre with a maximum of 60 iterations.

The capacity curve, which is a displacement-reaction curve, is the analysis's result that has been analysed. Specifically, the monitoring point above the center column, which record displacements and responses at each step, may be exported as a CCO file from ATENA 2D.

In this study, N pushdown studies have been carried out, leading to the development of N capacity curves, which account for the fact that the properties of the materials under study are subject to change at any different analysis. Figures below show the results of these elaborations respectively for the standard (on the

left) and the improved frames (on the right).

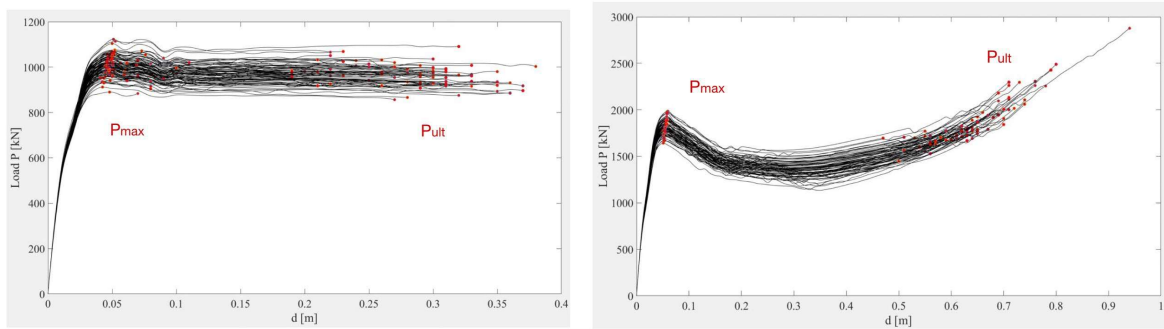


Figure 6.10: Results of pushdown analysis on the N simulations: a) curve displacement-load – Standard frame; b) curve displacement-load – Improved frame;

A peak in resistance, representing the flexural response, is seen in all the curves; this is followed by a softening interval and a region of constant resistance. When a system reaches its limit, failure occurs and the curves fall off quickly.

Since what occurs after the ultimate value has no importance, from a physical point of view, failure is reached, and ultimate capacity drops instantaneously.

It is easy to see the capacity recovery, in the catenary response, if it is there, as shown in Figure 5.22b. This occurs when the P_{ult} value is greater than the P_{max} value. It is important to note that in the majority of situations, the final resistance is lower than the peak one. This indicates that the catenary branch is regulated not by a catenary effect but rather by the ductility capacity of the reinforcing bars.

6.3.4 Dynamic amplification coefficient - DAF

The unintentional occurrence of a quick column loss in terms of structural reaction is a dynamic event caused by severe nonlinearities in geometry and material behaviour. Although DoD provisions [16] recommend having a dynamic non-linear analysis on the damaged structure, this is not necessarily the optimum approach due to the computational complexities in practical implementation. As a result, a static non-linear analysis with an associated dynamic technique may be a valid alternative. The DoD and GSA guidelines [16][42] permit this, when a static evaluation is employed, based on a constant dynamic amplification factor (DAF) $\lambda_d = 2$, for gravity loads above the lost column. However, since the

aforementioned figure was considered too conservative, an alternative technique may be employed to calculate the DAF numerically. Precisely, Izzuddin [1] provided a technique for computing a new range of λ_d on a steel multi-story structure.

The theory that supports this method is that the phenomenon of sudden column loss is analogous to the rapid application of gravity load on the involved sub-structure; at the beginning, at the moment of column failure, the gravity load is larger than the static structural resistance, due to the dynamic nature of the phenomenon, and as a result, the incremental of deformations is transformed into additional kinetic energy, which results in greater velocities. Increases in deformation lead to greater static structural resistance, which has the effect to reduce kinetic energy and so speeds. When the derivative of the dynamic displacement is zero—that is, when the kinetic energy has been brought back down to zero—the maximum dynamic displacement has been met. This corresponds to the point at which the energy absorbed by the structure is equal to the amount of work done by the gravitational loads.

The expressions of the internal energy U_n and external work W_n are followingly reported

The following are the formulations for internal energy, U_n , and external work, W_n :

$$U_n = \int_0^{u_{d,n}} P du_s \quad (6.2)$$

$$W_n = \lambda_n P_o u_{d,n} \quad (6.3)$$

External work W_n is the product of the level of rapidly applied gravity loading ($P_n = \lambda_n P_o$) and the corresponding maximum dynamic displacement ($u_{d,n}$), while internal energy U_n is equal to the area under the capacity curve up to $u_{d,n}$. The following diagram illustrates this point:

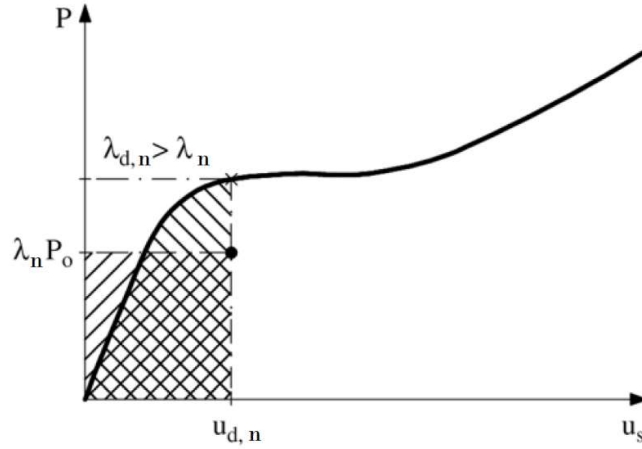


Figure 6.11: Energy balance approach (Izzuddin [1])

The dynamic amplification factor may be calculated using the preceding principles by equating (6.2) and (6.3):

$$\lambda_{d,n} = P_d/P_o \quad (6.4)$$

According to this, P_d is the dynamic load, i.e. the level of amplified loading that correspond to a dynamic displacement, computing as the point of the capacity curve corresponding to $u_{d,n}$.

The point on the capacity curve at which $u_{d,n}$ occurs is the dynamic load, P_d , which is the level of amplified loading corresponding to a dynamic displacement.

In order to determine the amount of rapid gravity loading that was applied, denoted by the symbol P-o, this can be interpreted as being equal in magnitude but opposite to the reaction that was applied at the point where the column was removed, in accordance with the procedure that was implemented before. There are two possible outcomes: either the structure is able to withstand the removal of the column or the equilibrium is not reached under those loading-material conditions. In the first case the two curves of external and internal work find a point of intersection.

Figures below shows a clear representation of the concept, following Izzuddin's research on the left we can visualize a frame which find equilibrium after the removal of the central column, while on the right this doesn't happen, the frame reach quickly collapse.

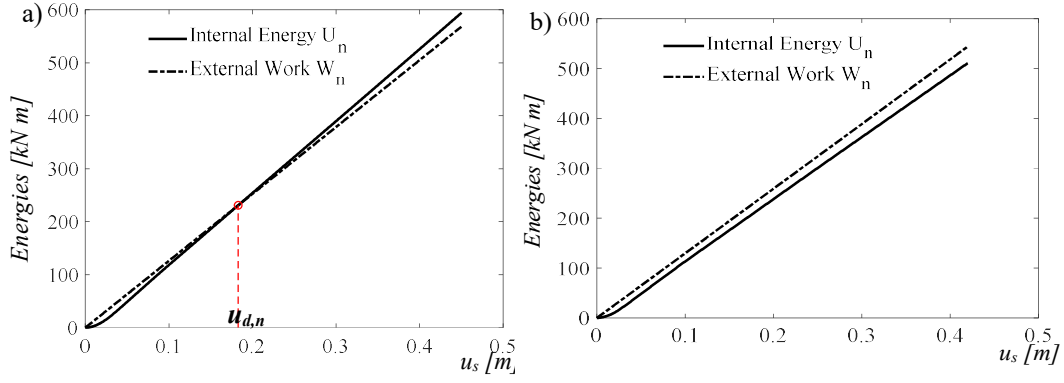


Figure 6.12: Energy curves: a) case where the equilibrium is reached b) case where the equilibrium is not reached

It was discovered that the dynamic displacement, which corresponds to the displacement at the intersection point ($u_{d,n}$) and the corresponding loading P_d (using capacity curves) are obtained for all of the situations in which equilibrium is achieved. Afterward, the DAF is determined using the formula according to the previous step.

For the other cases, where the intersection is not present, the DAF isn't computed and it was critically decided to increase the load by steps of 5 per thousand until reaching the collapse

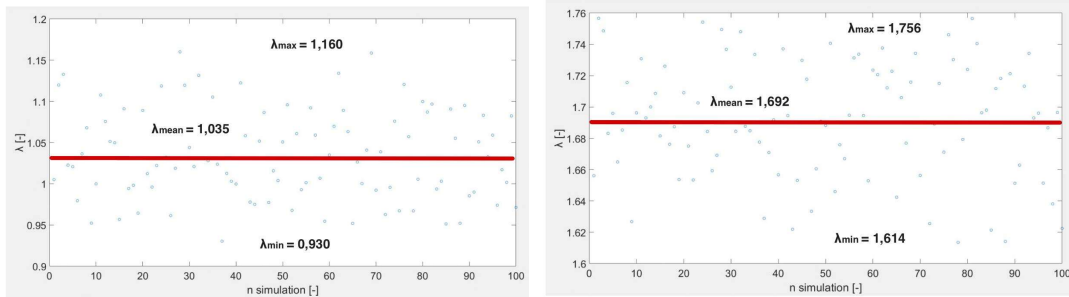


Figure 6.13: DAF sampled values for Standard frame (on the left) and Improved frame (on the right)

Figures 6.13 shows the values of the DAF as function of the number of simulations (from 1 to 100). On the left-hand side, the DAF regards the standard frame while on the right is shown DAF values about the improved one.

In the former the maximum amplification coefficient is $\lambda_{max} = 1.160$, the minimum is $\lambda_{min} = 0.930$ and the mean value is $\lambda_{mean} = 1.035$. Meanwhile in

the latter the maximum amplification coefficient is $\lambda_{max} = 1.756$, the minimum is $\lambda_{min} = 1.614$ and the mean value is $\lambda_{mean} = 1.692$.

It's easy to understand that the improved frame will have a better robustness behaviour just by observing much higher values of DAFs. It is also interesting to notice that in the standard frame there are many cases where DAF is lower than 1, indicating that the capacity curve's maximum value is less than the dynamic gravity loading. From a physical standpoint, this indicates that the structure cannot withstand gravity loads alone, even if without the column loss.

6.4 Analysis 2 - Reliability Analysis

Evaluating the dependability of this building, which was built according to robustness and seismic standards, is the very last thing that has to be done in order to achieve the objective of this thesis. This step needs to be taken in order to be successful. In order to accomplish this, the information that were derived from the previous analyses (the dynamic amplification factors), are incorporated into each of the N simulations. Next, the stresses at the critical nodes of the frame are analysed, and a local and then a global reliability assessment is carried out.

The frames that will be investigated are the ones that do not have the central column. More information on the applied loads and analysis procedures will be presented in the following sections.

6.4.1 Load cases in Atena

The load instances analysed are shown in the table below.

Table 6.5: Reliability analysis's load cases

Load case number	Description
1	Base support
2	Self-weight
3	Permanent structural loads
4	Permanent non-structural loads
5	Variable loads
6	Amplified columns weight
7	Amplified beams weight
8	Amplified permanent structural loads
9	Amplified variable loads
10	Amplified permanent non-structural loads
11	Temporary reaction

The self-weight is applied on the whole structure, as function of geometry and specific weight ρ . The other gravity loadings, defined in load cases 3,4 and 5, are applied as loads per meter on the upper horizontal lines of all the beams (apart from the variable loads where distinction is made between floors and roofing). The other load cases, i.e. from 6 to 10, regard only the lines of the beams of the central spans, since these are the only gravity loadings that should be amplified according to the DAFs previously computed. Finally, the temporary reaction is a load per meter applied oppositely to the gravity loadings, used to simulate the presence of the column. Thus, it is equal to the concentrated reaction P_o , divided by 0.6 m to obtain the load per meter, and applied at the line of the top of the column removed.

The self-weight acts uniformly over the whole structure and based on its architecture and specific weight. The additional gravity loadings, as specified by load cases 3, 4, and 5, are applied to the top horizontal lines of all the beams as loads per meter. In the remaining load scenarios (6-10) only the centre span beam lines are considered, since these are the only gravity loadings that should be amplified according to the DAFs previously obtained. Lastly, the column's existence may be reproduced by a transient response, which is a load per meter imposed in the opposite direction of the gravity loadings. Accordingly, the concentrated reaction, P_o , divided by 0.6 m to produce the distributed load, and applied at the line at the top of the column removed is the value.

6.4.2 Steps of the analysis

The analytical phases contain different assumptions based on the simulations, i.e., whether the equilibrium has been found or not according to energy-balance calculations, and on the value of λ .

The procedure was divided into 3 different steps: in the first one, to simulate the presence of the column, the structure was loaded gradually in 10 steps by standard loads while the opposite reaction that would provide the column was present (the latter calculated 1 time for all frames through Ftool with reasoning on areas of influence). In a second phase the fictitious reaction was removed in 10 steps of 10% each, finally only at this point the standard loads were increased by the dynamic factor DAF computed before. In the following pictures are presented

the two cases that I mentioned before about the theory of Izzuddin:

- when the two curves of internal and external work intersect, then the load has been increased by the exactly value found in more steps.
- when the two curves do not intersect, it has been critically decided to increase the load by steps of 0.005 each one until the collapse is reached.

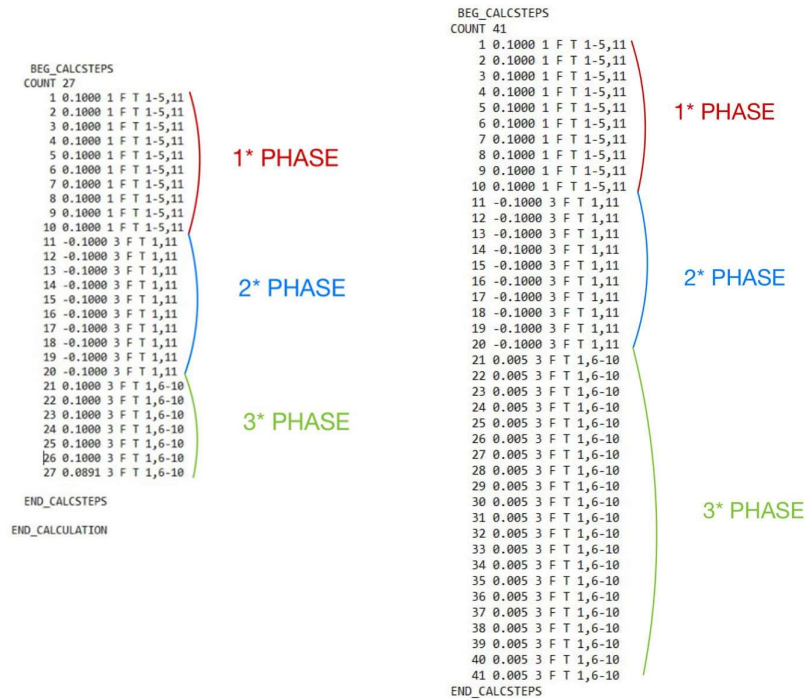


Figure 6.14: Load amplification's CCT format: simulations where equilibrium is reached (on the right); simulations where equilibrium is not reached (on the right)

Figure 6.15: Scheme of the failure probabilities at each sub-section, standard frameFigure 6.16: Load amplification's CCT format: simulations where equilibrium is reached (on the right); simulations where equilibrium is not reached (on the right)

In each of the N simulations, the first 20 load steps are the same. For instance, in the first ten, the frame is fully loaded with gravity loadings and the presence of the column is simulated via a transient response. Ten more steps are performed after this to fully suppress the reaction, simulating column loss, while the gravity loadings stay constant. In order to prevent numerical issues brought on by high loadings, the current scheme of 10 stages with a multiplier of 0.1 has been

established, with specific focus on the phase when the column is eliminated.

Different assumptions have been evaluated beginning by analysis step 21 depending on the simulations; in particular, an extra percentage of gravity loadings is introduced at this phase, but only on the center spans of the frame, as shown in the DAF discussion. If it is less than 1.0, as it is in certain circumstances where equilibrium has not been achieved, the structure is not likely to reach equilibrium even when subjected to static gravity loadings and will thus fail during the twentieth analysis step (even if without any accidental event).

6.4.3Outputs

Once the analysis has been conducted, the strains at the nodes will be the result to be studied for all N simulations. *TextPrintout* provides this information by exporting the *Principal Total Strains* at each node from the stage in which the gravity loadings of the core spans are amplified. A Matlab function was then developed to process these figures. In specifically, the stresses at various locations within the structures have been taken into account using the following scheme:

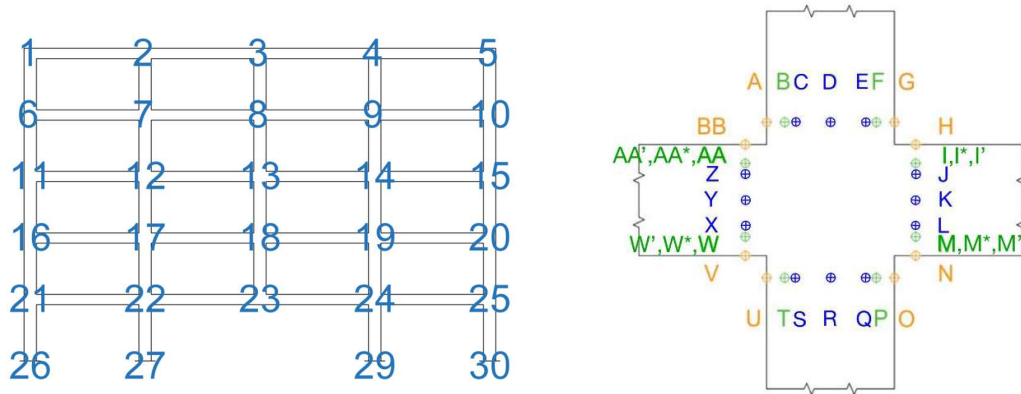


Figure 6.17: Strains evaluation's visualization: section location (on the left); nodes' location (on the right)

The inner nodes of the confined concrete, which are represented by the letters J, K, L, X, Y, and Z in blue, are a portion of the dissipative zone of the beams. The remaining inner nodes (in blue) denoted by the letters C, D, E, Q, R, and S are also nodes of the confined concrete, but since they are a part of the column, the constitutive equation is different. The exterior nodes, represented by the letters

A, G, H, N, O, U, V, and BB in orange, define the concrete cover, or non-confined concrete. The reinforcing longitudinal bars are represented by the intermediate nodes (in green) that are indicated by B, F, I, M, P, T, W, and AA. In our study, we additionally took into account four nodes (I, M, W, and AA) that are a part of stirrups as well as four additional nodes (I, M, W, and AA) that are a part of wall iron reinforcement.

In addition, a differentiation is established between the sections of the inner spans and the sections of the peripheral spans as follows:

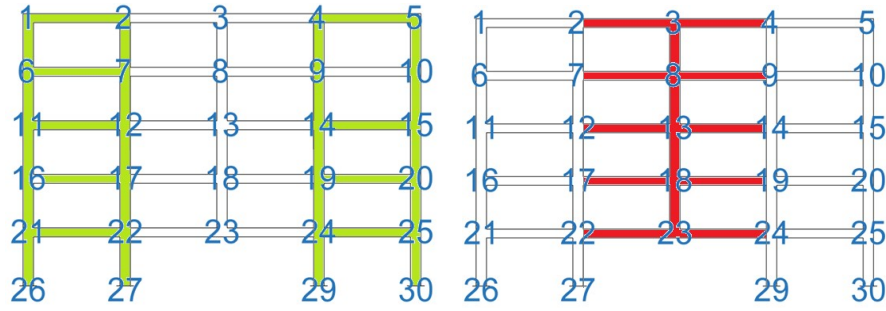


Figure 6.18: Scheme of the sections: indirectly affected members (on the left); directly affected members (on the right)

6.4.4 Computation of P_f^{max} : local probability of failure

The strains that were collected as an output for each section have been compared with the ultimate strains of both the reinforcement and the concrete. This was done for each section individually. The ultimate strain that is intended to be applied to the concrete is the one that corresponds to the peak. The technique that was carried out is composed of the following steps:

- 1) Since only the failure of concrete in compression needs to be evaluated, the data has been filtered to exclude nodes where the concrete is in tension, leaving a minimum realistic failure probability of $P_f = 10^{-7}$ at these nodes.
- 2) The values presented here do not take into account the nodes of the concrete cover, so the unconfined concrete, since the latter, despite being

lost in most nodes, is not a structural element that affects the overall stability of the entire frame.

- 3) A convolution integral computation is used to determine the failure probability P_f for each node.
- 4) The maximum of the probabilities (P_f^{max}) is used to determine the local probability of failure for each section. The section is meant to be one of the surfaces that make up the overall node.

The following equation shows how the convolution integral was employed for this situation:

$$P_f = P(S > R) = \int_{r=-\infty}^{\infty} \int_{s=-\infty}^r f_{S,R}(s, r) ds dr \quad (6.5)$$

where $f_R(x)$ is the probability density function of the resistance R (ultimate strains) and $f_S(x)$ is the probability density function of the demand S (strains at the nodes). The two PDFs are obtained respectively from the vector of the ultimate strain values, sampled N times, and the strains taken as outputs from the N FEM simulations. According to this, the convolution integral represents the probability that the strains at the nodes have reached or overcome the ultimate strains.

where $f_R(x)$ denotes the probability density function of resistance R (ultimate strains) and $f_S(x)$ denotes the probability density function of demand S . (strains at the nodes). The two PDFs are created by sampling the vector of ultimate strain values N times and using the strains as outputs from the N FEM simulations. This convolution integral reflects the probability that the strains at the nodes have reached or exceeded the ultimate strains.

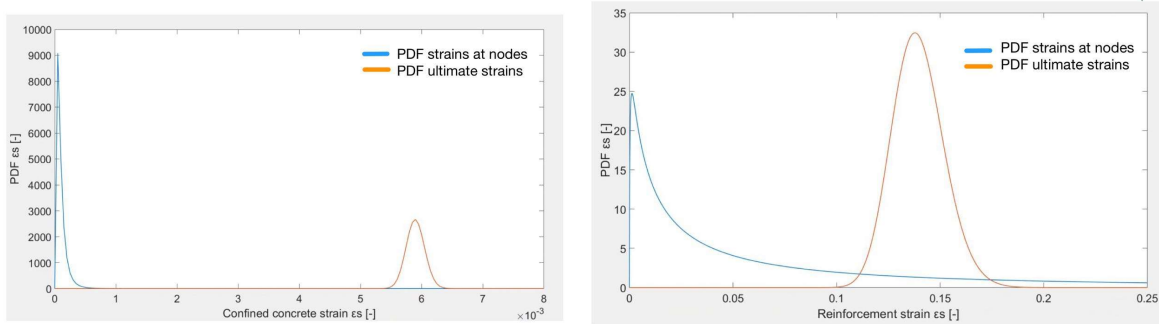


Figure 6.19: Convolution integral for the maximum P_f of directly affected sub-sections: beam confined concrete strain (on the left); beam reinforcement strain (on the right)

Different situations have been observed:

- For the sub-sections indirectly affected by the column loss, i.e. located outside the central spans, the P_f^{max} is lower than the limiting value everywhere for both the design frames
- Talking about the standard frame (Frame 1), for the sub-sections directly affected by the column loss (Figure 6.186.19), i.e. located inside the central spans, the P_f^{max} is always different than zero and with larger values, especially in the first floor, for the longitudinal reinforcement of the beams. While it is lower than the limiting value on the columns' nodes.
- Talking about the improved frame (Frame 2), for the sub-sections directly affected by the column loss (Figure 6.186.20), i.e. located inside the central spans, the P_f^{max} is lower than the limiting value everywhere, with exception of the first floor where P_f^{max} is comprised between 10^{-16} and 10^{-7} , for the longitudinal reinforcement of the beams. While it is lower than the limiting value on the columns' nodes.

This can be observed in the following schemes:

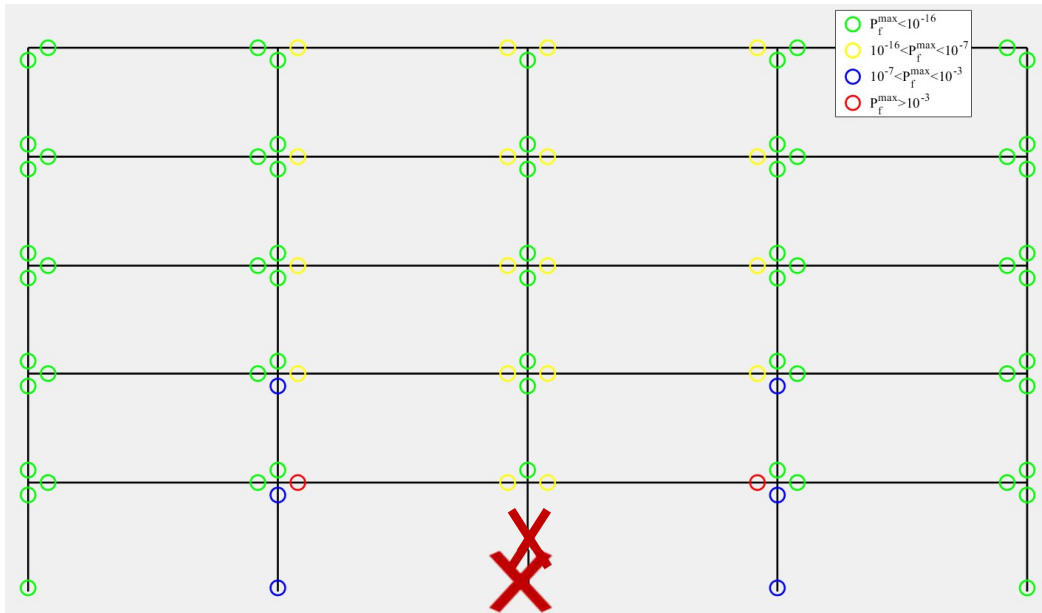


Figure 6.21: Scheme of the failure probabilities at each sub-section, standard frame

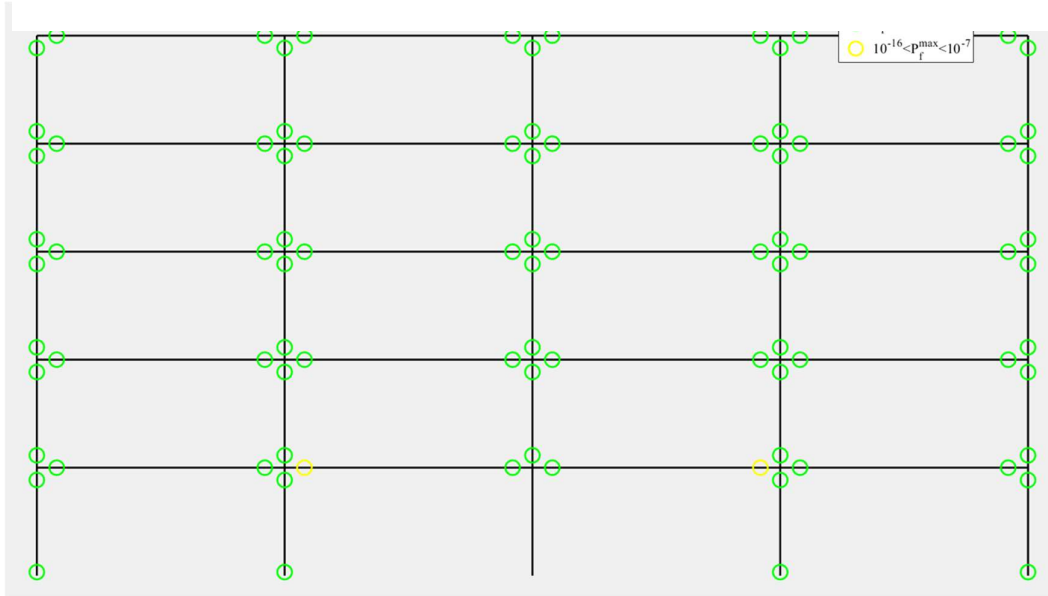


Figure 6.20: Scheme of the failure probabilities at each sub-section, improved frame

In addition, the observations presented in Figure 6.21 and Figure 6.22 demonstrate that, among the nodes of the central spans, there is a greater local probability of failure at the bars close to the joints beam column, and in particular in correspondence of the lateral pillars. This is as a result of the fact that plasticization takes place in order to make allowances for the displacement of the nodes in locations where the column has been removed. How we could expect,

larger values of P_f^{max} can be observed for the standard frame. These are, in fact, the things that are emphasized the most in these 3D visualization graphs.

Standard Frame:

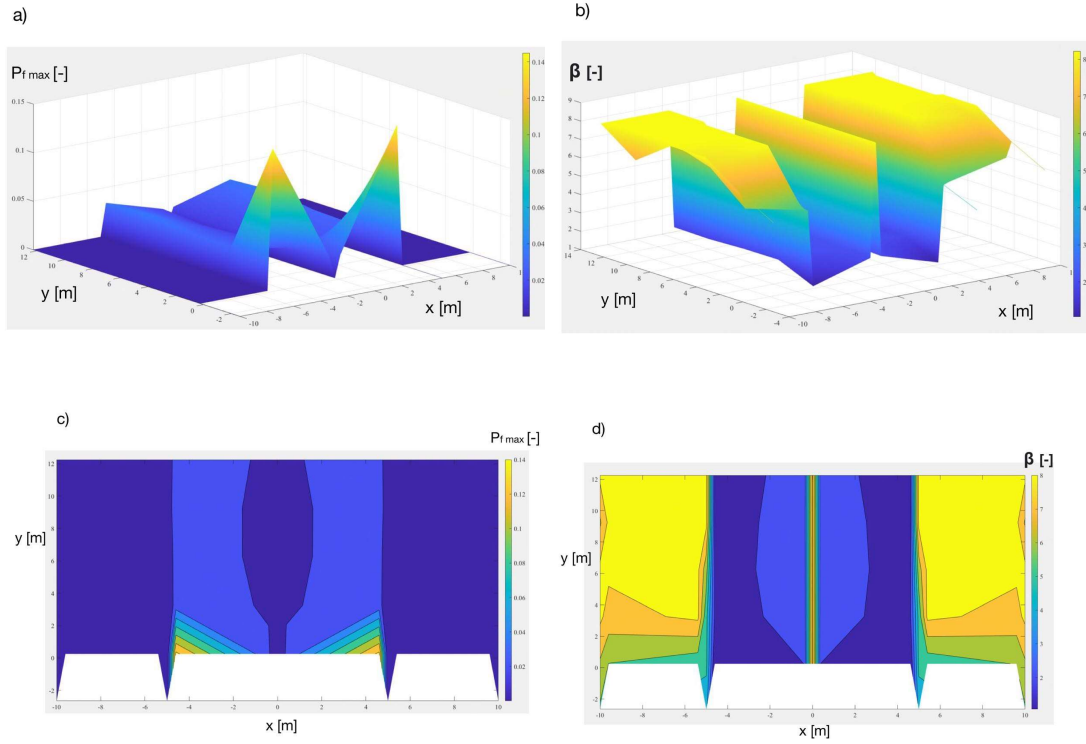
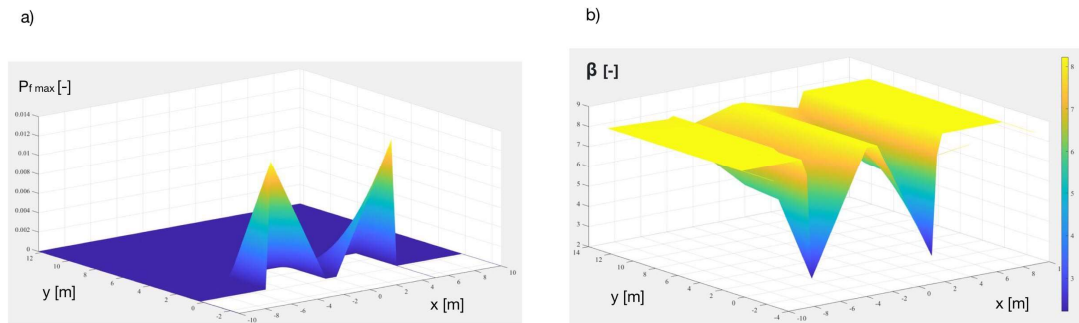


Figure 6.22: Failure probabilities and reliability indices of the standard frame's nodes: a) 3D plot of P_f ; b) 3D plot of β ; c) Contour plot of P_f ; d) Contour plot of β

Improved Frame:



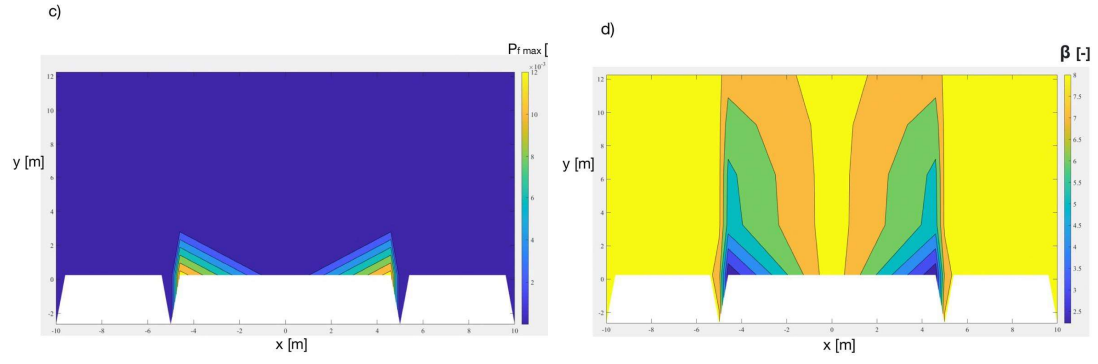


Figure 6.35: Failure probabilities and reliability indices of the improved frame's nodes: a) 3D plot of P_f ; b) 3D plot of β ; c) Contour plot of P_f ; d) Contour plot of β

7 Conclusions

This thesis study focused on a technique for assessing the reliability of 2 frames constructed with different design criteria in the seismically active city of L'Aquila.

The structural details has first been computed using capacity design and code requirements, using a design working life of 50 years. Starting from considerations taken from “Robustness assessment in reliability terms of reinforced oncrete structures in seismic zone”, E. Miceli [45], two differents frame had been analysed: the fist one designed literally following Italian and European code rules, while the second follows some robusteness improvements. In particular, the robustness has been enhanced by creating continuity of the bars along each beam, symmetry of the bars between the upper and lower chord and equality of the bars between the floors.

A probabilistic method has been adopted by sampling 10 basic variables with 100 values each: both material resistances and action loads.

By simulating the removal of the center column, a Static Non-Linear Study has been assessed as the most effective technique to carry out the reliability analysis. This has been done using the ATENA 2D program. With a preliminary analysis, the Pushdown, have been computed Dynamic Amplification Factors (DAFs) using a energy-balance method (“Progressive collapse of multi-storey buildings due to sudden column loss - Part I: Simplified assessment framework”, B. A. Izzuddin et al.[1]).

Then through a reliability analysis, by removing the central column and amplifying the loads only on the central spans of the frame, the results found in terms of probability of failure have been analysed, by comparing the ultimate strains with the strains at the nodes, for all the sections at the joints beam-column of the frame. This has highlighted that:

- The most stressed joints at the base are the two central ones: it is observed that the element in crisis is the longitudinal reinforcement towards the center of the frame, this underlines how equilibrium is reached during the 'first phase' in which the pillars act as a contrast to the

central beam that 'pushes' outwards after removing the column, that is, when the catenary mechanism has not yet developed.

- As we expected the frame designed according to criteria of robustness leads to values of P_f much lower than the frame designed according to codes criteria.
- Taking into account the iron cover, almost all the points have a $P_f \geq 10^{-1}$ so it was decided not to take it into account since the loss of it does not lead to the collapse of the building
- The most stressed joints and consequently with a major P_f are those corresponding to the two central spans straddling the point where the column is removed: here the longitudinal reinforcement irons are more stressed, another confirmation of the fact that the catenary mechanism has not yet been established (this in large displacements could put in crisis by traction even the wall irons because they are smaller in diameter and quantity than the longitudinal reinforcement).
- The frame designed according to robustness criteria has very low P_f values, not associated with a generalized collapse mechanism. We can therefore summarize that from this analysis the second frame turns out to be 'SAFE' against the removal of the central column at the base of it

8 References

- [1] B. A. Izzuddin, A. G. Vlassis, A. Y. Elghazouli, and D. A. Nethercot, "Progressive collapse of multi-storey buildings due to sudden column loss - Part I: Simplified assessment framework", *Eng. Struct.*, vol. 30, no. 5, pp. 1308–1318, May 2008.
- [2] fib, "fib Model Code for Concrete Structures", 2010 Weinheim, Germany: Wiley-VCH Verlag GmbH & Co. KGaA, 2013.
- [3] JCSS, "JCSS - Probabilistic Model Code", 2001.
- [4] CNR (Consiglio Nazionale delle Ricerche), "Istruzioni per la valutazione della robustezza nelle costruzioni", 2018.
- [5] European Committee for Standardization, "Eurocode: Basis of structural design", 1990.
- [6] European Committee for Standardization, "Eurocode 1: Action on structures - Part 1-7: General actions - Accidental actions", 1991.
- [7] European Committee for Standardization, "Eurocode 2: Design of concrete structures - Part 2: Concrete Bridges - Design and detailing rules", 2005.
- [8] Ministero delle Infrastrutture e dei Trasporti, "Norme tecniche delle costruzioni", 2008.
- [9] Ministero delle Infrastrutture e dei Trasporti, "Decreto 17 gennaio 2018: Aggiornamento delle "Norme tecniche per le costruzioni", 2018.
- [10] J. K. Mitchell and R. J. Blong, "Volcanic Hazards: A Sourcebook on the Effects of Eruptions", *Geogr. Rev.*, vol. 76, no. 1, p. 113, Jan. 1986.
- [11] J. Suda, A. Strauss, F. Rudolf-Miklau, and J. Hübl, "Safety assessment of barrier structures", *Struct. Infrastruct. Eng.*, vol. 5, no. 4, pp. 311–324, 2009.
- [12] European Committee for Standardization, "Eurocode 1: Actions on structures - Part 1-7: General actions - Accidental actions", 2006.
- [13] U.S. Nuclear Regulatory Commission, "Regulatory Guide 50.150 Aircraft impact assessment", Washington D.C., 2018.
- [14] M. E. Paté-Cornell, "Quantitative safety goals for risk management of industrial facilities", *Struct. Saf.*, vol. 13, no. 3, pp. 145–157, Mar. 1994.
- [15] ASCE/SEI 7-05, "Minimum Design Loads for Buildings and Other Structures", Reston, VA: American Society of Civil Engineers, 2005.
- [16] D. Stevens *et al.*, "DoD Research and Criteria for the Design of Buildings to Resist Progressive Collapse", *J. Struct. Eng.*, vol. 137, no. 9, pp. 870–880, Sep. 2011.

- [17] U. Starossek and M. Haberland, “Disproportionate Collapse: Terminology and Procedures”, *J. Perform. Constr. Facil.*, vol. 24, no. 6, pp. 519–528, Dec. 2010.
- [18] S. Kokot and G. Solomos, “Progressive collapse risk analysis: literature survey, relevant construction standards and guidelines”, Publications Office of the European Union, 2012.
- [19] H. S. Lew, Y. Bao, F. Sadek, J. A. Main, S. Pujol, and M. A. Sozen, “An Experimental and Computational Study of Reinforced Concrete Assemblies under a Column Removal Scenario”, Gaithersburg, MD, Oct. 2011.
- [20] M. Holicky, A. Materna, G. Sedlacek, and L. Sanpaolesi, "Implementation of Eurocodes Handbook 1 - Basis of structural design. Leonardo Da Vinci Project", Garston, Watford, UK, 2004.
- [21] M. Holicky *et al.*, "Implementation of Eurocodes Handbook 2 - Reliability backgrounds. Leonardo Da Vinci Project", Prague, 2005.
- [22] D. Gino, “Advances in reliability methods for reinforced concrete structures”, Politecnico di Torino, 2019.
- [23] A. Haldar and S. Mahadevan, “Probability, Reliability and Statistical Methods in Engineering Design”, *Bautechnik*, vol. 77, no. 5, May 2000.
- [24] International Standard Organization, “ISO 2394 - General principles on reliability for structures”, 1998.
- [25] A. Harbitz, “An efficient sampling method for probability of failure calculation”, *Struct. Saf.*, vol. 3, no. 2, pp. 109–115, Jan. 1986.
- [26] F. Mauro, “Robustezza strutturale di edifici intelaiati in calcestruzzo armato: analisi parametrica e nuove proposte progettuali”, Politecnico di Torino, 2019.
- [27] L. Capri, “Robustezza Strutturale di costruzioni multipiano in calcestruzzo armato: analisi parametrica di telai 2D per mezzo di modelli globali e locali”, Politecnico di Torino, 2019.
- [28] European Committee for Standardization, “Eurocode 2: Design of concrete structures - Part 1-1 : General rules and rules for buildings”, 2004.
- [29] European Committee for Standardization, “Eurocode 8: Design of structures for earthquake resistance - Part 1: General rules, seismic actions and rules for buildings”, 2003.
- [30] EN European Standard, “EN 206-1 Concrete - Part 1: Specification, performance, production and conformity”, 2000.
- [31] D. Grandić, “Shear resistance of reinforced concrete beams in dependence on concrete strength in compressive struts” , *Teh. Vjesn. Gaz.*, vol. 22, no. 4, pp. 925–934, Aug. 2015.
- [32] M. Saatcioglu and S. R. Razvi, “Strength and ductility of confined concrete”, *J. Struct. Eng. (United States)*, vol. 119, no. 10, pp. 3109–3110, 1993.

- [33] V. Červenka, L. Jendele, and J. Červenka, “ATENA Program Documentation Part 1 Theory”, 2013.
- [34] V. Červenka and J. Červenka, “ATENA Program Documentation Part 2-1 User’s Manual for ATENA 2D”, 2013.
- [35] A. J. Kappos, M. K. Chryssanthopoulos, and C. Dymiotis, “Uncertainty analysis of strength and ductility of confined reinforced concrete members”, *Eng. Struct.*, vol. 21, no. 3, pp. 195–208, 1999.
- [36] Y. Lu and X. Gu, “Probability analysis of RC member deformation limits for different performance levels and reliability of their deterministic calculations”, *Struct. Saf.*, vol. 26, no. 4, pp. 367–389, 2004.
- [37] A. Slobbe, Á. Rózsás, D. L. Allaix, and A. Bigaj-van Vliet, “On the value of a reliability-based nonlinear finite element analysis approach in the assessment of concrete structures”, *Struct. Concr.*, no. December 2018, pp. 1–16, 2019.
- [38] D. F. Wiśniewski, P. J. S. Cruz, A. A. R. Henriques, and R. A. D. Simões, “Probabilistic models for mechanical properties of concrete, reinforcing steel and pre-stressing steel”, *Struct. Infrastruct. Eng.*, vol. 8, no. 2, pp. 111–123, 2012.
- [39] Shamim, A. Sheikh, Dharmendra, V. Shah and S. K. Shafik, “Confinement of High-Strength Concrete Columns”, 1994.
- [40] S. Caprili and W. Salvatore, “Mechanical performance of steel reinforcing bars in uncorroded and corroded conditions”, *Data Br.*, vol. 18, pp. 1677–1695, Jun. 2018.
- [41] M. Ferraioli, A. Maria Avossa, and A. Mandara, “Assessment of Progressive Collapse Capacity of Earthquake-Resistant Steel Moment Frames Using Pushdown Analysis”, *Open Constr. Build. Technol. J.*, vol. 8, no. 1, pp. 324–336, Dec. 2014.
- [42] General Services Administration, “Progressive collapse analysis and design guidelines for new federal office buildings and major modernization projects”, Washington (DC, USA), 2003.
- [43] G. Xu and B. R. Ellingwood, “An energy-based partial pushdown analysis procedure for assessment of disproportionate collapse potential”, *J. Constr. Steel Res.*, vol. 67, no. 3, pp. 547–555, Mar. 2011.
- [44] H. R. Tavakoli, “Numerical Study of Progressive Collapse in Framed Structures: A New Approach for Dynamic Column Removal”, *Int. J. Eng.*, vol. 26, no. 7 (A), Jul. 2013.
- [45] E. Miceli, “Robustness assessment in reliability terms of reinforced oncrete structures in seismic zone”, Politecnico di Torino, 2020.
- [46] <https://www.cervenka.cz/products/aten/>

[47] <http://www.csi-italia.eu>

[48] <https://www.ingenio-web.it>